Università degli Studi di Padova

Università degli studi di Padova

Department of Physics

Master's Thesis in Physics

Extended Axion Dark Matter Landscape from Post-Inflationary Field Dynamics

Master Candidate

Camilla Midollini

Student ID 2152810

Supervisor

Prof. Francesco D'Eramo

University of Padova

Co-supervisor

Prof. Yann Mambrini

Université Paris-Saclay, IJC Lab

Academic Year
2025/2026

Abstract

The nature of Dark Matter remains one of the most significant unresolved problems in Physics. Throughout the years, various candidates have been proposed to account for this missing mass, starting from early candidates, such as neutrinos, that were afterwards excluded. Recently, the attention has shifted towards other models, one of which being the axion, which this work focuses on. The purpose of this study is the analysis of axions as a DM candidate, considering their production through different mechanisms with the goal of constraining the various parameters that come into play. This thesis is articulated as follows.

Chapters 1 to 4 contain the introduction, the contextualization of the framework we will be working in and present the focus of the thesis. Specifically, Chapter 1 describes the Standard Model of Particle Physics, along with its limitations and the need to go beyond it. In particular, the strong CP problem is briefly mentioned, as it will be thoroughly analyzed in Chapter 2. A simple and elegant solution to the strong CP problem was proposed by Peccei and Quinn and it involves the introduction of a dynamical field, the axion, into the theory. Chapter 3 explains this and describes the dynamics of the axion. The other necessary framework is the Standard Cosmological Model, or ΛCDM model. This model has, too, its shortcomings, such as the horizon and flatness problems. In order to provide a solution to them, the theory of inflation has been formulated, and is presented here in Chapter 4, the end of which describes its interplay with axions. Moreover, after this period of exponential expansion, a subsequent phase in which the Universe increases its temperature has to exist: reheating. The common link between these two frameworks is the existence of Dark Matter, which accounts for the majority of the matter content in the Universe and nevertheless is not made of any particle present in the SM. The purpose of this thesis is to hypothesize axions as a candidate for Dark Matter and study them in the context of the reheating phase.

Chapter 5 contains the main work of the thesis, starting with an analysis of the reheating phase for a T-model potential. Assuming that the inflaton decays

through three different channels, fermionic and bosonic decays and bosonic annihilations, and considering the axion field to start oscillating in this phase, one can relate the different parameters in play, such as the reheating temperature T_{rh} and the axion mass m_a, finding constraints on the former that depend on the bounds imposed on the latter.

Later on, axions are assumed to be produced via different mechanisms: either the misalignment mechanism, that sees axions gaining their abundance from oscillations around the minimum of the potential, or gravitational production, which involves gravitationally mediated scatterings of particles in the SM or of the inflaton condensate, with axions being produced in the final state. Again, knowing the experimental bounds on the DM relic abundance, it is possible to constrain the parameters of both reheating and of the axion field.

Lastly, a small deviation from the standard inflaton-driven inflation is studied, by considering the case in which Primordial Black Holes drive inflation. In this situation, their initial mass M_{in} and a parameter β, determining how dominant the PBHs are with respect to the rest of the content of the Universe, come into play and will be related to the usual T_{rh} and m_a.

Contents

1

Open problems in fundamental physics

Our understanding of physics as of today can be summarized using two models, one for infinitesimally small distances, the Standard Model (SM), describing the interactions between particles, and one for the infinitesimally large, the ΛCDM model, describing our Universe. In this chapter we will briefly present them and mention the problems that emerge within them.

1.1 Introduction to the Standard Model of particle physics

The Standard Model [14], [27] contains the description of all the interactions of the elementary particles that make up matter. These particles are classified into three different kinds: leptons, quarks and mediators.
To the first group, leptons, belong electrons e, muons μ, tauons τ and their respective neutrinos ν_e, ν_μ and ν_τ. The first three particles are characterized by electric charge $Q = -1$, whereas neutrinos are electromegnetically neutral. Their classification is symbolized through the lepton number L_i (with $i = e, \mu, \tau$), which identifies the corresponding leptonic family or generation. In addition to these particles, there are the six corresponding anti-leptons, with opposite quantum numbers.
The second group is formed by quarks, again divided in three generations for

a total of six flavours that, similarly to leptons, get labelled by a corresponding quantum number: u and d, c and s, t and b. The first element of each couple has electric charge $Q = \frac{2}{3}$, the second has $Q = -\frac{1}{3}$. Again we can consider reversed signs for antiquarks.
Lastly, we have mediators, which mediate, as the name suggests, all interactions. They constitute the gauge bosons, as they emerge from the gauge symmetries of the theory. In particular we have photons γ for the electromagnetic interaction, two W bosons and a Z boson for the weak interaction, 8 gluons that get exchanged between two quarks for the strong interaction and the graviton for gravity (which will however not be considered from here on, as it is not part of the SM). All the particles mentioned above add up to a number of 60 (6 quarks $\times$ 3 colours $\times$ 2 for their antiparticle, 6 leptons $\times$ 2 for their antiparticle, 12 gauge bosons), to which the SM adds an electrically neutral particle, the Higgs boson.

The gauge symmetry group of the model is $SU(3)_C \times SU(2)_L \times U(1)_Y$. This contains the symmetry group of the electroweak theory, $SU(2)_L \times U(1)_Y$, which again contains both the electromagnetic and the weak theories, having γ, $W^{\pm}$ and Z as gauge bosons.

The electroweak interaction Lagrangian is given by

$$\mathcal{L}_{EW} = \mathcal{L}_{CC} + \mathcal{L}_{NC} + \mathcal{L}_{em}. \tag{1.1}$$

While the two groups $SU(2)_L \times U(1)_Y$ are not the same as the QED and weak interactions groups [17] , they have the same structure. In particular $SU(2)_L$ is a non-abelian group with 3 generators ($N^2 - 1$ with $N = 2$ here gives 3 generators) that can be written in terms of the Pauli matrices: $\tau^a = \frac{\sigma^a}{2}$ with $a = 1, 2, 3$. The field strength tensor is

$$W^a_{\mu\nu} = \partial_\mu W^a_\nu - \partial_\nu W^a_\mu + g\epsilon^{abc} W^b_\mu W^c_\nu. \tag{1.2}$$

At the same time, $U(1)_Y$ is an abelian unitary group, therefore its generator is simply *1* and it has only one gauge boson B_μ, with field strenght tensor expressed as

$$B_{\mu\nu} = \partial_\mu B_\nu - \partial_\nu B_\mu. \tag{1.3}$$

$SU(3)_C$ is the QCD gauge symmetry group which has $N^2 - 1 = 8$ generators that can be written in terms of the Gell-Mann matrices: $T^A = \frac{\lambda^A}{2}$, where $A =$

$1, ..., 8$. As it is a non abelian group, its field strength tensor is

$$G^A_{\mu\nu} = \partial_\mu G^A_\nu - \partial_\nu G^A_\mu + g_s f^{ABC} G^B_\mu G^C_\nu. \tag{1.4}$$

The SM total Lagrangian is [51], in conclusion, obtained from [41]:

$$\mathcal{L}_{SM} = \mathcal{L}_f + \mathcal{L}_G + \mathcal{L}_{Higgs} + \mathcal{L}_{Yukawa}, \tag{1.5}$$

where

$$\mathcal{L}_f = \sum_{f=l,q} \bar{f} i \not{D} f = \bar{Q}_{L,i} \not{D} Q_{L,i} + \bar{\ell}_{L,i} \not{D} \ell_{L,i} + \bar{u}_{R,i} \not{D} u_{R,i} + \bar{d}_{R,i} \not{D} d_{R,i} + \bar{e}_{R,i} \not{D} e_{R,i}, \tag{1.6}$$

is the kinetic Lagrangian for fermions, constructed by summing over all left-handed doublets l_L and q_L and right-handed singlets e_R, u_R and d_R across the three generations (indexed by $i = 1, 2, 3$). It contains a covariant derivative that can be written to contain the three group generators with each coupling:

$$D_\mu = \partial_\mu - i g_s G^A_\mu T^A - i g W^a_\mu T^a - i g' Y B_\mu. \tag{1.7}$$

The second term is

$$\mathcal{L}_G = -\frac{1}{4} F^a_{\mu\nu} F^{a,\mu\nu} = -\frac{1}{4} G^A_{\mu\nu} G^{A,\mu\nu} - \frac{1}{4} W^a_{\mu\nu} W^{a,\mu\nu} - \frac{1}{4} B_{\mu\nu} B^{\mu\nu}, \tag{1.8}$$

which contains the gauge fields, the QCD gluons G^A_μ of $SU(3)_C$, the weak W^a_μ of $SU(2)_L$ and the B_μ of $U(1)_Y$.

Then, the Higgs sector:

$$\mathcal{L}_{Higgs} = |D_\mu H|^2 - V(H) = (D_\mu H)^\dagger (D^\mu H) - \lambda (H^\dagger H)^2 - \mu^2 H^\dagger H, \tag{1.9}$$

where H is the complex Higgs doublet and $\mu^2 < 0$. It is the only part of the SM to contain a dimensionful parameter, and to consequently set the energy scale of the electroweak theory, as $v^2/2 = \langle H^\dagger H \rangle = -\mu^2/2\lambda = (176GeV)^2$. The presence of this mass squared parameter μ^2 makes the term sensitive to quadratically divergent contributions from the self-energy corrections. Assuming the Standard Model to be an effective field theory, valid up to a high cutoff scale Λ, loop corrections drive the Higgs mass quadratically towards that cutoff ($\delta m^2 \propto \Lambda^2$). To keep the Higgs mass at its observed, lower value, different mathematical terms have to cancel each other out with severe fine-tuning. This fine-tuning issue is known as the hierarchy problem, and it serves as one of the primary motivations for introducing new physics beyond the Standard Model, such as Supersymmetry or composite Higgs models.

Lastly, the Yukawa sector, also known as the flavour sector:

$$\mathcal{L}_{Yukawa} = y^{ij}\psi^i\psi^j H^{(c)} = y_u^{ij}\bar{Q}_{L,i}u_{R,j}\tilde{H} + y_d^{ij}\bar{Q}_{L,i}d_{R,j}H + y_l^{ij}\bar{\ell}_{L,i}e_{R,j}H + h.c. \tag{1.10}$$

An important consequence of this structure to be mentioned is the Higgs mechanism, which applies to the electroweak sector during the spontaneous symmetry breaking of the gauge theory $SU(2)_L \times U(1)_Y \to U(1)_{em}$ [49]. Initially the gauge bosons are massless due to local gauge invariance. However, when the scalar doublet H acquires a non-zero vacuum expectation value v, three of its four scalar degrees of freedom manifest as massless Nambu-Goldstone bosons (ϕ^+, ϕ^-, and χ). These unphysical states get "eaten" by the $W^\pm$ and Z gauge fields, giving them their physical masses, while the photon γ remains massless.

1.1.1 Issues within the SM

We have seen how the Standard Model is the best theory to describe the interaction of particles. It is also, together with General Relativity and statistical mechanics, the main theoretical framework to describe the history of the Early Universe so far. However, in recent years empirical evidence started showing inconsistencies with the theoretical predictions of the Standard Model, highlighting its incompleteness. In this section we will mention some of these issues with a brief explanation.

Strong CP problem

Let us start with the Strong CP problem [46]. In the QCD Lagrangian of the SM seen in eq. (1.5) there could actually be an additional term:

$$\mathcal{L}_\theta = \theta\frac{g_s^2}{32\pi^2}G^A_{\mu\nu}\tilde{G}^{A,\mu\nu}, \tag{1.11}$$

which is T and CP violating, hence giving rise to the strong CP problem. We will not go into detail, as this issue will be discussed deeply in Chapter 2.

NEUTRINO MASS

In the SM neutrinos are strictly massless [15]. Since the SM particle content does not include right-handed neutrino fields ν_R, it is impossible to write a Dirac mass term of the form:

$$\mathcal{L}_{Dirac} = -m_\nu \bar{\nu}_L \nu_R + h.c. \tag{1.12}$$

Furthermore, a Majorana mass term, $\mathcal{L}_{Majorana} = -\frac{1}{2} m_L \nu_L^T C \nu_L$, is excluded as well. Such a term, in fact, not only violates the conservation of the total lepton number L by two units ($\Delta L = 2$), but it also explicitly violates the local $SU(2)_L \times U(1)_Y$ electroweak gauge symmetry, as the combination behaves as an electroweak triplet rather than a gauge singlet.

However, it has been observed that neutrinos undergo an oscillation phenomenon providing them with a mass. Evidence for this [11] comes from solar neutrino experiments (SNO), atmospheric neutrino observations (Super-Kamiokande), and reactor antineutrino monitoring (KamLAND). This was one of the first confirmations of the incompleteness of the SM and therefore of the need to dive deeper into Physics beyond the Standard Model.

To explain this behaviour, we can start by considering that the SM contains flavour eigenstates $|\nu_\alpha\rangle$, where $\alpha = e, \mu, \tau$. These states can be expressed as a superposition of the mass eigenstates $|\nu_i\rangle$, where $i = 1, 2, 3$, through:

$$|\nu_\alpha\rangle = \sum_i U^*_{\alpha i} |\nu_i\rangle, \tag{1.13}$$

where U is the unitary mixing matrix, parametrized by three mixing angles ($\theta_{12}, \theta_{23}, \theta_{13}$) and one Dirac CP-violating phase (δ_{CP}). Neutrino oscillation probabilities depend on the differences of the squares of the masses, defined as:

$$\Delta m^2_{ij} \equiv m^2_i - m^2_j. \tag{1.14}$$

An easy way to give Majorana masses to neutrinos is to add a non-renormalizable 5-dimension operator to the SM Lagrangian, known as the Weinberg operator.

$$-\mathcal{L}^{d=5}_\nu = \frac{1}{\Lambda} (\ell H)(H \ell) + h.c., \tag{1.15}$$

where ℓ is the left-handed lepton doublet spinor, H is the Higgs scalar doublet and Λ is the effective mass scale [1].

After spontaneous electroweak symmetry breaking, the Higgs field acquires its vacuum expectation value $\langle H \rangle = v/\sqrt{2}$, making this operator a mass term for neutrinos, with mass:

$$m_\nu \sim \frac{v^2}{\Lambda}. \tag{1.16}$$

1.2 Introduction to the ΛCDM model

The cosmological standard model [9] [40], or ΛCDM model, contains the framework able to describe the Universe as we know it today and to represent our best understanding of observational data [27] through six free parameters [20]: baryonic and cold dark matter energy densities $\Omega_b h^2$ and $\Omega_c h^2$, current Hubble rate value H_0, reionization optical depth τ, amplitude of the power spectrum A_s and spectral index n_s, predicting the existence of cosmic microwave background (CMB), of baryon acoustic oscillations (BAO), large-scale structures in the distribution of galaxies, the abundance of light elements, and the accelerated expansion of the Universe (which is attributed to the cosmological constant Λ as we will see in Sec. 1.2.1).
This model relies on the validity of the Standard Model of particles and on the theory of general relativity, and it describes a Universe that originated from the Big Bang, to which followed a phase of accelerated expansion.

We will now present some of the key features contained in the standard cosmological model that will be useful later on.
Firstly [62], the cosmological principle states that the Universe can be considered as spatially homogeneous and isotropic, at least on large scales [52]. The best evidence for it is the CMB that gives us temperature anisotropies of the order of $\leq 10^{-5}$. The metric used to describe this is the so called FLRW metric:

$$ds^2 = dt^2 - a(t)^2 \left[\frac{dr^2}{1 - kr^2} + r^2 d\theta^2 + r^2 \sin^2 \theta d\phi^2 \right], \tag{1.17}$$

where (t, r, θ, ϕ) are the comoving coordinates and $a(t)$ is the scale factor which measures the Universe expansion rate, telling how physical separations between objects grow with time as the Universe expands.

The parameter k represents the curvature of the Universe and it can be taken to be $-1, 0, +1$ depending on the geometry of the Universe. Lately, observations like the CMB have been indicating a strong compatibility with a flat geometry (even if it is impossible to prove it precisely), which would correspond to $k = 0$.

The dynamics of the expanding Universe become explicit when we solve Einstein's equations [25]:

$$R_{\mu\nu} - \frac{1}{2}g_{\mu\nu}R = 8\pi G T_{\mu\nu}. \tag{1.18}$$

Some useful equations needed in order to talk about our expanding Universe are the Friedmann equation

$$H^2 = \left(\frac{\dot{a}}{a}\right)^2 = \frac{8\pi G}{3}\rho - \frac{k}{a^2}, \tag{1.19}$$

and the fluid equation

$$\dot{\rho} + 3\frac{\dot{a}}{a}\left(\rho + p\right) = 0, \tag{1.20}$$

where we assume $c = 1$. Pressure and energy density are related by the so-called equation of state

$$p \equiv p(\rho) = \omega\rho. \tag{1.21}$$

Lastly, following from (1.19) and (1.20), the acceleration equation:

$$\frac{\ddot{a}}{a} = -\frac{4\pi G}{3}(\rho + 3p) = -\frac{4\pi G}{3}\rho(1 + 3\omega). \tag{1.22}$$

The contents of the Universe are radiation, relativistic particles (neutrinos), baryons, dark matter and the cosmological constant. The latter two give the name to the cosmological model, where CDM stands for cold dark matter (that together with baryons takes up approximately 32% of the total energy density), and Λ for the cosmological constant (taking up the remaining 68%); these, together with ordinary matter and their interactions through gravity are the basis of the model.

Analyzing the equation of state one can see how the Universe undergoes different phases of expansion, determined by the dominating species in that period of time. For $\omega = \frac{1}{3}$ the energy density of the Universe varies as $\rho \propto a^{-4}$; in this situation radiation dominates over the the other contents. For $\omega = 0$ we have the pressureless case, which corresponds to the matter dominated epoch, where $\rho \propto a^{-3}$. Lastly the cosmological constant comes to dominate whenever $\omega = -1$, for which the energy density stays constant.

1.2.1 Issues within the ΛCDM model

The formulation of the ΛCDM model is supported by the observation of CMB [10], under the assumption of a homogeneous and isotropic Universe. Specifically, experimental data allow us to consider the Universe as spatially flat, with the majority of its energy density due to dark energy and dark matter and just a fraction of it to ordinary matter; additionally they tell us about the structure formation, consequence of gravitational instability of quantum fluctuations in the Early Universe. However some of the features of this model, such as dark matter, dark energy and cosmic inflation are not yet understood at a fundamental level.

Similarly to the SM in particle physics, standard cosmology relies on a model with questions for which the answer has yet to be provided [23]. In this section these puzzles will be briefly presented along with the most plausible candidate to explain them: inflation.

Baryogenesis (baryon asymmetry)

While dark matter and dark energy, as we will see later on, make up approximately 95% of the energy density of the Universe, the remaining 5% is due to baryons [8]. The Standard Model explains how baryon and lepton numbers are conserved. However extensions of the SM such as the grand unified theories predict interactions that violate these two quantum numbers. This typically leads to the instability of the proton (nevertheless, the lifetime of the proton is quite long, approximately $10^{31} - 10^{32}$yr). These B-violating interactions were the first natural motivations to try to understand a process that could bring an initially baryon-symmetric Universe towards the observed asymmetry. Later on this was formalized by Sakharov [53]. The CPT theorem states, in fact, that for each particle X there exists its counter anti-particle $\bar{X}$ with same mass but opposite charge. This would naively lead to $n_X = n_{\bar{X}}$; however, observations contradict with this equality; it is almost impossible to find traces of antimatter on Earth if we don't consider CERN or Fermilab. For instance, experiments indicate a ratio of 10^{-4} between protons and antiprotons in cosmic rays, making cosmic rays an evidence for galactic asymmetry between baryons and antibaryons. On a cosmological scale, we could assume that this asymmetry only applies locally, and that perhaps at larger scales we could have clusters of galaxies made only of antimatter. As of today, though, the observable Universe is considered to possess a maximal baryon asymmetry, meaning that there are no free anti-baryons.

Data coming from the Big Bang Nucleosynthesis and from the CMB confirm a discrepancy of the number of baryons with respect to antibaryons in the Universe which is quantified by:

$$\eta_B \equiv \frac{n_B - n_{\bar{B}}}{n_\gamma} \approx 10^{-10}. \tag{1.23}$$

In standard cosmology there is no explanation as to how a Universe which was initially symmetric $n_b = n_{\bar{b}}$, today appears to have a big matter-antimatter asymmetry $n_b \gg n_{\bar{b}}$. The hypothesis is that the baryon asymmetry was generated in the early Universe. We could think that from the beginning more baryons with respect to antibaryons were created; in that case, however, a precise fine-tuning would be required in order to generate such a small value. Moreover, as we will see later on, inflation is a highly likely theory, and its happening would have washed away the difference, while in the subsequent reheating phase particles and antiparticles would have been created in equal abundance. So there needs to be a dynamical model generating this asymmetry. A model of baryogenesis needs to satisfy three conditions in order to explain this statement; they are called the Sakharov conditions:

- B violation: this is an obvious one; if you want a baryon asymmetry the baryon number has to be violated, otherwise you would get $n_b = n_{\bar{b}}$.

- C and CP violation: if they were conserved the probability of processes creating or destroying a particle would be the same as the ones of the corresponding antiparticle, hence generating no asymmetry.

- Non-equilibrium conditions: departure from chemical equilibrium is needed, otherwise same chemical potentials $\mu_b = \mu_{\bar{b}}$ would imply same distribution functions for baryons and antibaryons $f_b = f_{\bar{b}}$ and, consequently, same number density $n_b = n_{\bar{b}}$.

Even though these three conditions are already present in the SM (having the baryon number B symmetry broken by anomalies, seeing the CP violation in the electroweak sector through the CKM matrix and undergoing therml decouplings in the electroweak phase transition) [36], the SM fails to explain the observed value of η_B quantitatively. Consequently, the observed baryon asymmetry stands as evidence for physics beyond the Standard Model and, at the same time, as an attempt to the understanding of the dynamics of the Early Universe.

Large-scale smoothness: the problem of initial conditions

The metric employed to describe our Universe, which is expanding and with a certain curvature k, is the FLRW metric (1.17). This metric describes a space which is symmetric under rotation and spatial translation (meaning isotropic and homogeneous), but why is that so? What gives us compatibility with isotropy in the Universe is the CMB [5]. As we have said, the CMB allows us to measure fluctuations in temperature that might have been generated by fluctuations in the density of the primordial Universe, which then grew into the large-scale structure observable today, allowing us to consider the Universe as homogeneous. This constitutes the so called problem of initial conditions, and the explanation to the process responsible for the understanding of all structures formed in the Universe will be presented later on. The problem of initial conditions, also known as the Cauchy problem of the Universe, is formulated to highlight how the Big Bang requires a set of fine-tuned initial conditions to evolve to its current state. As we will see in Sec. 4.3, inflation is required to grow out of generic initial conditions. The fine tuning becomes necessary because we know that inhomogeneities are gravitationally unstable, therefore they grow with time; the CMB tells us that they were even smaller than today in the past, bringing them to an unnatural small value. As we will see with the flatness problem in 1.2.1, this unnaturality is explained if we hypothesise a phase of accelerated expansion: inflation.

The horizon problem

To fully understand the Horizon problem [27] we need to introduce a quantity called Hubble radius and specifically its comoving counterpart:

$$r_H(t) = \frac{R_C(t)}{a(t)} = \frac{1}{H(t)}\frac{1}{a(t)} = \frac{1}{\dot{a}(t)}, \tag{1.24}$$

where $a(t)$ is the scale factor, indicating how physical separations in the Universe grow with time, whereas $H(t)$ is the Hubble rate, indicating how fast these distances are changing as the Universe expands. Having defined it as above, the comoving Hubble radius' first derivative is the following:

$$\dot{r}_H = -\frac{\ddot{a}(t)}{\dot{a}(t)^2}, \tag{1.25}$$

which is always positive in the known eras of radiation and matter, given that the acceleration of the scale factor is determined by

$$\frac{\ddot{a}}{a} = -\frac{4}{3}\pi G(\rho + 3p). \tag{1.26}$$

This means that, considering the equation of state

$$p = \omega\rho, \tag{1.27}$$

we get the following condition:

$$\ddot{a} < 0 \leftrightarrow \omega > -\frac{1}{3}. \tag{1.28}$$

The fact that for radiation and matter epochs (respectively $\omega = 1/3$ and $\omega = 0$) we get a growing comoving Hubble radius means that sooner or later all scales λ will enter the horizon, allowing a growing causal connection region. The horizon problem emerges from an observational point of view: we observe regions that should not have been in causal contact before (because they are at a distance bigger than what light could have travelled given its finite velocity) sharing statistical properties, such as same values of temperatures up to fluctuations of the order of 10^{-5}. This could be explained if we considered a period of time, preceding the known ones, in which the comoving Hubble radius was decreasing, so that the scale λ enters the horizon at a certain time during radiation or matter, but just after having exited it during this new phase. This way the causal connection could be explained, considering that scales λ were already inside of the horizon in the past, which implies that even distant regions could share the same statistical properties. This new epoch is called inflation and its requirement is a decreasing Hubble radius, which implies a positive acceleration and an equation of state with $\omega < -\frac{1}{3}$, meaning a negative pressure. A good candidate would be Λ but its expansion is exponential, whereas we need inflation to end at a certain point to allow r_H to grow and scales to re-enter the horizon. Moreover, an additional requirement is that inflation needs to last long enough for all scales, even the largest probable today, to be able to have been inside of the horizon during the inflationary epoch. In order to be able to quantify this we introduce the number of e-folds:

$$N = \int_{t_i}^{t_f} H(t)dt = \ln\left(\frac{a_f}{a_i}\right). \tag{1.29}$$

Being N dependent on the scale factors at the beginning and at the end of inflation (corresponding respectively to the times t_i and t_f), we need N to be big enough to represent the correct enlarging of the Universe during the accelerated expansion. The condition imposed on the minimal number of e-folds derives from requiring that the biggest scale we can probe today was inside of the horizon when inflation took place. This means:

$$r_H(t_0) \leq r_H(t_i). \tag{1.30}$$

Substituting the definition of the comoving Hubble radius (1.24) and evaluating for the known H_0 and $H_i \simeq H_f \simeq T_f^4/M_P^2$ values, this translates into the condition: $N \in [56; 67]$, meaning that the Universe underwent an expansion of $\approx 10^{26}$ during inflation.

The flatness problem

The flatness problem is an issue arising in the Big Bang model related to the curvature k of the Universe. From Friedmann's equation, in fact, introducing the density parameter $\Omega(t) = \frac{\rho(t)}{\rho_c(t)}$, where the critical energy density is the one for a flat Universe, defined as $\rho_c(t) = 3H(t)^2 M_P^2$ we get:

$$H^2 = \frac{\rho}{3M_P^2} - \frac{k}{a^2} \longrightarrow \Omega(t) - 1 = \frac{k}{a^2H^2} = kr_H(t)^2 = \Omega_k(t). \tag{1.31}$$

We know that the comoving Hubble radius grows with time during the known epochs of radiation and matter, meaning that, if $k \neq 0$ the discrepancy of $\Omega(t)$ from 1 grows with time. As of today, we know that $|\Omega(t_0) - 1| < 10^{-3}$ which is a very small discrepancy. Again we encounter the problem previously mentioned: the fine tuning problem. As the discrepancy grows, and given that it is so small today, how small must it have been in the past? Seeing that the quantity $[\Omega^{-1}(t)-$

$1]\rho a^2 = \text{const}$ we can write the following equality:

$$[\Omega^{-1}(t) - 1]\rho(t)a(t)^2 = [\Omega_0^{-1} - 1]\rho_0 a_0^2. \tag{1.32}$$

Making the simplification of a Universe still dominated by matter today and considering t a generic time belonging to the radiation epoch, so that $\rho(t) = \rho_{eq}\left(\frac{a_{eq}}{a(t)}\right)^4$, we get the following relation:

$$[\Omega^{-1}(t) - 1] = [\Omega_0^{-1} - 1]\frac{a^2}{a_0 \cdot a_{eq}}. \tag{1.33}$$

Considering that $T \propto a(t)^{-1}$ we can easily find the discrepancy of $\Omega(t)$ with respect to 1 at any time, simply substituting the corresponding temperature. For instance at a time $t = t_P$ we get approximately 10^{-60}, and at $t = t_{BBN}$ approximately 10^{-19}, which are values too small to be obtained naturally and without imposing too precise initial conditions. The inflationary theory intervenes by adding a phase previous to radiation, at the beginning of which the discrepancy was way bigger than it is nowadays; as a consequence of the exponential expansion it was then pushed extremely close to 1, so close that today it still deviates by a small amount. This represents an explanation to the large scale smoothness mentioned in 1.2.1. A key feature for inflation is then its duration, as seen for the horizon problem. To solve the flatness problem inflation needs to have lasted long enough to be able to push $\Omega(t)$ very close to unity. In particular the condition (1.30) is still valid and the minimum number of e-folds is consistent with what was found in Sec. 1.2.1.

The entropy problem

The flatness problem is strictly connected to the entropy problem [52]. Looking at the Friedmann equation in a radiation dominated epoch:

$$H^2 \simeq \frac{\rho_R}{M_P^2} \simeq \frac{T^4}{M_P^2}. \tag{1.34}$$

This allows us to rewrite Eq. (1.31) as

$$\Omega(t) - 1 = \frac{k}{a^2H^2} \simeq \frac{kM_P^2}{a^2T^4} = \frac{kM_P^2}{S_U^{\frac{2}{3}}T^2}, \tag{1.35}$$

which comes from the entropy relation $S = sa^3 \propto a^3T^3$. We know that the discrepancy is very small, and we can compute it considering that the entropy inside a sphere with Hubble radius of the Universe at present day is of the order of 10^{90}. This comes from

$$S_U = \frac{4\pi}{3}H_0^{-3}s = \frac{4\pi}{3}H_0^{-3}\frac{2\pi^2}{45}g_*(T_0)T_0^3 \simeq 10^{90}. \tag{1.36}$$

Specifically, as mentioned before for the flatness problem, at a time $t = t_{Pl}$ the discrepancy would be of the order of 10^{-60}. So the flatness problem arises because the entropy in a comoving volume is conserved; if the expansion was non-adiabatic for some time during the early phase of the Universe, the problem could be solved. This means that the Universe has to go through a non-adiabatic period, which would generate the large entropy S_U observed today, in order to be able to solve the entropy and the flatness problem. During the accelerated expansion generated by inflation the Universe expands adiabatically, meaning that the non-adiabatic phase will take place during the phase transition between inflation and radiation. We postulate that the entropy changes by a quantity

$$S_f = Z^3 S_i \tag{1.37}$$

during inflation; since after inflation the Universe expands adiabatically, it is reasonable to state $S_f = S_U$, which implies $Z \sim 10^{30}$. Moreover, considering $S \sim (aT)^3$ we are able to infer

$$\left(\frac{a_f}{a_i}\right) \approx 10^{30}\left(\frac{T_i}{T_f}\right), \tag{1.38}$$

resulting in a number of e-folds N in accordance to the values indicated before.

Unwanted relics

Standard cosmology does not have a way to get rid of relics that were overproduced in the early stages of the Universe, that is to say superheavy particles, emerging from the spontaneous symmetry breaking in unified gauge theories, that survive annihilation and contribute too much to the energy density, meaning with $\Omega_X \gg 1$, contradicting present observations. Inflation would provide an accelerated expansion with $a(t) \propto e^{Ht}$ which would wash away the number density of these relics $n_X \propto a^{-3}$.

Dark energy

Within the ΛCDM model, dark energy is represented by the cosmological constant Λ [63]. This term was initially introduced by Einstein in his general relativity equations in order to allow for a static Universe configuration. He operated under the assumption that velocities of stars were negligible with respect to that of light. As no solution to the original equations could correspond to such a Universe he modified them by adding the cosmological constant:

$$R_{\mu\nu} - \frac{1}{2} g_{\mu\nu} R = 8\pi G T_{\mu\nu} - \Lambda g_{\mu\nu}. \tag{1.39}$$

This implies a modification in Friedmann's equation as

$$H^2 = \frac{8\pi G}{3}\rho - \frac{k}{a^2} + \frac{\Lambda}{3}, \tag{1.40}$$

such that the introduction of Λ, together with the curvature and the energy density, could enforce $H(t) = 0$, yielding a static Universe. Additionally, the acceleration equation gets modified as

$$\frac{\ddot{a}}{a} = -\frac{4\pi G}{3}\left(\rho + 3p\right) + \frac{\Lambda}{3}. \tag{1.41}$$

This demonstrates that a positive cosmological constant gives a positive contribution to the acceleration of the scale factor and acts as a repulsive force. Later on, the hypothesis of a static Universe was invalidated, making the term Λ temporarily unnecessary. Rewriting Eq. (1.40) with the knowledge that $H = \frac{\dot{a}}{a}$, one can easily see that the equation determining the motion of the scale factor is the following:

$$(\dot{a})^2 = (Ha)^2 = -k + \frac{1}{3}a^2(8\pi G\rho + \Lambda), \tag{1.42}$$

where even in the flat case, where $k = 0$, we can get expanding solutions for $\Lambda = 0$, provided that $\rho > 0$.

Nevertheless, the Λ term remains a fundamental feature of modern field theory and is still kept in the equations, as it is linked to the quantum vacuum. In the presence of gravity, the quantum fluctuations in the vacuum contribute to the expectation value of the energy-momentum tensor in the vacuum state. Because the vacuum must appear isotropic, homogeneous, and invariant under

Lorentz transformations to all observers, its vacuum expectation value must be proportional to the metric tensor:

$$\langle 0|T_{\mu\nu}|0\rangle = \langle T_{\mu\nu}\rangle = -\langle\rho\rangle g_{\mu\nu}. \tag{1.43}$$

Comparing this to the perfect fluid energy-momentum tensor, $T_{\mu\nu} = (\rho + p)u_\mu u_\nu + p g_{\mu\nu}$, forces the vacuum to obey an equation of state parameter $w \equiv p/\rho = -1$. This implies a constant energy density $\rho_\Lambda = \text{const}$, a negative pressure $p = -\rho$, a constant Hubble parameter and a resulting exponential de Sitter expansion of the scale factor $a(t) \propto e^{Ht}$.

While these properties mirror the dynamics of inflation, as will be explained in chapter 4, the inflationary theory does not solve the mystery of the cosmological constant.

The evidence for late-time cosmic acceleration [57] came at first from the redshift of far away type Ia supernovae and recently from the phenomenon of baryon acoustic oscillations. The Λ model described above well fits BAO and CMB data. Looking at BAO and CMB data one can understand how the rate of expansion of the Universe varies with time. In particular, baryonic and cold dark matter turn out to be insufficient to explain the Universe's late time acceleration [26]. From this emerged the need for an additional energy component driving the accelerated expansion, which could be represented by the vacuum energy seen before and consequently by Λ, which acts like a repulsive gravitational effect. We therefore maintain the term Λ to represent the vacuum energy density, which covers the dominant contribution to the total energy density: $\rho_\Lambda = 0.685\rho_c$.

Alternative models for DE [21] include quintessence, phantom energy and quintom DE.

1.3 Dark matter

Up until now we have presented the two frameworks necessary to understand particle physics and standard cosmology, along with their limitations. Among them, Dark Matter stands out as a hint to the need of new physics, and will therefore be a central theme in this dissertation.

Dark matter emerges as an issue for modern Physics, as it represents a set of particles that are not contained in the SM of particles but that have been shown to exist in our Universe making up approximately 27% of its energy density [13].

Historically, the first evidence of Dark Matter came from the measurement of the dispersion velocity of galaxies within the Coma Cluster, leading to the conclusion that the observed galaxies were moving too fast to remain gravitationally bound by the visible baryonic mass alone (which, by the way, takes up approximately 5% of the total energy density) but that there needed to be some missing mass. Later on, this anomaly was confirmed by flat rotation curves of disk galaxies and via gravitational lensing observations.

At the moment, the known properties of DM can be summarized in a couple of facts. Firstly, it has attractive gravitational interactions and it it stable, or at least with a very long lifetime, significantly longer than the age of the Universe. Moreover, it is electromagnetically neutral, it is not observed to be interacting with light and it can be assumed to be almost collisionless but self-interacting. It can be classified as either hot, warm or cold:

- hot DM: represents the case in which the DM particle decoupled from the thermal bath while relativistic and was still relativistic at equality;
- warm DM: when the particle decoupled while relativistic and became non-relativistic before equality;
- cold DM: if it decoupled while non-relativistic.

Among these, the favoured model is CDM, because HDM prevents small-scale structures from growing due to the process of free-streaming.

CMB data give us the following results: $\Omega_{DM}h^2 = 0.1187 \pm 0.0017$, $\Omega_b h^2 = 0.02214 \pm 0.00024$, where $h \equiv H_0/(100 \text{ km/s/Mpc}) \approx 0.674$ represents the dimensionless reduced Hubble parameter, representing the present expansion rate of the Universe. The big discrepancy between the DM and the baryon abundance confirms that most of the matter present in the Universe is non-baryonic and made of something unknown. This bound allows the exclusion of several historical candidates. Firstly, neutrinos, that possess a relic abundance which is mass-dependent $\Omega_\nu h^2 = \frac{\sum_i m_{\nu_i}}{94\text{eV}}$, were initially considered as candidates for DM. However, experiments placed an upper bound on their masses of $\sum m_\nu < 0.12$ eV [16], limiting their total contribution to $\Omega_\nu h^2 < 0.0013$, which is not enough compared to the value mentioned before for DM. Furthermore, neutrinos are ultra-light relativistic relics, therefore acting as hot dark matter, which does not fit the model of CDM wanted. Moreover, also astronomical objects known as

MACHOs ("Massive Astrophysical Compact Halo Objects") can be ruled out using gravitational microlensing effects. Apart from the few properties mentioned above and the few candidates ruled out, the actual nature of DM is yet to be established. Many experiments are underway to detect DM and many new candidates have been proposed, such as new generations of neutrinos, WIMPS (weakly interacting massive particles) and axions, on which we will focus in chapter 3.

For the sake of completeness, we mention what WIMPs are. WIMPs are one of the main current paradigms for explaining Dark Matter in the Universe. A WIMP is a heavy elementary particle χ, whose evolution number density n_χ in an expanding background is determined by the Boltzmann equation:

$$\frac{dn_\chi}{dt} + 3Hn_\chi = -\langle\sigma v\rangle \left(n_\chi^2 - n_{eq}^2\right), \tag{1.44}$$

where $H(t)$ is the Hubble rate, and $\langle\sigma v\rangle$ represents the thermally averaged annihilation cross-section of the DM particle. When $T \gg m_\chi$, the particle is relativistic and in thermal equilibrium with the thermal bath. As $T < m_\chi$, the value of $n_{eq} \propto e^{-m_\chi/T}$ undergoes an exponential Maxwell-Boltzmann suppression; the DM particles do not interact with the bath anymore, but only annihilate. Being decoupled from the bath, their density decreases, but not as steeply as $e^{-m_\chi/T}$. After a while, H comes to dominate over the annihilation rate $\langle\sigma v\rangle n_\chi$ and we recover the decoupling limit and $n \propto T^3$. This process is known as freeze-out. Solving the Boltzmann equation and analyzing the relic abundance of this particle species, one finds that the latter is not dependent on the mass of the particle, but only on the cross-section of the processes it is involved in. This is often called "WIMP miracle".

In conclusion, in the discussion above some of the issues encountered when describing particles in the Universe using the SM and ΛCDM model were presented. In order to solve them, many examples of physics beyond the Standard Model have been proposed. In this thesis, the focus will be only on a couple of them. Firstly the issue of Dark Matter, which is made of an unknown kind of elementary particle. Many DM candidates arise from physics beyond the Standard Model. Chapter 2 will focus on the strong CP problem; in relation to it in Chapter 3 we will investigate one of its possible solutions, the axion, whose interplay with inflation will be analyzed in Chapter 4.

2

Strong CP problem

As mentioned in chapter 1, one of the biggest inconsistencies of the Standard Model is the strong CP problem. In this chapter we outline its theoretical context and introduce one of the possible resolutions to it: the axion.

2.1 Brief introduction to QCD

Let us start with a concise description of the theory. Quantum chromodynamics, or QCD, is the theory describing interactions between quarks. Specifically, it is a non-abelian gauge theory with $N_C = 3$ colours and N_f flavours, the number of which depends on the energy scale being probed ($N_f = 6$ above the top mass, $N_f = 5$ below the top mass, $N_f = 4$ below the bottom mass and $N_f = 3$ below the charm). In this study we restrict our attention to $N_f = 2$, that corresponds to the up u and down d quarks. In this limit, the light quark masses are negligible compared to the typical QCD scale Λ_{QCD}.

The theory is described by the following Lagrangian:

$$\mathcal{L}_{QCD} = -\frac{1}{4}G^A_{\mu\nu}G^{A\mu\nu} + \bar{q}_{Li}i\gamma^\mu D_\mu q_{Li} + \bar{q}_{Rj}i\gamma^\mu D_\mu q_{Rj} - [\bar{q}_{Li}M_{ij}q_{Rj} + h.c.], \quad (2.1)$$

where M_{ij} is the quark mass matrix. If we assumed it to be zero, we could rotate independently left and right handed quark fields:

$$q_{L,Ri} \rightarrow U_{L,Rij}q_{L,Rj}. \quad (2.2)$$

The symmetry group under the condition $M = 0$ would then be $U(N_f)_L \times U(N_f)_R$, which acts independently on the left and right fields and is therefore called "chiral". Using the fact that $U(N) = SU(N) \times U(1)$, we can equivalently write it as:

$$SU(2)_L \times SU(2)_R \times U(1)_B \times U(1)_A. \tag{2.3}$$

Crucially, however, the axial transformation $U(1)_A$ is not a real symmetry at the quantum level due to an anomaly [59]. Consequently, the true classical global symmetry group of massless QCD is simply:

$$SU(2)_L \times SU(2)_R \times U(1)_B. \tag{2.4}$$

On the other hand, when $M \neq 0$, the only symmetry that survives is the vectorial one

$$U(1)_{V_1} \times ... \times U(1)_{V_{N_f}}, \tag{2.5}$$

which is the same for left and right and is therefore not chiral.

QCD is an asymptotically free theory, meaning that its coupling vanishes in the limit of high energies. In the IR, instead, the coupling grows, the phenomenon of confinement is reached and a quark condensate is formed. The latter is the vacuum expectation value of the composite operator $\Phi_{ij} = \bar{q}_{Li} q_{Rj}$, parameterized via the quark bilinear expression $\langle \bar{q}_{Li} q_{Rj} \rangle = -\sigma \delta_{ij}$, where σ is a constant. The condensate mixes left and right handed fields, hence it transforms as $\Phi \to L \Phi R^\dagger$ and chiral symmetry breaking is achieved:

$$SU(2)_L \times SU(2)_R \times U(1)_V \to SU(2)_V \times U(1)_V. \tag{2.6}$$

Passing from $3 + 3 + 1$ generators to $3 + 1$ tells us that after the SSB process 3 NGBs, the pions, emerge; in addition to the $SU(2)_A$ also the $U(1)_A$ symmetry is broken, leading to the η Goldstone boson. These fields can be rearranged into a 2×2 matrix Π. In reality, the quark masses are not actually exactly vanishing, therefore these 4 bosons will be only pseudo-Nambu-Goldstone bosons with a mass that will be proportional to m_u, m_d.

2.2 The $U(1)_A$ problem

Having established the framework of the QCD theory, we can now introduce the strong CP problem starting from the first clue that something was missing from the Lagrangian seen in Eq. (2.1): the $U(1)_A$ problem.
It was mentioned that $U(1)_A$ is not a real but an apparent symmetry of the QCD Lagrangian in the limit of vanishing quark masses. We can work under this assumption considering that $m_u, m_d \ll \Lambda_{QCD}$, which implies that taking a limit for $m_f \longrightarrow 0$ is reasonable. Under this assumption, one would expect strong interactions to have a large global symmetry and hence be $U(2)_V \times U(2)_A$ (where $U(2)_V = SU(2)_V \times U(1)_B$) invariant.

These unitary transformations, vectorial and axial, act respectively as:

$$q_f \longrightarrow e^{i\alpha_a \frac{T_a}{2}} q_f, \tag{2.7}$$

$$q_f \longrightarrow e^{i\gamma_5 \alpha_a \frac{T_a}{2}} q_f. \tag{2.8}$$

However, as it turns out, there is no $U(1)_A$ symmetry for strong interactions. Experimentally, in fact, it is observed that $U(2)_V$ is a good approximate symmetry of nature, whereas the axial symmetry breaks down spontaneously as seen from the existence of quark condensates $\langle \bar{u}u \rangle = \langle \bar{d}d \rangle \neq 0$. (The formation of these condensates mixes left and right fields: $\langle \bar{q}q \rangle = \langle \bar{q}_L q_R + \bar{q}_R q_L \rangle$. Under vector rotations $SU(2)_V$ the condensate is invariant, but under $SU(2)_A$ it changes, meaning that the condensate is not invariant under axial transformations, implying that $SU(2)_A$ is spontaneously broken). Because of the breaking of this symmetry operated by the quark condensate, one expects the emergence of Nambu-Goldstone bosons: η and the π mesons. When including the masses of the u and d quarks, these bosons should get similar masses; for instance the singlet meson is made of

$$\eta \approx \frac{1}{\sqrt{2}}(u\bar{u} + d\bar{d}), \tag{2.9}$$

which is made of the same quarks as the neutral pion:

$$\pi^0 \approx \frac{1}{\sqrt{2}}(u\bar{u} - d\bar{d}). \tag{2.10}$$

This would imply the two masses to be close in value: $m_\eta \approx m_\pi$. However, experimentally one finds $m_\eta^2 \gg m_\pi^2$, showing that $U(1)_A$ cannot be a real symmetry of QCD. The formal explanation following these observations comes from the fact that its associated current, in this limit, has a non-vanishing divergence due to the chiral anomaly.

2.2.1 Historical reasons behind the $U(1)_A$ problem

First of all let us mention some of the inconsistencies appearing in the QCD Lagrangian.

The $\pi^0 \to \gamma\gamma$ decay

Experimentally the neutral pion is observed to decay into two photons, however there is no term in $\mathcal{L}_{QCD}$ that accounts for this process. One can show that in a theory with an unbroken $SU(2)_L \times SU(2)_R$ chiral symmetry, the decay $\pi^0 \to \gamma\gamma$ should be forbidden. This is an indicator that something is missing in the Lagrangian. A term describing this decay should include $F_{\mu\nu}$ to account for the photons in the interaction, moreover the $F_{\mu\nu}$ combination should be odd under parity, since π_0 is P-odd as well.

Missing light meson

The quark condensate has been said to break the $U(1)_A$ if that was a symmetry. Our theory has a $SU(2)_L \times SU(2)_R \times U(1)_B$ symmetry, with $3 + 3 + 1$ generators. After the $SU(2)_L \times SU(2)_R \to SU(2)_V$ symmetry breaking we end up with $3 + 1$, hence we have 3 NGBs. If $U(1)_A$ was a symmetry of our theory it would be broken by the quark condensate, hence we should get an additional Goldstone boson, for a total of 4. This additional NGB should be as light as pions; the fact that we do not observe it in nature is an further hint at the problem related to the $U(1)_A$ symmetry.

The sign of M

Under an axial rotation in Eq. (2.1) we have that LH and RH fields rotate with an opposite phase due to the structure of γ_5, so the mass term that we include in the Lagrangian for $M_{ij} \neq 0$ transforms under the $U(1)_A$ symmetry with a total phase of $M \to e^{-2i\alpha} M$; this tells us that if $U(1)_A$ was an actual symmetry of QCD the sign of M would have no physical consequences.

THE $\Pi(x) \to -\Pi(x)$ SYMMETRY

In the chiral Lagrangian, when neglecting the mass term, an accidental symmetry acting as $\Pi(x) \to -\Pi(x)$, where Π is the matrix containing pions and the η mentioned before, is found. This would imply that only an even number of pions can interact, contrasting with the observed process $K^+K^- \to \pi^+\pi^0\pi^-$. Once again, this indicates that something is missing in the theory previously described.

2.2.2 SOLUTIONS TO THE $U(1)_A$ PROBLEM

Let us sketch what a chiral anomaly is [46] [64] in order to fully understand the issue and its solution, which will rely on the structure of the QCD vacuum. Consider a model of a theory with a single fermion field ψ and a global symmetry $U(1)_V \times U(1)_A$. At the classical level this has two conserved currents: a vectorial one

$$J^\mu_V = \bar{\psi}\gamma^\mu\psi, \tag{2.11}$$

which satisfies $\partial_\mu J^\mu_V = 0$, and an axial one

$$J^\mu_A = \bar{\psi}\gamma^\mu\gamma_5\psi, \tag{2.12}$$

where $\partial_\mu J^\mu_A = 2im\bar{\psi}\gamma_5\psi \xrightarrow{m\to 0} 0$. The conservation of the axial current emerges therefore exclusively in the massless fermion limit. At the quantum level instead, you cannot preserve both currents simultaneously, hence the chiral anomaly. The divergence of the axial current is non-vanishing, in accordance to the massive case, even in the massless limit. For a non-Abelian theory it can be expressed by

$$\partial_\mu J^\mu_A = \frac{\alpha_g^2}{4\pi} F_a^{\alpha\beta}\tilde{F}_{a,\alpha\beta}, \tag{2.13}$$

which is called Adler-Bell-Jackiw anomaly. The notation involving the dual field strength tensor here is

$$F^{\mu\nu}\tilde{F}_{\mu\nu} = \frac{1}{2}\epsilon_{\mu\nu\alpha\beta}F^{\alpha\beta}F^{\mu\nu}. \tag{2.14}$$

A derivation of this quantum breaking was formulated by Fujikawa, who showed that in the path integral formulation, after a chiral rotation the measure transforms depending on a Jacobian, which is related to the anomaly.

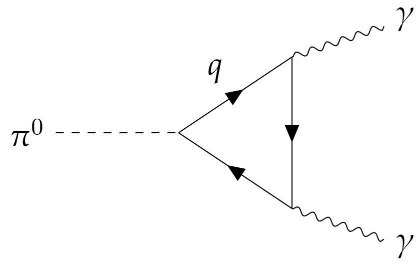

In the context of QCD, as mentioned, the theory with N_f flavors has $SU(N_f)_V\times SU(N_f)_A\times U(1)_V\times U(1)_A$ as a global symmetry. The chiral anomaly is contained in the $U(1)_A$ current, which for $N_f = 2$ looks like:

$$J_5^\mu = \frac{1}{2}[\bar{u}\gamma^\mu\gamma_5 u + \bar{d}\gamma^\mu\gamma_5 d]. \tag{2.15}$$

Evaluating its quantum divergence gives

$$\partial_\mu J_5^\mu = \frac{g_s^2}{32\pi^2} N_f G_a^{\alpha\beta}\tilde{G}_{a,\alpha\beta} = N_f Q, \tag{2.16}$$

which is explicitly non-vanishing and hence confirming the anomaly in accordance to Eq. (2.13). Under a global $U(1)_A$ transformation

$$q_f \to e^{i\frac{\alpha}{2}\gamma_5} q_f, \tag{2.17}$$

this chiral anomaly affects the action as

$$\delta W = \alpha \int d^4x \partial_\mu J_5^\mu = \alpha N_f \frac{g_s^2}{32\pi^2} \int d^4x G_a^{\alpha\beta}\tilde{G}_{a,\alpha\beta} = \alpha N_f \int d^4x Q. \tag{2.18}$$

However, the integrand can be expressed as a total divergence:

$$G_a^{\alpha\beta}\tilde{G}_{a,\alpha\beta} = \partial_\mu K^\mu, \tag{2.19}$$

where K^μ is a current introduced by Bardeen, specifically [47]

$$K^\mu = \epsilon^{\mu\alpha\beta\gamma} A_{a\alpha}\left(G_{\alpha\beta\gamma} - \frac{g_s}{3} f_{abc} A_{b\beta} A_{c\gamma}\right). \tag{2.20}$$

Substituting this relation into the variation of the action transforms the volume integral into a surface integral:

$$\delta W = \alpha N \frac{g_S^2}{32\pi^2} \int d^4x \partial_\mu K^\mu = \alpha N \frac{g_S^2}{32\pi^2} \int d\sigma_\mu K^\mu. \tag{2.21}$$

Imposing the boundary condition that the gauge fields vanish at infinity, $A_a^\mu = 0$, this surface integral vanishes, preserving $U(1)_A$ as a true symmetry of QCD despite the anomaly. However, it actually turns out that the boundary condition on the gauge field A_a^μ is to approach a pure gauge configuration at infinity rather than strictly vanishing. This would prevent the integral (2.21) from vanishing, meaning $U(1)_A$ is not a true symmetry of QCD [48] [24]. Specifically one can show that the configurations $\int \partial\sigma_\mu K^\mu \neq 0$ contribute to the vacuum-to-vacuum transition amplitude for QCD.

To better grasp the resolution of the problem, one needs to understand the vacuum structure of non-Abelian gauge theories [46]. Classically, the vacuum state corresponds to the vanishing of the field strength tensor, hence either the trivial $A_\mu^0 = 0$ or to gauge fields being a gauge transformation of zero. For instance, let us consider the $SU(2)$ gauge theory with coupling constant g_s. We work in a temporal gauge, where $A_a^0 = 0$ with $a = 1, 2, 3$ and the spatial components of the gauge fields are time independent: $A_a^i(\vec{r})$. In the temporal gauge there is still some residual gauge freedom. Under a spatial gauge transformation $\Omega(\vec{r}) \in SU(2)$, the fields transform as:

$$A^i(\vec{r}) \to \Omega(\vec{r}) A^i(\vec{r}) \Omega(\vec{r})^{-1} + \frac{i}{g_s} \Omega(\vec{r}) \nabla^i \Omega(\vec{r})^{-1}. \tag{2.22}$$

This states that in the $A_a^0 = 0$ gauge, $A_i = 0$ is not the only vacuum, but any configuration looking like $A_i = \frac{i}{g_s}\Omega(\vec{r})\nabla^i\Omega(\vec{r})^{-1}$ also has zero energy. These degenerate vacuum configurations can be classified through their behaviour at spatial infinity, when $\vec{r} \to \infty$:

$$\Omega_n \xrightarrow{\vec{r}\to\infty} e^{2\pi i n}. \tag{2.23}$$

Each configuration is indexed by an integer number n, defined explicitly as:

$$n = \frac{i g_s^3}{24\pi^2} \int d^3r Tr \epsilon_{ijk} A_n^i(\vec{r}) A_n^j(\vec{r}) A_n^k(\vec{r}). \tag{2.24}$$

Since infinitly many n values exist, there are infinite degenerate vacuum states in the quantum theory, which can be labelled as $|n\rangle$. The n-vacuum state is not fully gauge invariant, in fact:

$$\Omega_1|n\rangle = |n+1\rangle. \tag{2.25}$$

However the vacuum of a gauge theory needs to be invariant under gauge transformations, therefore the true vacuum needs to be a superposition of these n-states. This defines the θ-vacuum:

$$|\theta\rangle = \sum_n e^{-in\theta}|n\rangle, \tag{2.26}$$

which is now explicitly gauge invariant, given that

$$\Omega_1|\theta\rangle = \sum_n e^{-in\theta}\Omega_1|n\rangle = \sum_n e^{-in\theta}|n+1\rangle = e^{i\theta}|\theta\rangle. \tag{2.27}$$

This θ-vacuum is the correct vacuum state for gauge theories, and it modifies the quantum dynamics of the theory. The vacuum-to-vacuum transition amplitude is given by:

$$_+\langle\theta|\theta\rangle_- = \sum_{m,n} e^{im\theta}e^{-in\theta}{}_+\langle m|n\rangle_- = \sum_\nu e^{i\nu\theta}\left[\sum_n {}_+\langle n+\nu|n\rangle_-\right], \tag{2.28}$$

where $|\theta\rangle_\pm$ are the θ-vacuum states at $t=\pm\infty$ and we performed a change of variables such that $\nu = m-n$, with the parameter ν representing the vacuum-to-vacuum transition index:

$$\nu = n|_{t=+\infty} - n|_{t=-\infty} = \frac{g_s^2}{32\pi^2}\int \partial\sigma_\mu K^\mu|_{t=-\infty}^{t=+\infty} = \frac{g_s^2}{32\pi^2}\int d^4x G_a^{\mu\nu}\tilde{G}_{a,\mu\nu}. \tag{2.29}$$

By re-expressing this transition amplitude directly within the path integral framework, one can absorb the topological phase factor $e^{i\nu\theta}$ into a redefinition of the action, so that in the transition amplitude the effective action contains $S_{eff}[A] = S[A] + \nu\theta$:

$$_+\langle\theta|\theta\rangle_- = \sum_n \int \delta A_\mu e^{iS_{eff}[A]}\delta\left[\nu - \frac{g_s^2}{32\pi^2}\int d^4x G_a^{\mu\nu}\tilde{G}_{a,\mu\nu}\right]. \tag{2.30}$$

This way, the effective action acquires an extra term:

$$S_{eff}[A] = S[A] + \theta \frac{g_s^2}{32\pi^2} \int d^4x G_a^{\mu\nu} \tilde{G}_{a,\mu\nu}. \tag{2.31}$$

This complex structure of the vacuum basically adds an extra parameter-dependent term to the canonical QCD Lagrangian:

$$\mathcal{L}_{QCD} \rightarrow \mathcal{L}_{QCD} + \mathcal{L}_\theta, \tag{2.32}$$

where

$$\mathcal{L}_\theta = \theta \frac{g_s^2}{32\pi^2} G_a^{\alpha\beta} \tilde{G}_{a,\alpha\beta}. \tag{2.33}$$

While the presence of $\mathcal{L}_\theta$ solves the $U(1)_A$ problem, it presents another issue: since the $G\tilde{G}$ operator violates parity P and time reversal T while preserving charge conjugation C, it explicitly breaks the CP symmetry. Moreover, as it will be seen in the following section, the parameter θ appearing in the Lagrangian needs to be extremely small. These two characteristic of $\mathcal{L}_\theta$ constitute the so-called strong CP problem.

2.3 Introduction to the strong CP problem

Classically, the strong CP problem is manifested in the electric dipole moment of the neutron, d_n [18]. A theoretical calculation would lead to a value of the order of $10^{-13}e$ cm, precisely from:

$$|d_n| \approx 10^{-13}\sqrt{1 - \cos\theta}\, e \cdot \text{cm}, \tag{2.34}$$

whereas the best measurement, as of right now, gives a value of $|d_n| \leq 10^{-26} e \cdot \text{cm}$. The parameter θ that characterizes the Strong CP problem is expected to be of order $\mathcal{O}(1)$ given the naturalness principle, but here we would get an extremely fine-tuned value, of the order of $\theta \leq 10^{-13}$. Why is it so small?
The solution to this problem, proposed by Quinn and Peccei, comes from not treating this parameter as a static constant but from thinking of the angle between the two bonds (one $\frac{2}{3}$ up quark bounded to two $-\frac{1}{3}$ down quarks) as if it were dynamical: even if it is not initially 0 it then relaxes to that value, solving naturally the strong CP problem.

At the quantum level, summing up the results of Sec. 2.2.2, analyzing the low-energy QCD theory requires the addition of the following term in the Lagrangian:

$$\mathcal{L}_{QCD} \supset \frac{\theta g_s^2}{32\pi^2} G_a^{\mu\nu} \tilde{G}_{a,\mu\nu}, \tag{2.35}$$

where $G^a_{\mu\nu}$ is the gluon field strength (and $\tilde{G}_{a,\mu\nu} = \frac{1}{2}\epsilon_{\mu\nu\rho\sigma} G_a^{\rho\sigma}$). The theory has a $SU(2)$ gauge group and four global symmetries: $SU(2)_V \times SU(2)_A \times U(1)_V \times U(1)_A$. As previously explored studying the structure of the θ-vacuum of QCD, this term explicitly violates parity and time-reversal symmetries, hence representing the source of CP violation within the strong interactions of the SM.

2.4 Possible solutions to the strong CP problem

In Section 2.2.2 the emergence of the strong CP problem was presented. This turns out to be even more complicated if one adds electroweak interactions. We know, in fact, that the quark mass term looked like:

$$\mathcal{L}_{mass} = -\bar{q}_{Li} M_{ij} q_{Rj} - \bar{q}_{Ri} M^\dagger_{ij} q_{Lj}, \tag{2.36}$$

with non diagonal quark mass matrices. They can however be diagonalized by performing a unitary $U(1)_A$ transformation on the quark fields, that can be proven to be:

$$q_R \to q'_R = U_R q_R = \exp\left[\frac{i}{2n_f} \mathrm{Arg}\det M\right] q_R \equiv \exp\left[\frac{i}{2}\alpha\right] q_R, \tag{2.37}$$

$$q_L \to q'_L = U_L q_L = \exp\left[-\frac{i}{2n_f} \mathrm{Arg}\det M\right] q_L \equiv \exp\left[-\frac{i}{2}\alpha\right] q_L. \tag{2.38}$$

Moreover, the $U(1)_A$ chiral transformation that rotates the fields also shifts the θ-vacuum as:

$$e^{i\alpha Q_5}|\theta\rangle = |\theta + \alpha n_f\rangle. \tag{2.39}$$

Essentially, by performing the electroweak chiral rotation to fix the quark masses, the QCD vacuum is rotating too. This leads to an effective CP-violating term:

$$\mathcal{L}^{eff}_{CP-violating} = \bar{\theta} \frac{g_s^2}{32\pi^2} G_a^{\alpha\beta} \tilde{G}_{a,\alpha\beta}, \tag{2.40}$$

where the CP violating parameter accounts for both the strong and the electroweak contributions:

$$\bar{\theta} = \theta + \mathrm{Arg}\det M. \tag{2.41}$$

There are three possible solutions proposed to solve the question of why θ is so close to zero [48]:

- An anomalously small value of $\bar{\theta}$;
- Spontaneously broken CP symmetry;
- An additional global chiral symmetry spontaneously driving $\bar{\theta} \to 0$.

Out of these three possibilities, the last option is the most natural solution to the strong CP problem. We will however briefly mention the others too, for the sake of completeness.

The first option mentioned sees the hypothesis that $\bar{\theta}$ is simply a static constant fixed by anthropic reasons or by inconventional dynamics to be very small, of order $O(10^{-10})$. This, however, looks like an unlikely scenario.

If, instead, CP is a symmetry of nature which gets spontaneously broken, this forces the tree-level parameter to vanish identically $\bar{\theta}_{tree} = 0$. However, if CP is spontaneously broken, $\bar{\theta}$ gets induced back at 1-loop level, meaning that to get small values of it one needs to make sure that $\bar{\theta}_{1-loop} = 0$. Theories with this characteristic exist but they are difficult to reconcile with experiments.

2.4.1 The axion as solution

We now focus on the most popular and simplest solution to the strong CP problem, given by axions.

This mechanism, proposed by Peccei and Quinn, postulates the existence of a global chiral $U(1)_{PQ}$ symmetry that is spontaneously broken at a high energy scale f_a, known as the axion decay constant. The axion $a(x)$ emerges as the pseudo-Nambu-Goldstone boson of this broken symmetry. Under a $U(1)_{PQ}$ transformation, the axion field transforms via a shift:

$$a(x) \xrightarrow{U(1)_{PQ}} a(x) + \alpha f_a. \tag{2.42}$$

Going back to our theory, it can be shown that spontaneous breaking of the $U(1)_{PQ}$ symmetry provides a mechanism to dynamically eliminate the $\theta G\tilde{G}$

term, which is the CP violating term, hence fixing the issue. Rather than treating $\bar{\theta}$ as a static CP-violating angle, the PQ mechanism introduces the axion field $a(x)$, allowing us to replace the static CP-violating term of the theory with the dynamical CP-conserving axion:

$$\bar{\theta} \to \frac{a(x)}{f_a}. \tag{2.43}$$

The $U(1)_{PQ}$ symmetry is anomalous with respect to QCD. Due to this chiral anomaly, the shift in the field generates an additional term in the action, meaning that the axion field promotes the static $\bar{\theta}$ parameter to a dynamical degree of freedom.

The effective Lagrangian coming out after the addition of this axion field needs to be invariant under a $U(1)_{PQ}$ transformation and can therefore be written as:

$$\mathcal{L}_{TOT} = \mathcal{L}_{SM} + \bar{\theta}\frac{g_s^2}{32\pi^2}G_a^{\mu\nu}\tilde{G}_{a,\mu\nu} - \frac{1}{2}\partial_\mu a \partial^\mu a + \mathcal{L}^{int}_{axion}\left[\frac{\partial_\mu a}{f_a}\ \psi\right] + \xi\frac{a}{f_a}\frac{g_s^2}{32\pi^2}G_a^{\mu\nu}\tilde{G}_{a,\mu\nu}. \tag{2.44}$$

Here the first two terms are the SM Lagrangian together with the CP violating term; the third is the kinetic term for axions and the fourth describes the interactions that the axion can have with the other fields ψ of the theory. The last term, the ξ term, ensures the chiral anomaly (as it contains the field $a(x)$ directly and not its derivatives and reflects the anomaly when the axion undergoes the $U(1)_{PQ}$ symmetry):

$$\partial_\mu J^\mu_{PQ} = \xi\frac{g_s^2}{32\pi^2}G_a^{\mu\nu}\tilde{G}_{a,\mu\nu}. \tag{2.45}$$

Since the $G\tilde{G}$ term contains the axion field directly, QCD instanton effects induce an effective potential for the newly introduced dynamical field. At low energies below the QCD scale, this effective potential is periodic:

$$V_{\text{eff}}(a) \sim \cos\left(\bar{\theta} + \xi\frac{\langle a\rangle}{f_a}\right). \tag{2.46}$$

To find the ground state configuration of the vacuum, we minimize the effective potential with respect to the expectation value of the axion field:

$$\left\langle\frac{\partial V_{\text{eff}}}{\partial a}\right\rangle \sim \frac{\xi}{f_a}\left\langle\sin\left(\bar{\theta} + \xi\frac{\langle a\rangle}{f_a}\right)\right\rangle = 0. \tag{2.47}$$

The minimum of this potential occurs when the argument vanishes:

$$\langle a \rangle = -\frac{f_a}{\xi}\bar{\theta}. \tag{2.48}$$

Evaluating the total Lagrangian at this ground state configuration, the CP-violating parameter $\bar{\theta}$ is dynamically cancelled out by the axion's background VEV. CP-violating term is dynamically driven to zero, therefore solving the strong CP problem.

3

Axion Dark Matter

3.1 The axion as a Dark Matter candidate

The axion field introduced in the previous section is not only useful in the resolution of the strong CP problem, but it can also be a viable candidate for Dark Matter [45]. As seen in Sec. 1.3, observations demonstrate that the vast majority of the matter content in the Universe is not made up of any known particle of the SM. We will here propose the axion, a light and weakly coupled scalar, as a DM candidate. In the Early Universe, a relic abundance of axions can be produced either from the misalignment mechanism or the decay of topological defects, such as cosmic strings and domain walls.

It is to be noted that the word "axion" is a general term that delineates different categories. It may either refer to the QCD axion, which as seen in chapter 2 emerged from the breaking of the PQ symmetry introduced to fix the strong CP problem. A key feature of the QCD axion is that its mass is not an independent parameter, but it is related to the axion decay constant f_a, which fixes the axion's zero-temperature mass $m_{a,0}$. Their inverse relationship is specifically evaluated as:

$$m_a = (5.70 \pm 0.007)\mu eV \left(\frac{10^{12} GeV}{f_a} \right). \tag{3.1}$$

Consequently, the mass has a temperature dependence, parametrized by a power law:

$$m_a(T) = m_{a,0} \left(\frac{T}{\Lambda_{QCD}} \right)^{-n}, \tag{3.2}$$

which from lattice QCD calculations [39] is compatible with $n = 4$.

Otherwise it can refer to ALPs, axion-like-particles, which is a broader and more generic classification of heavier particles sharing the shift symmetry properties, but that do not give a solution to the strong CP problem. In fact, in models of QCD axions there is a strict relation between mass and decay constant, which is related as $g_{a\gamma\gamma} \sim 1/f_a$ to the coupling to the photon [32]. For ALPs, on the other hand, the mass and the decay constant are independent from each other.

Finally, axions also play a role in supergravity and string theory frameworks, but such axions will not be investigated in this thesis.

3.2 Axion cosmology

In order to see how the axion goes from a theoretical solution of the strong CP problem to a viable CDM candidate, we analyze its field evolution [58] [23]. Two important processes determine the behaviour of the axion: firstly spontaneous symmetry breaking of the $U(1)_{PQ}$ symmetry occurs at some high energy Peccei-Quinn scale f_a, when the field introduced to fix the strong CP problem is driven to its vacuum expectation value $\langle\Phi\rangle = f_a$, identifying the axion as a Goldstone boson; then at lower temperatures non-perturbative effects become relevant. Let us see in detail what happens.

We start this discussion by keeping in mind that the axion is a pseudo-Nambu-Goldstone boson emerging from a spontaneously broken $U(1)_{PQ}$ symmetry during the Peccei-Quinn phase transition, which happens at a temperature $T \sim f_a$ where f_a is some high scale. As we had seen, the axion emerges as a solution to solve the strong CP problem. Specifically the Peccei-Quinn model sees the introduction of the complex scalar field $\Phi = |\Phi|e^{i\theta}$, where the phase θ can be interpreted as the axion and $|\Phi|$ is the radial component living on the classical potential

$$V_{PQ}(\Phi) = \frac{\lambda}{8}\left(|\Phi|^2 - f_a^2\right)^2, \tag{3.3}$$

where λ is a dimensionless coupling constant. This potential exhibits an invariance under global $U(1)_{PQ}$ phase rotations $\Phi \to \Phi e^{i\alpha}$. As the Universe cools below a critical temperature $T \sim f_a$, the system undergoes a spontaneous symmetry-breaking phase transition. The complex field acquires a non-vanishing vev, $\langle|\Phi|\rangle = f_a$, minimizing its potential energy by settling into the rim of the so-called "Mexican hat" potential. We can parameterize the field fluctuations around this vacuum configuration in terms of its massive radial degree of freedom $r(x)$ and its massless angular phase degree of freedom $\theta(x)$:

$$\Phi(x) = \frac{1}{\sqrt{2}}\left(f_a + r(x)\right) e^{i\theta(x)}. \tag{3.4}$$

The phase $\theta(x)$ corresponds to the broken symmetry generator and represents a massless Nambu-Goldstone boson. From here on, we will define the canonically normalized axion field as:

$$a(x) = f_a \theta(x). \tag{3.5}$$

The axion field therefore possesses a shift symmetry $a(x) \rightarrow a(x)+\text{const}$, keeping it initially massless at this initial high temperature stage, $T \gg \Lambda_{\text{QCD}}$.

The second process is an explicit symmetry breaking, followed by instanton effects. As the temperature decreases to lower energy scales $T \sim \Lambda_{\text{QCD}}$, in fact, the exact shift symmetry responsible for the masslessness of the axion field is explicitly broken. At this stage, when $T \ll f_a$, non-perturbative effects, such as instantons, which are tunneling effects between different topological vacuums of QCD, get switched on, explicitly breaking the $U(1)_{PQ}$ shift symmetry and turning the axion into a pseudo-Nambu-Goldstone boson. This simply means that the axion is no longer massless, but it gets a temperature-dependent mass. These processes tilt the previously symmetric potential, generating a new periodic potential ($\theta \rightarrow \theta + 2n\pi f_a$) for the angular field. In order to keep the minimum at $\theta = 0$ and therefore enforcing the dynamic cancellation of the CP violating term, it is usually chosen to have the form:

$$V_{\text{QCD}}(\theta) = \chi(T)(1 - \cos\theta) \implies V_{\text{QCD}}(a) = \chi(T)\left[1 - \cos\left(\frac{a}{f_a}\right)\right], \tag{3.6}$$

where $\chi(T)$ represents the finite-temperature topological susceptibility of the QCD vacuum.

More on this will be revisited in Section 3.2.1.

There are four possible cosmological ways in which a relic abundance of axions can be produced:

- Production via decay of a parent particle, with mass much larger than the axion's;
- Thermal production, happening when axions are coupled to the SM;

- Production via decay of a topological defect;
- The misalignment mechanism, which will be thoroughly analyzed in the following section;

In the subsequent sections we will summarize these production mechanisms [39], specifically focusing on the misalignement mechanism, which will be needed further on in this thesis. For completeness we briefly mention the other three too, even though the first two do not produce axions as a CDM candidate.

3.2.1 The misalignment mechanism

We want to explain how to reconcile the oscillating behaviour of a classical field with the cosmological behaviour that matter requires. We therefore describe the mechanism that will be needed throughout this work, in order to describe the abundance of axion DM, specifically to explain the axion dark matter production: the misalignment mechanism.

Scalar misalignment

At first we briefly describe the misalignment mechanism for a generic scalar field ϕ, so we could think of the axion as a background field [36], homogeneous and time-dependant like the inflaton in Chapter 4. The scalar field has an initial value $\phi_i \neq 0$ which is displaced from the potential minimum. After a symmetry breaking occurring during a phase transition, the field is able to move towards the minimum. As can be seen from Appendix B, then, the equation of motion for this field for a harmonic potential and constant mass m_ϕ, is:

$$\ddot{\phi} + 3H\dot{\phi} + m_\phi^2 \phi = 0. \tag{3.7}$$

Considering that we are interested in DM production, this dynamics will take place before matter-radiation equality; hence, we can consider $H = \frac{1}{2t}$. The solution to this equation can be found to be

$$\phi(t) = \phi_i \left(\frac{2}{m_\phi t}\right)^{\frac{1}{4}} \Gamma\left(\frac{5}{4}\right) J_{\frac{1}{4}}(m_\phi t), \tag{3.8}$$

where $J_n(x)$ is the Bessel function and $\Gamma(x)$ is the gamma function.

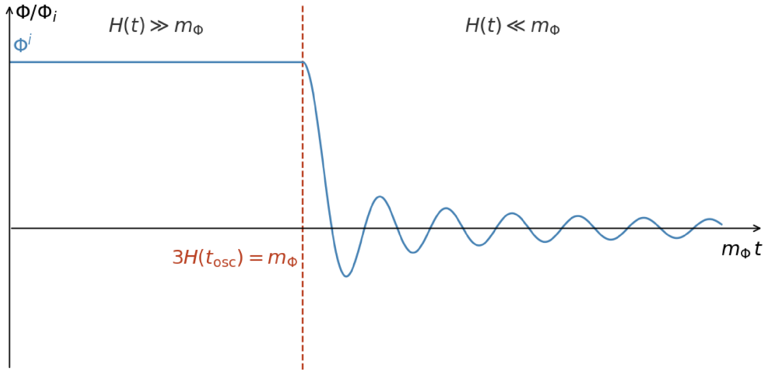

Figure 3.1: Dynamics of the $\phi(t)$ field as a function of time and mass. At first the field is kept on the plateau of the potential due to the friction of H, but at later times H becomes negligible and the field is allowed to roll down and starts oscillating near the minimum.

We briefly present the justification as to why this is the right solution to the equation of motion. A generic Bessel differential equation has the form

$$x^2\frac{d^2y}{dx^2} + x\frac{dy}{dx} + (x^2 - \nu^2)y = 0. \tag{3.9}$$

In order to see the correspondence with (3.7) we perform a change of variable: $x = m_\phi t$, which implies $\dot{\phi} = \frac{d\phi}{dt} = m_\phi \frac{d\phi}{dx}$ and $\ddot{\phi} = \frac{d^2\phi}{dt^2} = m_\phi^2 \frac{d^2\phi}{dx^2}$. After the change the equation becomes

$$\frac{d^2\phi}{dx^2} + \frac{3}{2x}\frac{d\phi}{dx} + \phi = 0. \tag{3.10}$$

Now we use the following ansatz: $\phi(x) = x^{-\frac{1}{4}}u(x)$, which inserted in the previous equation gives

$$x^2\frac{d^2u}{dx^2} + x\frac{du}{dx} + \left(x^2 - \frac{1}{16}\right)u = 0, \tag{3.11}$$

which matches Bessel's equation (3.9) in the case $\nu = \frac{1}{4}$. A general solution is a combination of Bessel's functions of first and second kind:

$$u(x) = c_1 J_{\frac{1}{4}}(x) + c_2 Y_{\frac{1}{4}}(x), \tag{3.12}$$

which implies

$$\phi(x) = (m_\phi t)^{-\frac{1}{4}}[c_1 J_{\frac{1}{4}}(m_\phi t) + c_2 Y_{\frac{1}{4}}(m_\phi t)]. \tag{3.13}$$

The only thing left now is the evaluation of the constants c_1, c_2, which we achieve by imposing the initial conditions $\phi(0) = \phi_i$ and $\dot{\phi}(0) = 0$ at $t \to 0$. Since

$Y_{\frac{1}{4}}(x) \propto x^{-\frac{1}{4}}$, in order to prevent ϕ from diverging at $t = 0$, one needs to impose $c_2 = 0$. Moreover $J_\nu(x) \simeq \frac{1}{\Gamma(\nu+1)}(\frac{x}{2})^\nu$, so at $t = 0$ $\phi(0) = \phi_i = c_1(m_\phi t)^{-\frac{1}{4}}\frac{1}{\Gamma(\frac{5}{4})}(\frac{m_\phi t}{2})^{\frac{1}{4}}$ and therefore $c_1 = \phi_i 2^{\frac{1}{4}}\Gamma(\frac{5}{4})$, which inserted into Eq. (3.13) gives the solution presented in Eq. (3.8).

As we are interested in the late time behaviour, we can use the WKB approximation and the ansatz

$$\phi(t) = \mathcal{A}(t) cos(m_\phi t + \alpha), \tag{3.14}$$

with an arbitrary phase α and the function $\mathcal{A}$ slowly varying ($\dot{\mathcal{A}}/m_\phi \sim H/m_\phi \ll 1$). This basically represents a slowly decaying envelope and a fast oscillating part. In the equation of motion this gives $\mathcal{A}(t) \propto t^{-\frac{3}{4}} \propto a^{-\frac{3}{2}}$. The solution to this equation is [38]

$$\phi(t) = \phi_i cos(m_\phi t)\left(\frac{a_i}{a}\right)^{\frac{3}{2}}. \tag{3.15}$$

Assuming that the field starts from a misaligned value different from 0 ($\phi_i \neq 0$ and $\dot{\phi}_i = 0$) the energy density can be written as

$$\rho_\phi = \frac{1}{2}\dot{\phi}^2 + \frac{1}{2}m_\phi^2\phi^2 = \frac{1}{2}m_\phi^2(\phi_i)^2\left(\frac{a_i}{a}\right)^3 \propto a^{-3}, \tag{3.16}$$

which tells us that at late times $H \ll m_a$ this field behaves like pressureless matter; ϕ is indeed a cold dark matter candidate. It is also worth mentioning that at early times $H \gg m_a$, instead, the Hubble friction dominates maintaining the axion at its initial value and its energy density to a constant value ρ_ϕ = const. The equation of state in this period of time gives a value of $\omega = -1$, meaning that this field behaves as a contribution to the vacuum energy. For this reason, axions can not only be considered as DM contributions, but also in DE and inflation models.

Having said that ϕ can be a good candidate for DM, we can try to make sense of it as such by evaluating its abundance.

$$\Omega_\phi h^2 = \frac{\rho_\phi^0}{\rho_c/h^2} = 0.12, \tag{3.17}$$

where the experimental value of the DM abundance has been placed on the RHS.

As seen from Eq. (3.16) the energy density scales as

$$\rho_\phi(t_0) = \rho_\phi(T_0) = \rho_\phi(t_{osc})\left(\frac{a_0}{a_{osc}}\right)^{-3} = \rho(T_{osc})\frac{g_{*s}(T_0)}{g_{*s}(T_{osc})}\left(\frac{T_0}{T_{osc}}\right)^3. \tag{3.18}$$

Considering $\phi(T_{osc}) = \phi_i$, hence $\rho(T_{osc}) = \frac{1}{2}m_\phi^2\phi_i^2$, and identifying the oscillation temperature through the condition $3H(T_{osc}) = m_\phi$, meaning $T_{osc} = (\frac{M_P}{\pi}\sqrt{\frac{10}{g_*(T_{osc})}}m_\phi)^{\frac{1}{2}}$, one finds

$$\Omega_\phi h^2 = \frac{1}{2}\frac{T_0^3}{\rho_c/h^2}\frac{g_*(T_0)}{g_*(T_{osc})}\left(\frac{\pi}{M_P}\sqrt{\frac{g_*(T_{osc})}{10}}\right)^{\frac{3}{2}}\phi_i^2 m_\phi^{\frac{1}{2}}. \tag{3.19}$$

Axion misalignment

Let us now focus on the more specific process, not just scalar but axion misalignment mechanism. The misalignment mechanism takes its name from the fact that the axion field is initially displaced and then a dynamical process brings this value to the potential minimum. This is due to the fact that the axion mass is temperature dependent; at very high temperatures we mentioned that it is basically massless, which implies that no value of θ is preferred, therefore there is no reason why it should be zero. Consequently, at early times we expect the axion field to be misaligned with the minimum of the potential and the specific initial value will be determined by some stochastic process. At temperatures around $T \sim \Lambda_{QCD}$ the axion acquires a mass, which becomes comparable to the rate H, making the axion field start rolling towards the minimum $\theta = 0$, where it will oscillate analogously to the inflaton field, with the only exception that the axion field does not decay.

For the QCD axion, the $U(1)_{PQ}$ symmetry is explicitly broken by non-perturbative topological effects. This implies that, in order to evaluate this mechanism, one must account for the coupling of the axion field to gluons. The effective potential for the complex scalar field Φ will then be expressed as the sum of the high-energy Peccei-Quinn potential and the low-energy QCD instanton potential:

$$V(\Phi) = V_{PQ}(|\Phi|) + V_{QCD}(\theta) = \frac{\lambda}{8}(|\Phi|^2 - f_a^2)^2 + \chi(T)(1 - \cos\theta). \tag{3.20}$$

We will express the term $\chi(T)$, the QCD topological susceptibility, as a temperature-dependent axion mass: $\chi(T) = \tilde{m}_a^2(T)f_a^2$. With this change, the potential would go as:

$$V_a = \tilde{m}_a(t)^2 f_a^2 \left[1 - \cos\left(\frac{a}{f_a}\right)\right], \tag{3.21}$$

which can be expanded, with a dominant term that will coincide with the mass term

$$V_a \approx \frac{1}{2}\tilde{m}_a(t)^2 a^2. \tag{3.22}$$

From (3.21) we can see that the potential energy for the axion is periodic; it is then easy to compute the equations of motion for the field θ, and consequently simply for $a(x)$, in an expanding Universe;

$$\ddot{\theta} + 3H\dot{\theta} + \tilde{m}_a^2(T)\sin(\theta) = 0 \tag{3.23}$$

This equation is very similar to (3.7); in particular for very small values of θ we can make the approximation $sin\theta \approx \theta$ which leads to the same dynamics as the scalar case. For values $\theta_i \approx \pi$ we will not have a harmonic oscillator solution approximation but the cosine-like potential.

As briefly mentioned in the introduction of the chapter, we assume the QCD axion mass scaling:

$$\tilde{m}_a^2(T) = \begin{cases} m_a^2\left(\frac{T}{T_{QCD}}\right)^{-n} & \text{for } T > T_{QCD} \\ m_a^2 & \text{for } T < T_{QCD} \end{cases} \tag{3.24}$$

where m_a is the axion mass at T_0. Again, in [54] a good fit for this expression shows that the power is compatible with $n \approx 8$.

Considering this relation, the solution to $\theta(t)$ evolving in a cosmological background can be computed.

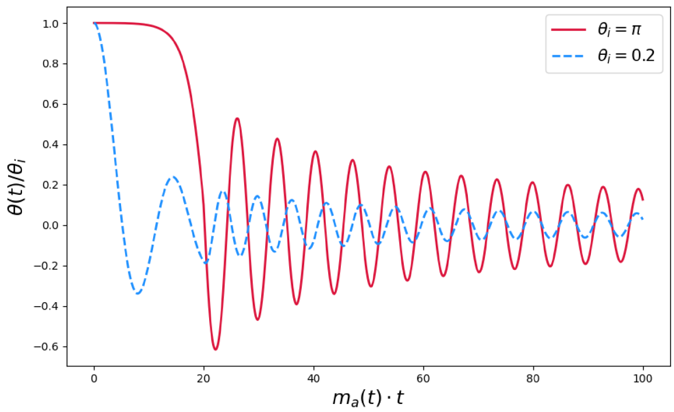

Figure 3.2: Dynamics of the normalized $\theta(t)$ field as a function of axion mass and time, imposing different initial conditions. The dashed blue line represents the approximated solution, which is possible for a small value of θ_i, so that $\sin\theta \approx \theta$. In red, instead, the real solution to Eq. (3.23) with an initial value of $\theta_i = \pi$; at first the field is kept on the plateau of the potential due to the friction of H, but at later times H becomes negligible and the field is allowed to roll down and starts oscillating near the minimum.

As we did before, we now want to get an expression for the energy density $\rho_a(T)$, so we start from the number density

$$n_a(T_0) = n_a(T_{osc})\left(\frac{a_0}{a_{osc}}\right)^{-3}. \tag{3.25}$$

Having assumed, in this particular case, that the field starts from an initial value $\theta_i f_a$ and that $\dot{\theta}_i = 0$, we can say

$$n_a(T_{osc}) = \frac{\rho_a(T_{osc})}{m_a(T_{osc})} \approx \frac{1}{2}\tilde{m}_a(T_{osc}) f_a^2 \theta_i^2. \tag{3.26}$$

Seeing that the number density of axions varies as a^{-3} we understand that it only decreases as the volume of the Universe expands, ensuring that the number of axions per comoving volume is conserved even as the mass changes.

From this we get an expression for the energy density today:

$$\begin{aligned}\rho_a(T_0) &= n_a(T_0)\cdot m_a \\ &= \frac{1}{2}\tilde{m}_a(T_{osc})f_a^2\theta_i^2\left(\frac{a_0}{a_{osc}}\right)^{-3}\cdot m_a \\ &= \frac{1}{2}f_a^2\theta_i^2 m_a\tilde{m}_a(T_{osc})\left(\frac{g_{*s}(T_0)}{g_{*s}(T_{osc})}\right)\left(\frac{T_0}{T_{osc}}\right)^3,\end{aligned} \tag{3.27}$$

which allows us to get an expression for the relic abundance:

$$\Omega_a h^2 = \frac{\rho_a(T_0)}{\rho_c/h^2} = \frac{1}{2}\frac{\theta_i^2 f_a^2 m_a\tilde{m}_a(T_{osc})}{\rho_c/h^2}\left(\frac{g_{*s}(T_0)}{g_{*s}(T_{osc})}\right)\frac{T_0^3}{T_{osc}^3}. \tag{3.28}$$

Now imposing again the oscillation condition $3H \approx m_a(T)$, which in this case is a good approximation [61], we find:

$$T_{osc} = \left(\frac{M_P}{\pi}\sqrt{\frac{10}{g_*(T_{osc})}}m_a\right)^{\frac{2}{4+n}} T_{QCD}^{\frac{n}{n+4}}, \tag{3.29}$$

where we consider $n = 0$ in the case in which $T < T_{QCD}$. Now, substituting this in Eq. (3.28) and employing the relation between decay constant and axion mass of Eq. (3.1), one gets:

$$\Omega_a h^2 = \frac{1}{2}\theta_i^2(5.7\cdot 10^{-3}GeV^2)^2\frac{g_{*s}(T_0)}{g_{*s}(T_{osc})}\frac{T_0^3}{\rho_c/h^2}\left(\frac{M_P}{\pi}\sqrt{\frac{10}{g_*(T_{osc})}}m_a\right)^{-\frac{6+n}{4+n}} T_{QCD}^{-\frac{n}{n+4}}. \tag{3.30}$$

As we will see in chapter 5, the fact that the relic abundance has an experimental upper bound of $\Omega_{DM}h^2 < 0.12$ allows us to constrain the parameter space of the DM candidate we are considering. In this case $\Omega_a h^2 \propto \theta_i^2 m_a^{-\frac{6+n}{4+n}}$, which relates the two axionic parameters, the initial misalignment angle and the mass of the axion.

However, there is an epoch in cosmology that may change the analysis until now performed: inflation. Chapter 4 describes the reasons why an inflationary era is needed in cosmology and concludes, in Section 4.4, by looking at the possible scenarios of axions being born before or after inflation takes place.

3.2.2 Other production mechanisms

Apart from the misalignment mechanism, which will be one of the main processes studied in this thesis to explain the production of axions as DM, some other mechanisms were mentioned above.

A population of axions can be produced from the decay of a parent particle X coupled to the axion field, provided that the kinematic condition $m_X > m_a$ is satisfied. These axions are relativistic if the decay happens after they decoupled from the SM. In this situation axions are classified as dark radiation, which can affect the CMB in different ways. Of course, these relativistic axions cannot be a candidate for cold DM.

Another mechanism is thermal production, meaning when axions are created and annihilated during interactions happening among particles in the thermal bath. During these processes the number density of axions, $n_a^{th}(t)$, will evolve according to Boltzmann's equations:

$$\frac{dn_a^{th}}{dt} + 3Hn_a^{th} = \Gamma(n_a^{eq} - n_a^{th}), \tag{3.31}$$

where the rate can be expressed as $\Gamma = \sum_i n_i \langle \sigma_i v \rangle$ and the equilibrium number density is $n_a^{eq} = \frac{\zeta(3)}{\pi^2} T^3$. The relative strength between H and Γ determines the evolution of the process. Specifically, whenever $\Gamma > H$, axions reach a thermal distribution and may constitute the population of thermal axions observed today, provided that inflation did not dilute them.

Lastly, axions can be produced from the decay of a topological defect. The breaking of the $U(1)_{PQ}$ symmetry leads to topological defects, which in our case are domain walls and axionic strings, that will later decay into cold axions. Specifically, these are formed from the winding around the θ angle that leads to a string-like topological defect along the length of the region enclosed by the winding. It is important to distinguish the pre-inflationary scenario $H_I < f_a$ when the PQ symmetry gets broken before inflation takes place, with the consequence that all topological defects get washed away, and the post-inflationary scenario $H_I > f_a$, in which their decay produces axions. This distinction will be further analyzed in chapter 4.

4

Inflation

In Section 1.2.1 some drawbacks regarding the ΛCDM model were presented. Some of them, like the smoothness, flatness, horizon and entropy problems, have already hinted at a possible explanation, which relies on the theory of inflation. A note to be made here [5] is that the flatness and horizon problems are not strict inconsistencies of the Standard cosmological model, since we could have a Universe evolving homogeneously, as observations suggest, if the initial value of Ω was close to unity. The flatness of the Universe cannot, therefore, be predicted by the model, but it must be assumed in the initial conditions.
Let us now study the characteristics that the inflationary theory needs to have in order to solve the problems listed above.

4.1 Inflation dynamics

In order to solve these issues we need a field satisfying accelerated expansion and negative pressure:

$$\ddot{a} > 0 \leftrightarrow p < -\frac{1}{3}\rho. \tag{4.1}$$

The best candidate for this is a simple scalar field. The reason for this choice emerges from an analogy with the cosmological constant Λ. To Λ is, in fact, associated a stress-energy tensor that can be written in the form of a perfect fluid:

$$T^{\Lambda}_{\mu\nu} = (p_\Lambda + \rho_\Lambda)u_\mu u_\nu + p_\Lambda g_{\mu\nu} = p_\Lambda g_{\mu\nu}, \tag{4.2}$$

where the last equality comes from the equation of state of the cosmological constant, $\omega = -1$. As seen, Λ can be interpreted as the energy of the quantum vacuum state of the system.

Taking the vacuum expectation value one gets:

$$\langle 0|T^{\Lambda}_{\mu\nu}|0\rangle = \langle T^{\Lambda}_{\mu\nu}\rangle = -\langle\rho\rangle g_{\mu\nu}. \tag{4.3}$$

If, on the other hand, we consider a scalar field ϕ with the Lagrangian

$$\mathcal{L}_{\phi} = -\frac{1}{2}g^{\mu\nu}\partial_{\mu}\phi\partial_{\nu}\phi - V(\phi) \tag{4.4}$$

and an associated stress-energy tensor

$$T^{\phi}_{\mu\nu} = \partial_{\mu}\phi\partial_{\nu}\phi + g_{\mu\nu}\mathcal{L}, \tag{4.5}$$

and we also assume that $\langle\phi\rangle$ = constant, we get

$$T^{\phi}_{\mu\nu} = -V(\langle\phi\rangle)g_{\mu\nu}, \tag{4.6}$$

which mimics the expression seen for the cosmological constant. Since Λ exhibits a negative pressure and driving an exponential expansion, it would be a good candidate as it would satisfy the requests of Eq. (4.1); the only issue with it is that inflation needs to end at some point, in order to allow scales to re-enter the horizon. This is why we consider the scalar field ϕ, imposing, however, that its vacuum expectation value is not constant but depends on time

$$\langle 0|\phi|0\rangle = f(t) \neq \text{constant}, \tag{4.7}$$

so that we can have a dynamical evolution determining the end of the accelerated expansion that we call inflation. Of course, as we are interested in an isotropic evolution, we don't consider anything that has a preferred direction, as a vector or spinor field, which would violate rotational invariance. Hence the field is scalar.

To sum up, inflation is the theory describing the dynamical evolution of a weakly coupled scalar field which was initially displaced from the minimum of its potential.

For the sake of completeness, we mention that the Lagrangian in Eq. (4.4) could contain an additional term related to the coupling of the inflaton field to gravity, $+\xi\phi^2 R$, but we will here consider a minimally coupled model, meaning $\xi = 0$.

4.1.1 Equation of motion of the scalar field

We now want to analyze the dynamics of the evolution of the scalar field, rolling on a potential $V(\phi)$, from whose minimum $\phi = \sigma$ it was initially displaced, moving in a background RW space-time with expansion rate H and having a certain energy density ρ_ϕ.

Looking at the calculations performed in Appendix B, we can start analyzing this dynamics from the equations of motion:

$$\ddot{\phi} + 3H\dot{\phi} - \frac{\nabla^2\phi}{a^2} = -\frac{\partial V}{\partial \phi}. \tag{4.8}$$

This equation of motion represents the inflaton field rolling down the scalar potential $V(\phi)$ with a friction given by H and it has two different regimes: the first one, in which the friction dominates and ϕ rolls at an asymptotic velocity, and a second one, when the friction becomes negligible and the field ends up in the rapid oscillation regime.

Expressing the scalar field as a sum of a classical background and field fluctuations:

$$\phi(\vec{x}, t) = \phi_0(t) + \delta\phi(\vec{x}, t), \tag{4.9}$$

where we assume a homogeneous scalar field with quantum fluctuations treated as small corrections ($\delta\phi(\vec{x}, t) \ll \phi_0(t)$), we get that our system is well defined by these two equations for the background field:

$$\begin{cases} \ddot{\phi} + 3H\dot{\phi} = -\frac{\partial V}{\partial \phi} \\ H^2 = \frac{8\pi G}{3}\left(\frac{1}{2}\dot{\phi}^2 + V(\phi)\right) = \frac{8\pi G}{3}\rho_\phi \end{cases} . \tag{4.10}$$

Moreover, it is useful to write the following relations, that emerge from the components of the stress-energy tensor [52]

$$T_{00} = \frac{\dot{\phi}^2}{2} + V(\phi) = \rho_\phi, \tag{4.11}$$

$$\frac{T_i^i}{3} = \frac{\dot{\phi}^2}{2} - V(\phi) = p_\phi, \tag{4.12}$$

which clearly show that in the limit $V(\phi) \gg \dot{\phi}^2$ the kinetic term is negligible and we get the analogous to the cosmological constant: $p_\phi \simeq -\rho_\phi$.

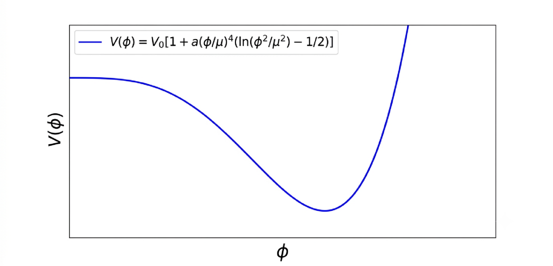

(a) Small field potential.

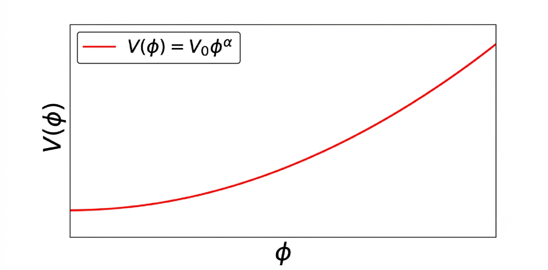

(b) Large field potential.

Figure 4.1: Two examples of inflationary potentials are presented in the figure. On the left side the small field model shows clearly the plateau allowing slow-roll and hence inflation, with a consequent minimum and steep region after inflation ends. On the right side the field will again be initially displaced from the minimum and will be able to roll down at a later stage.

4.1.2 Slow-roll regime

As mentioned above, for inflation to take place we need to impose some conditions, such as the kinetic term being negligible with respect to the potential (hence a sufficiently flat potential on which the inflaton field is able to slow-roll) and the field's acceleration being suppressed. These can be summarised in what are called the slow-roll conditions:

$$\begin{cases} \frac{1}{2}\dot{\phi}(t)^2 \ll V(\phi) \Rightarrow H^2 = \frac{8\pi G}{3}V(\phi) \\ \ddot{\phi} \ll 3H\dot{\phi} \Rightarrow 3H\dot{\phi} = -V' \end{cases}, \tag{4.13}$$

where the derivative is $' \equiv \frac{\partial}{\partial\phi}$. These equations describe the evolution of a scalar field where the background is evolving too; the second equation, in particular, is analoguous to a viscometer one, where the viscous term is the Universe in expansion, represented by the Hubble rate $H = \frac{\dot{a}}{a}$, and it states that the friction due to the expansion is balanced by the acceleration due to the slope of the potential.

In order to quantify the slow-roll regime dynamics we define two parameters, ϵ and η, as:

$$\epsilon \equiv \frac{M_P^2}{2V^2}\left(\frac{\partial V}{\partial \phi}\right)^2, \tag{4.14}$$

$$\eta \equiv \frac{M_P^2}{V}\frac{\partial^2 V}{\partial \phi^2}. \tag{4.15}$$

From the slow-roll conditions, and consequent approximation to the equations of motion seen in Eq. (4.13), one can show that

$$\frac{\dot{\phi}^2/2}{V} \simeq \frac{1}{2V}\frac{1}{9H^2}\left(\frac{\partial V}{\partial \phi}\right)^2 \simeq \frac{M_P^2}{6V^2}\left(\frac{\partial V}{\partial \phi}\right)^2 = \frac{\epsilon}{3}. \tag{4.16}$$

From this expression, one can see that the first slow-roll condition becomes:

$$\epsilon \ll 1. \tag{4.17}$$

We can also see this when computing the second derivative of the scale factor and requiring it to be positive during inflation (acceleration expansion):

$$\ddot{a} = \dot{\dot{a}} = \dot{a}H + a\dot{H} = aH^2 + a\dot{H} = aH^2\big(1 + \frac{\dot{H}}{H^2}\big) = aH^2(1-\epsilon) > 0. \tag{4.18}$$

As we need not only to impose a positive acceleration, but also that inflation lasts long enough to solve the horizon and the flatness problem, we need a second condition, which from the definition in Eq. (4.15) is simply

$$\eta \ll 1. \tag{4.19}$$

During inflation, the slow roll parameters ϵ and η can be considered approximately constant, considering that the potential $V(\phi)$ is flat. Indeed, as we are working at first order, it can be checked that $\dot{\epsilon}$, $\dot{\eta} = \mathcal{O}(\epsilon^2, \eta^2)$.

4.1.3 Coherent oscillations: Reheating

The reheating phase is a post-inflationary period, coming before the radiation era, in which the Universe is reheated. This happens after the accelerated expansion, when the temperature goes as $T \propto a^{-1} \propto e^{-Ht}$. Inflation ends when the curvature of the potential is not negligible anymore, in other words, in the regime in which $V'' \gg H^2$. The flat region is already passed, slow roll cannot happen anymore and the scalar field rolls down towards the minimum of the potential $\phi = \sigma$, where it starts oscillating with a high frequency $\omega^2 = V''(\sigma)$. This oscillation results in an unstability of the inflaton field, which starts decaying into other forms of matter and radiation with rate Γ_ϕ, generating the particle content of the Standard Model and maybe Dark Matter. The equation of motion in this period of time needs to account for the decay rate and therefore gets then modified into:

$$\ddot{\phi} + (3H + \Gamma_\phi)\dot{\phi} + V'(\phi) = 0. \tag{4.20}$$

Remembering that the energy density of the inflaton field could be written as

$$\rho_\phi = \frac{1}{2}\dot{\phi}^2 + V(\phi), \tag{4.21}$$

one can derive it with respect to time, and substitute the result in Eq. (4.20) after this got multiplied by $\dot{\phi}$:

$$\ddot{\phi}\dot{\phi} + 3H\dot{\phi}^2 + \Gamma_\phi\dot{\phi}^2 + V'(\phi)\dot{\phi} = 0, \tag{4.22}$$

which in terms of ρ_ϕ becomes

$$\dot{\rho}_\phi + \dot{\phi}^2(3H^2 + \Gamma_\phi) = 0. \tag{4.23}$$

Assuming rapid oscillations of the field once it reaches the minimum of the potential, ϕ oscillates sinusoidally ($\phi = \phi_0 \sin(\omega t)$), hence $V(\phi) = \frac{1}{2}\omega^2\phi^2 = \frac{1}{2}\omega^2\phi_0 \sin^2(\omega t)$ and $\frac{1}{2}\dot{\phi}^2 = \frac{1}{2}\omega^2\phi_0 \cos^2(\omega t)$. Since $\langle\sin^2(x)\rangle = \langle\cos^2(x)\rangle = \frac{1}{2}$, we can take the average over a period of oscillation:

$$\frac{1}{2}\langle\dot{\phi}^2\rangle_{cycle} = \langle V(\phi)\rangle_{cycle} \Rightarrow \rho_\phi = \langle\dot{\phi}^2\rangle_{cycle}, \tag{4.24}$$

which allows us to modify Eq. (4.23) in terms of the energy density:

$$\dot{\rho_\phi} + (3H + \Gamma_\phi)\rho_\phi = 0. \tag{4.25}$$

In this case, the equation of state looks like

$$\omega = \frac{p}{\rho} = \frac{\langle \frac{1}{2}\dot{\phi}^2 - V(\phi)\rangle}{\langle \frac{1}{2}\dot{\phi}^2 + V(\phi)\rangle} = 0, \tag{4.26}$$

suggesting that ϕ behaves as pressureless matter in this oscillating phase. Moreover, equation (4.25) represents the decay of this massive particle species, with solution given by:

$$\rho_\phi = M^4 \left(\frac{a}{a_{osc}}\right)^{-3} e^{-\Gamma_\phi (t - t_{osc})}, \tag{4.27}$$

where M^4 is the vacuum energy of the inflaton field at that time and t_{osc} is the time at which oscillations start. To the equation involving ρ_ϕ we can add the equation regarding the energy density in the relativistic decay products; the equation related to the energy density of radiation and the Friedman equation now becomes:

$$\dot{\rho_R} + 4H\rho_R = \Gamma_\phi \rho_\phi; \tag{4.28}$$

$$H^2 = \frac{8}{3}\pi G(\rho_\phi + \rho_R). \tag{4.29}$$

These two equations, together with Eq. (4.27), describe the reheating process, in which the inflaton field ϕ oscillating decays into massive light particles. ϕ particles oscillate starting from the time $t_{osc} \simeq H^{-1} \simeq \frac{M_P}{M^2}$ until $t \simeq \Gamma_\phi^{-1}$. The way they are written makes it easy to compare the rate at which the decay happens with respect to the expansion rate, allowing to identify when these processes are happening. Between these two times the field is decaying, but not in an effective way yet, and light particles begin being produced. The non-relativistic ϕ particles dominate the energy density of the Universe, which is hence behaving as in a matter-like epoch, where $a(t) \propto t^{\frac{2}{3}}$ (and consequently $H = \frac{2}{3t}$) and ρ_R doesn't go as the usual a^{-4} behaviour. Substituting these values in Eq. (4.28) we obtain:

$$\dot{\rho_R} + 4\frac{2}{3t}\rho_R = \Gamma_\phi \rho_\phi = \Gamma_\phi \rho_{osc}\left(\frac{a}{a_{osc}}\right)^{-3} \simeq \Gamma_\phi M^4 \left(\frac{t}{t_{osc}}\right)^{-2} \simeq \frac{\Gamma_\phi M_P^2}{t^2}. \tag{4.30}$$

The approximate solution to this is given by:

$$\rho_R \simeq \frac{M_P^2 \Gamma_\phi}{10\pi t}\left[1 - \left(\frac{t}{t_{osc}}\right)^{-\frac{5}{3}}\right] \simeq \frac{(6/\pi)^{\frac{1}{2}}}{10} M_P \Gamma_\phi M^2 \left(\frac{a}{a_{osc}}\right)^{-\frac{3}{2}}\left[1 - \left(\frac{a}{a_{osc}}\right)^{-\frac{5}{2}}\right]. \tag{4.31}$$

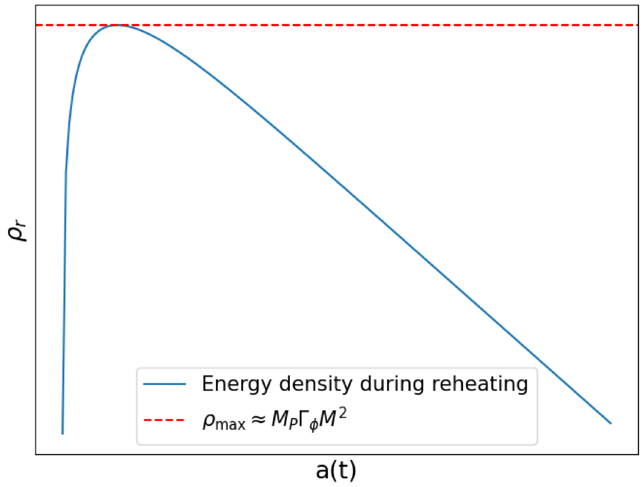

Figure 4.2: Energy density plot during reheating. The graph represents a growth of ρ_R from zero until a maximum value $\rho_{max} \simeq M_P \Gamma_\phi M^2$, after which it decreases as $a^{-\frac{3}{2}}$ instead of a^{-4}.

The maximum temperature achieved in correspondence to ρ_{max} is

$$T_{max} \simeq 0.8 g_*^{-\frac{1}{4}} M^{\frac{1}{2}} (\Gamma_\phi M_P)^{\frac{1}{4}}. \tag{4.32}$$

Between the beginning of oscillations and the time in which the decays become efficient, the entropy goes as:

$$s \propto T^3 \approx \rho_R^{\frac{3}{4}} \approx a^{-\frac{9}{8}} \longrightarrow S = s a^3 \propto a^{\frac{15}{8}}, \tag{4.33}$$

which shows how the total entropy is not constant, but it increases with the scale factor.

Eventually, decays become efficient and the Universe starts to become radiation dominated, with $\rho_R \propto a^{-4}$. The temperature at the beginning of this phase is obtained through the matching of the Friedmann equation during radiation, where the time is $t_{decay} \sim \Gamma_\phi^{-1}$:

$$\left(\frac{1}{2 t_{decay}} \right)^2 = H^2 \simeq \frac{\rho_R}{3 M_P^2} \simeq \frac{g_*}{3 M_P^2} \frac{\pi^2}{30} T^4, \tag{4.34}$$

which gives the following result for the reheating temperature:

$$T_{rh} \equiv T(t = \Gamma_\phi^{-1}) = \left(\frac{2}{\pi}\sqrt{\frac{10}{g_*}}\Gamma_\phi M_P\right)^{\frac{1}{2}}. \tag{4.35}$$

We will see in Sec. 5 how this expression gets modified if one assumes that the potential is not quadratic.

4.2 Quantum fluctuations of the inflaton field

Up until now the background evolution of the inflaton field was studied. If we introduce the quantum fluctuations around the classical background, as seen in Eq. (4.9), the general equations of motion (4.8) can be applied to both contributions and one gets:

$$\begin{cases} \delta\ddot{\phi} + 3H\delta\dot{\phi} - \frac{\nabla^2\delta\phi}{a^2} = -V''\delta\phi \\ \ddot{\phi}_0 + 3H\dot{\phi}_0 - \frac{\nabla^2\phi_0}{a^2} = -V' \end{cases}. \tag{4.36}$$

The second equation of this system can be derived so that we can compare $\dot{\phi}_0$ and $\delta\phi$:

$$\ddot{\dot{\phi}}_0 + 3H\dot{\dot{\phi}}_0 = -V''\dot{\phi}_0, \tag{4.37}$$

where we also neglected the laplacian due to the fact that ϕ_0 only depends on time coordinates; considering the large scale regime in which $k \ll aH$, we can neglect also $\frac{\nabla^2\delta\phi}{a^2}$. Comparing (4.36) and (4.37), one can see that $\delta\phi$ and $\dot{\phi}_0$ have the same equation of motion in the large scale approximation, meaning that the two solutions may not be independent. Checking the Wronskian, one is able to infer a dependence between the two quantities $\delta\phi \propto \dot{\phi}_0$, which we can express as

$$\delta\phi(\vec{x}, t) = -\delta t(\vec{x})\dot{\phi}_0(t), \tag{4.38}$$

where $\delta t(\vec{x})$ represents the local time shift of the inflaton that, due to quantum fluctuations, slow rolls down the potential at slightly different rates. This way we can write the inflaton field, considering both the background and the quantum fluctuations, as

$$\phi(\vec{x}, t) = \phi_0(t - \delta t(\vec{x})), \tag{4.39}$$

which tells us that the effect of these fluctuations is making all of the Universe experience the same values of ϕ but at slightly different times; for instance different patches of the Universe will end inflation at different times.

4.2.1 Quantum fluctuations solutions

Let us now solve the equation

$$\delta\ddot{\phi} + 3H\delta\dot{\phi} - \frac{\nabla^2\delta\phi}{a^2} = -V''\delta\phi. \tag{4.40}$$

Going into Fourier space:

$$\delta\phi(\vec{x},t) = \frac{1}{(2\pi)^3}\int d^3k e^{i\vec{k}\cdot\vec{x}}\delta\phi(k,t), \tag{4.41}$$

and quantizing the field, rescaling it as $\delta\phi = \frac{\delta\hat{\phi}}{a(t)}$, one gets:

$$\delta\hat{\phi}(\vec{x},\tau) = \frac{1}{(2\pi)^3}\int d^3k[u_k(\tau)\hat{a}_k e^{-i\vec{k}\cdot\vec{x}} + u_k^*(\tau)\hat{a}_k^\dagger e^{i\vec{k}\cdot\vec{x}}], \tag{4.42}$$

where we can assume the so-called Bunch-Davies vacuum choice:

$$u_k(\tau) \approx \frac{e^{-ik\tau}}{\sqrt{2k}}. \tag{4.43}$$

In Fourier space, using $|\delta\hat{\phi}_k| = |u_k|$, the KG equations become:

$$u_k''(\tau) + \left[k^2 - \frac{a''}{a} + \frac{\partial^2 V}{\partial\phi^2}a^2\right]u_k(\tau) = 0. \tag{4.44}$$

For the massless case, the second derivative term vanishes and one can identify two regimes.

- Sub-Horizon regime $k \gg aH$. The EOM reduces to

$$u_k'' + k^2 u_k = 0 \Rightarrow u_k(\tau) = \frac{1}{\sqrt{2k}}e^{-ik\tau}, \tag{4.45}$$

  which identifies an oscillating solution, specifically:

$$\delta\phi_k = \frac{1}{a}\frac{1}{\sqrt{2k}}e^{-ik\tau}. \tag{4.46}$$

- Super-Horizon regime $k \ll aH$. The EOM reduces to

$$u_k'' - \frac{a''}{a}u_k = 0 \Rightarrow u_k(\tau) = B(k)a(\tau) + A(k)a^{-2(\tau)}. \tag{4.47}$$

  Neglecting the decaying term that gets washed away by inflation, this implies:

$$\delta\phi_k = B(k) = \text{constant}. \tag{4.48}$$

  Fluctuations get then frozen on super-horizon scales. After the expansion, couples of particle-antiparticle cannot annihilate anymore, hence a net amount of particles is generated.

4.3 Cosmic no-Hair Theorem

We conclude this chapter by mentioning something that confirms the theory of inflation as an attractor solution towards a homogeneous and isotropic Universe.

Up until now, inflation has been analyzed in the context of a flat FRW cosmological model. If we start from different initial conditions, though, like an anisotropic or non-homogeneous Universe, is inflation still a valid theory? The answer should be yes if we want to have validity for the most general conditions, solving the problem of initial data. This explanation takes the name of Cosmic no-Hair Theorem.

Consider for example a Bianchi model with

$$H^2 = \frac{8\pi G\rho_{TOT}}{3} + F(a_x, a_y, a_z), \tag{4.49}$$

which represents an anisotropic Universe where the anisotropies get collected in the F function, which depends on the three different scale factors of the three directions of the 3-dimensional space. Defining a mean scale factor, that accounts for the different evolutions along the x, y and z axes of the Universe, we can write

$$V = a_x \cdot a_y \cdot a_z \longrightarrow \overline{a} \propto V^{\frac{1}{3}}. \tag{4.50}$$

The key concept here is that F goes at least like $\overline{a}^{-2}$, whereas in ρ_{TOT} there are $\rho_{matter} \propto \overline{a}^{-3}$, $\rho_{radiation} \propto \overline{a}^{-4}$ and ρ_Λ which is constant. Wald's theorem uses this to show that a cosmological model with non-zero vacuum energy asymptotically evolves to a de Sitter state. As the Universe expands, the F term becomes more and more negligible and the cosmological constant energy density term starts to dominate; this way all anisotropies will disappear, demonstrating how the expanding Universe predicted by inflation constitutes an attractor solution towards a homogeneous and isotropic state, solving in a sense the problem of initial conditions.

4.4 Axion interplay with inflation

There are two possible scenarios involving axion fields during inflation: axion-driven inflation and axions DM fields as spectators during inflation [38].

Regarding the first case, we have already seen in this chapter how inflation is an expansion theory driven by a scalar field ϕ slow-rolling on a potential $V(\phi)$. Axions are good inflaton candidates, considering that the shift symmetry protects the flatness of the potential from quantum corrections. Inflation is followed by a period of reheating, in which the inflaton field decays; because of this, if inflation is axion-driven, that axion is not DM, therefore it is not the QCD axion. As this thesis focuses on the axion as a DM candidate, this scenario will not be analysed further.

Let us then focus on the case of axions as spectator fields during inflation. To understand this we consider that the temperature of the Universe during inflation, obtained from the Hawking radiation emitted from the de-Sitter horizon, is

$$T_I = \frac{H_I}{2\pi} = M_p\sqrt{A_s\frac{r_T}{8}}, \tag{4.51}$$

where H_I is the inflationary Hubble scale, A_s the scalar amplitude and r_T is the tensor-to-scalar ratio. Experimental constraints on these values imply an upper bound on H_I, which translates into $\frac{H_I}{2\pi} < 1.4 \cdot 10^{13} GeV$. The two conditions of unbroken or broken symmetry during inflation can be equivalently expressed as either $f_a < \frac{H_I}{2\pi}$ or $f_a > \frac{H_I}{2\pi}$.

4.4.1 PQ symmetry unbroken during inflation: $f_a < \frac{H_I}{2\pi}$

In this first case, during inflation the $U(1)$ symmetry is unbroken and the field has zero vev. The symmetry then breaks after inflation, when the temperature drops below f_a. Since the decay constant is larger than the scale of non-perturbative physics, the axion has no potential at this time, and thus θ_i has no preferred value, meaning that it follows a uniform distribution on $[-\pi;\pi]$. This initial value, as we will see, fixes the axion relic abundance. On average, this initial angle will have a value of:

$$\langle\theta_i^2\rangle = \frac{1}{2\pi}\int_{-\pi}^{+\pi}\theta^2 d\theta = \frac{\pi^2}{3}. \tag{4.52}$$

There is a consequence to the symmetry being broken after inflation, which is the rise of topological defects, such as axion strings and domain walls. When the PQ symmetry breaks after inflation, some of those defects will remain in the present Universe and may create problems, which will however not be discussed here.

4.4.2 PQ symmetry broken during inflation: $f_a > \frac{H_I}{2\pi}$

In this scenario, the rapid expansion of inflation washes all the phase transition relics away. If in the previous case the PQ symmetry breaking established causally disconnected patches, each with a different value of the initial θ_i and produced topological defects, here each patch of θ_i is stretched out, meaning that a single uniform value of the initial θ_i, which is completely random, is everywhere. Therefore:

$$\langle\theta_i^2\rangle = \text{constant}. \tag{4.53}$$

5

Axionic Dark Matter during Reheating

5.1 Post-inflationary inflaton oscillations

As seen in Section 4, inflation is a period of exponential expansion in which the inflaton field ϕ slow-rolls along a potential $V(\phi)$, followed by a period of oscillation of the field along the minimum of the potential, that takes the name of reheating. Up until now we have considered a quadratic potential $V(\phi) = \frac{1}{2}m_\phi^2\phi^2$, that allowed harmonic oscillations and ensured a constant mass $V'' = m_\phi$ for the field [29]. We will now, however, consider an α-attractor model that goes as $V \sim \phi^k$, specifically the T-model, whose name derives from the fact that it contains different powers of the $\tanh$ function [22]:

$$V(\phi) = \lambda M_P^4 \left[\sqrt{6}\tanh\left(\frac{\phi}{\sqrt{6}M_P}\right)\right]^k \simeq \lambda M_P^4 \times \begin{cases} 1 & \text{for } \phi \gg M_P \\ \left(\frac{\phi}{\sqrt{6}M_P}\right)^k & \text{for } \phi \ll M_P \end{cases}, \tag{5.1}$$

where $M = M_P$ is the Planck mass, and λ is a coupling whose values will be presented later on. Depending on the value of k we have harmonic ($k = 2$) or anharmonic ($k > 2$) oscillations during reheating.

This is a good potential, as it is sufficiently flat for larger values of ϕ, so that the inflaton can have its slow-roll regime, and yet it allows oscillations around the minimum at $\phi = 0$.

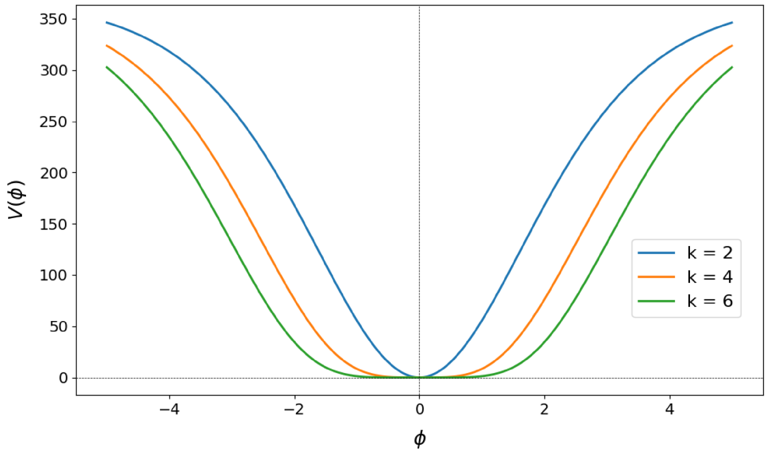

Figure 5.1: Plot of the potential for different values of k.

Taylor expanding this potential around the origin, when $\phi \ll M_P$, we are left with

$$V(\phi) = \lambda \frac{\phi^k}{M_P^{k-4}}. \tag{5.2}$$

The equation of motion used in chapter 4 is still valid, so we rewrite it here, leaving $V(\phi)$ implicit for simplicity:

$$\ddot{\phi} + (3H + \Gamma_\phi)\dot{\phi} + V'(\phi) = 0. \tag{5.3}$$

The inflaton is a time dependent field which we can parametrize as

$$\phi(t) = \phi_0(t) \cdot \mathcal{P}(t), \tag{5.4}$$

where $\mathcal{P}(t)$ encodes the harmonicities or anharmonicities over a short time scale and $\phi_0(t)$, a decaying envelope function [43], tracks the amplitude of oscillations and only changes noticeably over longer time scales.

The difference from the previous chapter lies in the model of potential used. Multiplying (5.3) by ϕ, we get to

$$\phi\ddot{\phi} + (3H + \Gamma_\phi)\phi\dot{\phi} + \phi V'(\phi) = 0. \tag{5.5}$$

Then we use the fact that $\frac{d}{dt}(\phi\dot{\phi}) = \dot{\phi}^2 + \phi\ddot{\phi}$ to substitute the first term in the equation:

$$\frac{d}{dt}(\phi\dot{\phi}) - \dot{\phi}^2 + (3H + \Gamma_\phi)\phi\dot{\phi} + \phi V'(\phi) = 0. \tag{5.6}$$

In this case, we can assume that the inflaton decays slowly so that Γ_ϕ and H can be considered as constants over a cycle. Then averaging over one oscillation brings the first and the third term to zero, allowing us to get the following relation:

$$\langle\dot{\phi}^2\rangle \simeq \langle\phi V'(\phi)\rangle = k\langle V(\phi)\rangle, \tag{5.7}$$

which then leads to

$$\rho_\phi \simeq \frac{1}{2}\langle\dot{\phi}^2\rangle + \langle V(\phi)\rangle \simeq \frac{k+2}{2}\langle V(\phi)\rangle = V(\phi_0), \tag{5.8}$$

$$P_\phi \simeq \frac{1}{2}\langle\dot{\phi}^2\rangle - \langle V(\phi)\rangle \simeq \frac{k-2}{2}\langle V(\phi)\rangle = \frac{k-2}{k+2}V(\phi_0), \tag{5.9}$$

where in the first equation, Eq. (5.8), the equality with $V(\phi_0)$ comes from the consideration that at the maximum oscillation amplitude, $\phi = \phi_0$, the inflaton stops moving, meaning that its kinetic energy is zero and we can take $\rho_\phi = V(\phi_0)$. These two together imply a modification of the equation of state that will now be

$$\omega_\phi = \frac{k-2}{k+2}. \tag{5.10}$$

As anticipated, for $k = 2$ we get $\omega_\phi = 0$ meaning matter, whereas for $k = 4$ we obtain a correspondence with radiation. This k-dependent ω_ϕ will appear in the Boltzmann equations describing the evolution of the energy density respectively of the inflaton and of radiation during reheating:

$$\frac{d\rho_\phi}{dt} + 3H(1+\omega_\phi)\rho_\phi = -(1+\omega_\phi)\Gamma_\phi\rho_\phi, \tag{5.11}$$

$$\frac{d\rho_R}{dt} + 4H\rho_R = +(1+\omega_\phi)\Gamma_\phi\rho_\phi, \tag{5.12}$$

where the difference in signs on the RHS is due to the fact that ϕ is decaying, hence diminishing its energy density, whereas the product of the decay injects energy density into the thermal bath, hence the positive sign in equation (5.12). These two, together with the Friedmann equation

$$H = \sqrt{\frac{\rho_\phi + \rho_R}{3M_P^2}}, \tag{5.13}$$

tell us that the oscillations of the inflaton around the minimum of the potential allow an energy transfer from the inflaton to the particles emerging from the decays, which will thermalize and form the thermal bath.

The reheating process depends not only on the form of the potential chosen, but also on the couplings of the inflaton to other fields [30]. The decay rate Γ_ϕ appearing in Eqs. (5.11) and (5.12) gets contributions that we can summarize in the following three different processes:

- The $\phi \to \bar{f} f$ fermionic decay, which appears in the Lagrangian as $\mathcal{L} \supset y\phi\bar{f} f$;
- The $\phi \to bb$ bosonic decay, which appears in the Lagrangian as $\mathcal{L} \supset \mu\phi bb$;
- The $\phi\phi \to bb$ bosonic annihilation, which appears in the Lagrangian as $\mathcal{L} \supset \sigma\phi^2 b^2$.

As it will now be shown, the effective inflaton mass is field dependent, the decay rate will therefore be modified and consequently the temperature will too, no longer scaling as $T \propto a^{-1}$. Similarly the maximum and reheat temperaure evaluated in Section 4.1.3 will now change as well.

Let us first analyze the inflaton decay into two fermions. In our model, since the potential is no longer quadratic, the inflaton mass, which is defined through the second derivative of the potential itself, gets modified as

$$m_\phi^2(t) = V''(\phi_0(t)) = k(k-1)\lambda M_P^2 \left(\frac{\phi_0(t)}{M_P}\right)^{k-2}. \tag{5.14}$$

It is now evident that the mass is no longer constant but it has a time dependence due to $\phi_0(t)$. This modifies the decay rate, making it time-dependent too:

$$\Gamma_{\phi\to\bar{f}f}(t) \equiv \frac{y_{\text{eff}}^2(k)}{8\pi} m_\phi(t). \tag{5.15}$$

The details of this calculation can be found in appendix C.

Similarly, the other two processes will now have decay rates that look like:

$$\Gamma_{\phi\to bb}(t) \equiv \frac{\mu_{\text{eff}}^2(k)}{8\pi m_\phi(t)}; \tag{5.16}$$

$$\Gamma_{\phi\phi\to bb}(t) \equiv \frac{\sigma^2_{\text{eff}}(k)}{8\pi}\frac{\rho_\phi}{m^3_\phi(t)}. \tag{5.17}$$

The rates computed assumed that the decay products, fermionic or bosonic, had no mass. In reality, they do get a mass, just like the inflaton does during the oscillations. Since they emerge from the interaction with ϕ their masses are effective masses:

$$m^2_{\text{eff}} \equiv \begin{cases} y^2\phi^2 & \text{for } \phi \to \bar{f}f \\ 2\mu\phi & \text{for } \phi \to bb \\ 2\sigma\phi^2 & \text{for } \phi\phi \to bb \end{cases}, \tag{5.18}$$

that come from comparing the interaction Lagrangian terms for the three processes with the mass terms: $m\bar{\psi}\psi$ for fermions and $\frac{1}{2}m^2b^2$ for bosons. These effective masses get kinematic constraints due to the fact that the inflaton needs to be heavier than the two particles produced, resulting in the condition $m^2_{eff}(t) \ll m^2_\phi$.

Inverting the relations (5.8), (5.14) we can express the envelope ϕ_0 and the inflaton mass in terms of the energy density ρ_ϕ; specifically:

$$\phi_0 = \left(\frac{\rho_\phi}{\lambda}M_P^{k-4}\right)^{\frac{1}{k}}, \tag{5.19}$$

$$m_\phi = \sqrt{k(k-1)}\sqrt{\lambda}M_P\left(\frac{\rho_\phi}{\lambda M_P^4}\right)^{\frac{k-2}{2k}}. \tag{5.20}$$

Substituting these two values in the results found for the decay rates (5.15), (5.16), (5.17) we get :

$$\begin{aligned} \Gamma_{\phi\to\bar{f}f} &= \frac{y^2_{\text{eff}}}{8\pi}m_\phi = \frac{y^2_{\text{eff}}}{8\pi}\sqrt{k(k-1)}\lambda^{\frac{1}{2}}M_P\left(\frac{\rho_\phi}{\lambda M_P^4}\right)^{\frac{k-2}{2k}} \\ &= \frac{y^2_{\text{eff}}}{8\pi}\sqrt{k(k-1)}\lambda^{\frac{1}{k}}M_P\left(\frac{\rho_\phi}{M_P^4}\right)^{\frac{1}{2}-\frac{1}{k}}. \end{aligned} \tag{5.21}$$

The same can be done for the bosonic decay:

$$
\begin{aligned}
\Gamma_{\phi\to bb} = \frac{\mu_{\text{eff}}^2}{8\pi m_\phi} &= \frac{\mu_{\text{eff}}^2}{8\pi}\frac{1}{\sqrt{k(k-1)}}\frac{1}{\lambda^{\frac{1}{2}}}\cdot\frac{1}{M_P}\lambda^{\frac{k-2}{2k}}\left(\frac{\rho_\phi}{M_P^4}\right)^{-\frac{k-2}{2k}} \\
&= \frac{\mu_{\text{eff}}^2}{8\pi}\frac{1}{\sqrt{k(k-1)}}\frac{1}{\lambda^{\frac{1}{k}}}\cdot\frac{1}{M_P}\left(\frac{\rho_\phi}{M_P^4}\right)^{\frac{1}{k}-\frac{1}{2}},
\end{aligned}
\tag{5.22}
$$

and the bosonic annihilation:

$$
\begin{aligned}
\Gamma_{\phi\phi\to bb} = \frac{\sigma_{\text{eff}}^2}{8\pi}\frac{\rho_\phi}{m_\phi} &= \frac{\sigma_{\text{eff}}^2}{8\pi}\frac{1}{[k(k-1)]^{\frac{3}{2}}}\frac{1}{\lambda^{\frac{3}{2}}}\cdot\frac{1}{M_P^3}\rho_\phi\lambda^{3\frac{k-2}{2k}}\left(\frac{\rho_\phi}{M_P^4}\right)^{-\frac{3(k-2)}{2k}} \\
&= \frac{\sigma_{\text{eff}}^2}{8\pi}\frac{1}{[k(k-1)]^{\frac{3}{2}}}\frac{1}{\lambda^{\frac{3}{k}}}\cdot M_P\left(\frac{\rho_\phi}{M_P^4}\right)^{\frac{3}{k}-\frac{1}{2}}.
\end{aligned}
\tag{5.23}
$$

To simplify the notation we can group the three expressions into:

$$
\Gamma_\phi(t) = \gamma_\phi\left(\frac{\rho_\phi}{M_P^4}\right)^l, \tag{5.24}
$$

where

$$
\gamma_\phi = \begin{cases} \frac{y_{\text{eff}}^2}{8\pi}\sqrt{k(k-1)}\lambda^{\frac{1}{k}}M_P & \text{for } \phi\to\bar{f}f \\ \frac{\mu_{\text{eff}}^2}{8\pi}\frac{1}{\sqrt{k(k-1)}}\frac{1}{\lambda^{\frac{1}{k}}}\cdot\frac{1}{M_P} & \text{for } \phi\to bb \\ \frac{\sigma_{\text{eff}}^2}{8\pi}\frac{1}{[k(k-1)]^{\frac{3}{2}}}\frac{1}{\lambda^{\frac{3}{k}}}\cdot M_P & \text{for } \phi\phi\to bb \end{cases} \tag{5.25}
$$

encodes the square of the coupling for each process and

$$
l = \begin{cases} \frac{1}{2}-\frac{1}{k} & \text{for } \phi\to\bar{f}f \\ \frac{1}{k}-\frac{1}{2} & \text{for } \phi\to bb \\ \frac{3}{k}-\frac{1}{2} & \text{for } \phi\phi\to bb \end{cases} \tag{5.26}
$$

is the parameter characterizing the specfic decay channel.

We now want to get an expression for the radiation energy density, so we consider equation (5.11), we multiply by $a^{\frac{6k}{k+2}}$ both sides, we replace ω_ϕ with Eq. (5.10), we use this last equation to substitute Γ_ϕ and we replace the temporal derivative with $\frac{d}{dt} = aH\frac{d}{da}$. Altogether this gives

$$aH\frac{d}{da}(\rho_\phi)a^{\frac{6k}{k+2}} = -3H\left(1+\frac{k-2}{k+2}\right)\rho_\phi a^{\frac{6k}{k+2}} - \gamma_\phi\frac{\rho_\phi^l}{M_P^{4l}}\left(1+\frac{k-2}{k+2}\right)\rho_\phi a^{\frac{6k}{k+2}}. \quad (5.27)$$

The left hand side can be rewritten using integration by parts:

$$\frac{d}{da}(\rho_\phi)a^{\frac{6k}{k+2}} = \frac{d}{da}(\rho_\phi a^{\frac{6k}{k+2}}) - \rho_\phi\frac{6k}{k+2}a^{\frac{6k}{k+2}-1}, \quad (5.28)$$

where you can see that the second term on the RHS cancels with the first term on the RHS of equation (5.27). The final equation then looks like

$$\frac{d}{da}(\rho_\phi a^{\frac{6k}{k+2}}) = -\frac{\gamma_\phi}{aH}\frac{2k}{k+2}\frac{\rho_\phi^{l+1}}{M_P^{4l}}a^{\frac{6k}{k+2}}. \quad (5.29)$$

This expression gets simplified assuming that $\gamma_\phi \ll H$ at early times, rendering the RHS negligible and ensuring that the quantity in the parenthesis remains constant:

$$\rho_\phi(a) = \rho_{end}\left(\frac{a}{a_{end}}\right)^{-\frac{6k}{k+2}}. \quad (5.30)$$

This is the expression of how the energy density for the inflaton field evolves in time, or with the scale parameter, and it will be useful for some following computations. Let us now derive the radiation energy density. First of all we can see that

$$\frac{d}{dt}(\rho_R a^4) = \dot{\rho}_R a^4 + 4a^3\dot{a}\rho_R = a^4(\dot{\rho}_R + 4H\rho_R), \quad (5.31)$$

which highlights a similarity with the LHS of (5.12). We can again get the relation

$$\dot{\rho}_R + 4H\rho_R = \frac{1}{a^4}aH\frac{d}{da}(\rho_R a^4). \quad (5.32)$$

Therefore

$$\frac{1}{a^4}\frac{d}{da}(\rho_R a^4) = \frac{2k}{k+2}\frac{\gamma_\phi}{aH}\frac{\rho_\phi^{l+1}}{M_P^{4l}}. \quad (5.33)$$

The integration of this, considering ρ_ϕ as in Eq. (5.30) and $H^2 \propto \rho_\phi$, meaning that $H = H_{end}\left(\frac{a_{end}}{a}\right)^{\frac{3k}{k+2}}$, gives:

$$\rho_R = \frac{2k}{k+8-6kl}\frac{\gamma_\phi}{H_{end}}\frac{\rho_{end}^{l+1}}{M_P^{4l}}\left(\frac{a_{end}}{a}\right)^4\left[\left(\frac{a}{a_{end}}\right)^{\frac{k+8-6kl}{k+2}} - 1\right]. \tag{5.34}$$

Considering $a \gg a_{end}$ at later times, for the case in which $8 + k - 6kl > 0$, we can get rid of the 1 factor into parenthesis and get an expression of the radiation energy density depending on a:

$$\begin{aligned}\rho_R^{a\gg a_{end}} &= \frac{2k}{k+8-6kl}\frac{\gamma_\phi}{H_{end}}\frac{\rho_{end}^{l+1}}{M_P^{4l}}\left(\frac{a}{a_{end}}\right)^{\frac{k+8-6kl}{k+2}-4} \\ &\propto a^{\frac{-3k-6kl}{k+2}}.\end{aligned} \tag{5.35}$$

Then knowing the relation $\rho_R \propto T^4$ it is easy to derive the relation between the temperature and the scale factor, which in our $V \sim \phi^k$ model becomes k-dependent:

$$T \propto a^{-\frac{3k+6kl}{4k+8}}. \tag{5.36}$$

It needs to be noted how in the case in which $k + 8 - 6kl < 0$ and still in the limit $a \gg a_{end}$, only the -1 term survives inside the brackets and Eq. (5.34) simply reduces to

$$\begin{aligned}\rho_R^{a\gg a_{end}} &= \frac{2k}{6kl-k-8}\frac{\gamma_\phi}{H_{end}}\frac{\rho_{end}^{l+1}}{M_P^{4l}}\left(\frac{a_{end}}{a}\right)^4 \\ &\propto a^{-4},\end{aligned} \tag{5.37}$$

meaning that the temperature would here scale as

$$T \propto a^{-1}. \tag{5.38}$$

decay channel	dependence	$k=2$	$k=4$	$k=6$
$\phi \to \bar{f}f$	$T \propto a^{-\frac{3k-3}{2k+4}}$	$T \propto a^{-\frac{3}{8}}$	$T \propto a^{-\frac{3}{4}}$	$T \propto a^{-\frac{15}{16}}$
$\phi \to bb$	$T \propto a^{-\frac{3}{2k+4}}$	$T \propto a^{-\frac{3}{8}}$	$T \propto a^{-\frac{1}{4}}$	$T \propto a^{-\frac{3}{16}}$
$\phi\phi \to bb$	$T \propto a^{-\frac{9}{2k+4}}$	$T \propto a^{-1}$	$T \propto a^{-\frac{3}{4}}$	$T \propto a^{-\frac{9}{16}}$

Table 5.1: Sum up of the temperature behaviour for the three different decay channels in the T-model.

We can now compute the maximum temperature by imposing the maximum condition on the ρ_R curve, which is simply $\frac{d\rho_R}{da} = 0$.

Not considering the constant factors in Eq. (5.34), as they will get cancelled, we find

$$\begin{aligned} 0 &= \frac{d}{da}\left[\left(\frac{a}{a_{end}}\right)^{\frac{k+8-6kl}{k+2}-4} - \left(\frac{a}{a_{end}}\right)^{-4}\right] \\ &= \left(\frac{k+8-6kl}{k+2} - 4\right)\left(\frac{a}{a_{end}}\right)^{\frac{k+8-6kl}{k+2}-5} \cdot \frac{1}{a_{end}} + 4\left(\frac{a}{a_{end}}\right)^{-5} \cdot \frac{1}{a_{end}}. \end{aligned} \tag{5.39}$$

Being a_{max} the value that satisfies this relation, it is easy to see that

$$a_{max} = a_{end}\left(\frac{4k+8}{3k+6kl}\right)^{\frac{k+2}{k+8-6kl}}. \tag{5.40}$$

Plugging this value in Eq. (5.34) we can find the maximum of the curve:

$$\begin{aligned} \rho_R^{max} = \rho_R(a_{max}) &= \frac{2k}{k+8-6kl}\frac{\gamma_\phi}{H_{end}}\frac{\rho_{end}^{l+1}}{M_P^{4l}}\left(\frac{4k+8}{3k+6kl}\right)^{-\frac{4k+8}{k+8-6kl}}\left[\left(\frac{4k+8}{3k+6kl}\right)^{\frac{k+8-6kl}{k+2}\cdot\frac{k+2}{k+8-6kl}} - 1\right] \\ &= \frac{2k}{k+8-6kl}\frac{\gamma_\phi}{H_{end}}\frac{\rho_{end}^{l+1}}{M_P^{4l}}\left(\frac{4k+8}{3k+6kl}\right)^{-\frac{4k+8}{k+8-6kl}}\left[\frac{4k+8-3k-6kl}{3k+6kl}\right] \\ &= \frac{2}{3+6l}\frac{\gamma_\phi}{H_{end}}\frac{\rho_{end}^{l+1}}{M_P^{4l}}\left(\frac{4k+8}{3k+6kl}\right)^{-\frac{4k+8}{k+8-6kl}}. \end{aligned} \tag{5.41}$$

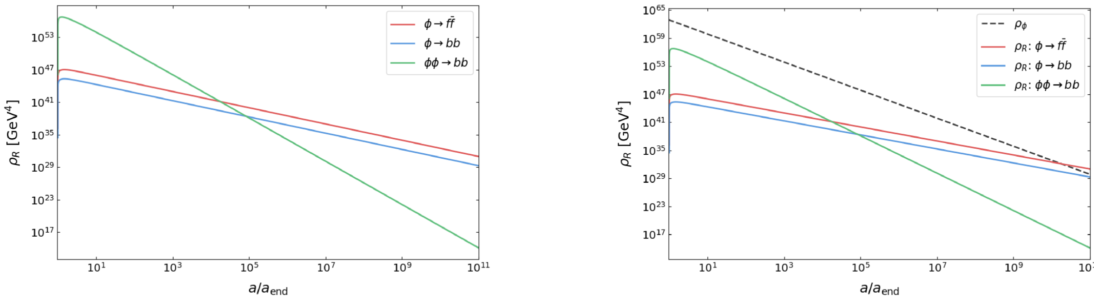

Figure 5.2: Energy density plot for the three different processes as a function of the scale factor. The values used are $k = 2$, $y = \sigma = 10^{-7}$, $\mu = 10^{-13}M_P$, $\rho_{end} = (5.2 \cdot 10^{15} GeV)^4$. On the right the inflaton energy density has been added; depending on the parameters, the two curves will intersect identifying the reheating temperature.

And consequently [28]

$$T_{max} = \left(\frac{30}{g_\rho \pi^2} \rho_R^{max} \right)^{\frac{1}{4}}. \tag{5.42}$$

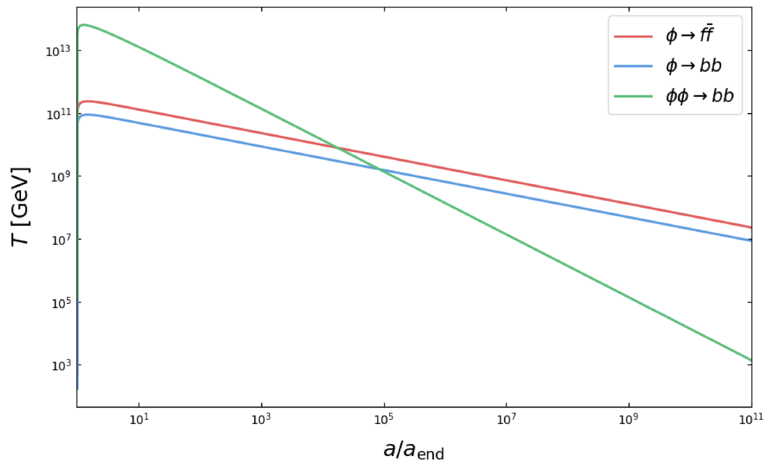

Figure 5.3: Temperature plot for the three different processes as a function of the scale factor. The values used are $k = 2$, $y = \sigma = 10^{-7}$, $\mu = 10^{-13}M_P$, $\rho_{end} = (5.2 \cdot 10^{15} GeV)^4$.

Another useful computation is the evaluation of the reheat temperature T_{RH}, which is defined as the curves of the energy density of radiation and of the inflaton field cross each other and can therefore be found imposing the condition:

$$\rho_R(T_{rh}) = \rho_\phi(T_{rh}). \tag{5.43}$$

Putting together equations (5.35) and (5.30), the condition simply becomes

$$\frac{2k}{k+8-6kl}\frac{\gamma_\phi}{H_{end}}\frac{\rho_{end}^{l+1}}{M_P^{4l}}\left(\frac{a_{end}}{a_{rh}}\right)^{\frac{3k+6kl}{k+2}} = \rho_{end}\left(\frac{a_{rh}}{a_{end}}\right)^{-\frac{6k}{k+2}}, \tag{5.44}$$

which allows us to figure out the redshift between the time of reheating and the end of inflation

$$\begin{aligned}\frac{a_{rh}}{a_{end}} &= \left[\frac{k+8-6kl}{2k}\frac{H_{end}}{\gamma_\phi}\frac{M_P^{4l}}{\rho_{end}^{l}}\right]^{\frac{k+2}{3k-6kl}} \\ &= \left[\frac{k+8-6kl}{2k}\frac{M_P^{4l-1}\rho_{end}^{\frac{1}{2}-l}}{\sqrt{3}\gamma_\phi}\right]^{\frac{k+2}{3k-6kl}}.\end{aligned} \tag{5.45}$$

valid for $8+k-6kl > 0$. Instead, in the case in which $8+k-6kl < 0$, the condition becomes

$$\frac{2k}{6kl-k-8}\frac{\gamma_\phi}{H_{end}}\frac{\rho_{end}^{l+1}}{M_P^{4l}}\left(\frac{a_{end}}{a_{rh}}\right)^{4} = \rho_{end}\left(\frac{a_{rh}}{a_{end}}\right)^{-\frac{6k}{k+2}}, \tag{5.46}$$

and one finds

$$\frac{a_{rh}}{a_{end}} = \left[\frac{6kl-k-8}{2k}\frac{M_P^{4l-1}\rho_{end}^{\frac{1}{2}-l}}{\sqrt{3}\gamma_\phi}\right]^{\frac{k+2}{2k-8}}. \tag{5.47}$$

Now we simply plug this back in one of the two equations for ρ, as they coincide at t_{rh}, to get the value of the energy density at reheating. For $8+k-6kl > 0$ we find:

$$\begin{aligned}\rho_{rh} &= \rho_{end}\left(\frac{a_{rh}}{a_{end}}\right)^{-\frac{6k}{k+2}} \\ &= \rho_{end}\left[\frac{k+8-6kl}{2k}\frac{M_P^{4l-1}\rho_{end}^{\frac{1}{2}-1}}{\sqrt{3}\gamma_\phi}\right]^{-\frac{6k}{k+2}\frac{k+2}{3k-6kl}} \\ &= \rho_{end}\left[\frac{k+8-6kl}{2k}\frac{M_P^{4l-1}\rho_{end}^{\frac{1}{2}-1}}{\sqrt{3}\gamma_\phi}\right]^{-\frac{2}{1-2l}}.\end{aligned} \tag{5.48}$$

Lastly, we use this relation to get the value of T_{rh} which will look like:

$$\begin{aligned} T_{rh} = \left(\frac{30}{g_*(T_{rh})\pi^2}\right)^{\frac{1}{4}} \rho_{rh}^{\frac{1}{4}} &= \left(\frac{30}{g_*(T_{rh})\pi^2}\right)^{\frac{1}{4}} \rho_{end}^{\frac{1}{4}} \left[\frac{k+8-6kl}{2k} \cdot \frac{M_P^{4l-1}\rho_{end}^{\frac{1}{2}-l}}{\sqrt{3}\gamma_\phi}\right]^{-\frac{1}{2-4l}} \\ &= \left(\frac{30}{g_*(T_{rh})\pi^2}\right)^{\frac{1}{4}} \left[\frac{k+8-6kl}{2k} \cdot \frac{M_P^{4l-1}}{\sqrt{3}\gamma_\phi}\right]^{-\frac{1}{2-4l}} \rho_{end}^{\frac{1}{4}} \rho_{end}^{-(\frac{1}{2}-l)(\frac{1}{2-4l})} \\ &= \left(\frac{30}{g_*(T_{rh})\pi^2}\right)^{\frac{1}{4}} \left[\frac{k+8-6kl}{2k} \cdot \frac{M_P^{4l-1}}{\sqrt{3}\gamma_\phi}\right]^{-\frac{1}{2-4l}} . \end{aligned} \tag{5.49}$$

The same procedure can be applied for the case in which $8+k-6kl < 0$; using Eq. (5.47) for the redshift we get the same structure for the energy density, but with the opposit sign inside of the squared parenthesis and a different exponent, specifically $-\frac{3k}{k-4}$. We then find the following reheating temperature:

$$T_{rh} = \left(\frac{30}{g_*(T_{rh})\pi^2}\right)^{\frac{1}{4}} \left[\frac{6kl-k-8}{2k} \cdot \frac{M_P^{4l-1}}{\sqrt{3}\gamma_\phi} \cdot \rho_{end}^{\frac{k-6kl+8}{6k}}\right]^{-\frac{3k}{4k-16}} . \tag{5.50}$$

5.2 Axions produced via Misalignment during Reheating

In this section we will analyze the production of QCD axions via the standard misalignment mechanism, already seen in chapter 3, during the epoch of reheating. Specifically we will have a DM abundance which we will assume to be produced by axions when the misalignment mechanism takes place after the inflaton domination, where the temperature is no longer simply inversely dependent on the scale factor. In chapter 3 we already presented the Lagrangian term for the axion field and its consequent equations of motion:

$$\ddot{\theta} + 3H\dot{\theta} + \tilde{m}_a^2(t)\sin\theta = 0, \tag{5.51}$$

where $\theta(t) \equiv \frac{a(t)}{f_a}$. We will now analyse different temperature regimes, namely when the oscillations of the axion field takes place either before or after the reheating phase started.

5.2.1 Misalignment after reheating: $T_{rh} \geq T_{osc}$

The dynamics of the axion field is encoded in the previous equation; for example this tells us that the axion will start to oscillate at a temperature T_{osc} which is reached at the condition $3H(T_{osc}) \equiv \tilde{m}_a(T_{osc})$. We will consider

$$H^2(T) = \frac{\rho(T)}{3M_P^2} \tag{5.52}$$

and, as seen in Chapter 3, the mass gets a temperature dependence such as

$$\tilde{m}_a(T) = m_a \times \begin{cases} \left(\frac{T_{QCD}}{T}\right)^4 & \text{for } T > T_{QCD} \\ 1 & \text{for } T < T_{QCD} \end{cases}, \tag{5.53}$$

where m_a is the axion mass at zero temperature and can be expressed as

$$m_a \simeq 5.7 \times 10^{-6} \left(\frac{10^{12} GeV}{f_a}\right) eV. \tag{5.54}$$

Plugging these two expressions into the oscillation condition required we get the following oscillation temperature:

$$T_{osc} \simeq \begin{cases} \left(\sqrt{\frac{10}{g_*(T_{osc})}} \frac{M_P}{\pi} m_a\right)^{\frac{1}{2}} & \text{for } T_{osc} \leq T_{QCD} \\ \left(\sqrt{\frac{10}{g_*(T_{osc})}} \frac{M_P}{\pi} m_a T_{QCD}^4\right)^{\frac{1}{6}} & \text{for } T_{osc} \geq T_{QCD} \end{cases}, \tag{5.55}$$

where, since misalignement and hence oscillations started after reheating took place, radiation domination has been assumed, meaning $H \propto T^2$.

5.2.2 Misalignment during reheating: $T_{rh} < T_{osc}$

In this case, instead, we take into consideration oscillations of the axion that start during the reheating period.

We can now discuss two additional scenarios.

$T_{QCD} < T_{osc}$

We can check that from Eq. (5.53) the axion mass is temperature dependent. In this regime one gets the expression for the oscillation temperature by imposing once again $3H(T_{osc}) = \tilde{m}_a(T_{osc})$. We can use the relation between the Hubble rate and temperature

$$H \sim \rho^{\frac{1}{2}} \sim a^{-\frac{3}{2}(1+\omega_\phi)} = a^{-\frac{3k}{k+2}}, \tag{5.56}$$

in our model, where $\omega_\phi = \frac{k-2}{k+2}$. This tells us that the relation between the Hubble rate and the scale factor is

$$H(a) = H(a_{rh})\left(\frac{a_{rh}}{a}\right)^{\frac{3k}{k+2}}, \tag{5.57}$$

which is in agreement with the result found in the previous section.
And using the temperature dependence on the scale factor written in Eq. (5.36), due to the fact that the inflaton is decaying during reheating:

$$H(T) = H(T_{rh})\left(\frac{T}{T_{rh}}\right)^{\frac{4}{1+2l}}. \tag{5.58}$$

Matching this expression with (5.53) in the oscillation condition:

$$\pi\sqrt{\frac{g_*(T_{rh})}{10}}\frac{T_{rh}^2}{M_P}\left(\frac{T_{osc}}{T_{rh}}\right)^{\frac{4}{1+2l}} = m_a\left(\frac{T_{osc}}{T_{QCD}}\right)^{-4}. \tag{5.59}$$

After a simple manipulation this yields

$$T_{osc} = T_{rh}\left(\frac{1}{\pi}\sqrt{\frac{10}{g_*(T_{rh})}}\frac{m_a \cdot T_{QCD}^4 \cdot M_P}{T_{rh}^6}\right)^{\frac{1+2l}{8+8l}}. \tag{5.60}$$

$T_{QCD} > T_{osc}$

In this case (5.53) tells us that the axion mass is constant, so the matching equation will just be

$$\pi\sqrt{\frac{g_*(T_{rh})}{10}}\frac{T_{rh}^2}{M_P}\left(\frac{T_{osc}}{T_{rh}}\right)^{\frac{4}{1+2l}} = m_a, \tag{5.61}$$

which implies

$$T_{osc} = T_{rh}\left(\frac{1}{\pi}\sqrt{\frac{10}{g_*(T_{rh})}}\frac{m_a \cdot M_P}{T_{rh}^2}\right)^{\frac{1+2l}{4}}. \tag{5.62}$$

We will now use the two equations (5.60) or (5.62) and (5.49) or (5.50), that express respectively the oscillation and the reheating temperature, to impose constraints related to the regime that we are interested in analyzing, specifically when $t_{rh} > t_{osc}$, meaning when the axion field starts oscillating while the inflaton is decaying and injecting entropy in the thermal bath. We therefore look at the inequality

$$T_{osc} > T_{rh}, \tag{5.63}$$

which gives us different constraints depending on the regime we are working on. The goal is to find a constraint on the value of the couplings that will depend on a function $f(m_a, k, l)$ of the continuous variable m_a and of the two discrete variables k and l, representing respectively the power of the model chosen and the decay channel that we are probing.

Let us first analyze the possibility in which $8 + k - 6kl > 0$, as surely the fermionic and bosonic decays will always satisfy those conditions for the potentials studied in this thesis ($k = 2, 4, 6$). The only situation in which this is not satisfied is the bosonic annihilation for $k = 2$, which will then analyzed separately.

Consider again the case in which $T_{QCD} < T_{osc}$; in this case we use Eq. (5.60) to get the wanted relation

$$\left(\frac{30}{g_*(T_{rh})\pi^2}\right)^{\frac{1}{4}}\left[\frac{2k}{k+8-6kl}\frac{\sqrt{3}\gamma_\phi}{M_P^{4l-1}}\right]^{\frac{1}{2-4l}} < \left(\frac{1}{\pi}\sqrt{\frac{10}{g_*(T_{rh})}}m_a M_P T_{QCD}^4\right)^{\frac{1}{6}}. \tag{5.64}$$

Through algebraic manipulation, we can extract a constraint on γ_ϕ that looks like

$$\gamma_\phi < \frac{k+8-6kl}{2k}\cdot\frac{M_P^{4l-1}}{\sqrt{3}}\left[\left(\frac{g_*(T_{rh})\pi^2}{30}\right)^{\frac{1}{4}}\cdot\left(\sqrt{\frac{1}{\pi^2}\frac{10}{g_*(T_{rh})}}\cdot m_a M_P T_{QCD}^4\right)^{\frac{1}{6}}\right]^{2-4l}. \tag{5.65}$$

This is the function $f(m_a, k, l)$ that was mentioned before. We know that γ_ϕ is related to the couplings of the three interactions discussed in the previous section; this means that expliciting this dependence we can obtain constraints on the three couplings y_{eff}, μ_{eff} and σ_{eff}.
Expliciting γ_ϕ, the couplings will have constraints that look like:

$$y_{\text{eff}}^2 < \frac{4\pi}{\sqrt{3}}\frac{14-2k}{k^{\frac{3}{2}}\sqrt{k-1}}\lambda^{-\frac{1}{k}}\left(\frac{\pi^4 g_*(T_{rh})^2}{3\cdot 900}\frac{1}{M_P^{10}}T_{QCD}^8\right)^{\frac{1}{3k}}\cdot m_a^{\frac{2}{3k}} \tag{5.66}$$

for the fermionic decay;

$$\mu_{\text{eff}}^2 < \frac{4\pi}{\sqrt{3}}\sqrt{\frac{k-1}{k}}(4k+2)M_P^{\frac{4}{k}-2}\lambda^{\frac{1}{k}}\left(\frac{\sqrt{10}\cdot g_*(T_{rh})}{30^{\frac{3}{2}}}\cdot\pi^2 M_P T_{QCD}^4\right)^{\frac{2}{3}(1-\frac{1}{k})}\cdot m_a^{\frac{2}{3}(1-\frac{1}{k})} \tag{5.67}$$

for the bosonic decay;

$$\sigma_{\text{eff}}^2 < \frac{4\pi}{\sqrt{3}}\sqrt{k}(k-1)^{\frac{3}{2}}(4k-10)\lambda^{\frac{3}{k}}\left(\frac{\sqrt{10}}{M_P^5}\frac{g_*(T_{rh})}{30^{\frac{3}{2}}}\pi^2 T_{QCD}^4\right)^{\frac{2}{3}(1-\frac{3}{k})}\cdot m_a^{\frac{2}{3}(1-\frac{3}{k})} \tag{5.68}$$

for the bosonic annihilation. Again, it is to be noted that this last derivation is only valid for the case in which $k = 4, 6$. For the bosonic annihilation in the case $k = 2$ the term $8 + k - 6kl = -2 < 0$, meaning that the reheating temperature used has to be (5.50). Moreover in this regime the temperature scales as $T \propto a^{-1}$, so the Hubble dependence on it changes too. We can obtain for $T_{QCD} < T_{osc}$ and $k = 2$ an oscillation temperature of

$$T_{osc} = \left[\frac{M_P}{\pi}\sqrt{\frac{10}{g_*(T_{rh})}}m_a T_{QCD}^4\right]^{\frac{1}{6}}, \tag{5.69}$$

which is consistently in agreement to eq. (5.55). The condition $T_{osc} > T_{rh}$ gives then the constraint

$$\left(\frac{30}{g_*(T_{rh})\pi^2}\right)^{\frac{1}{4}}\left[2\sqrt{3}\frac{\gamma_\phi}{M_P^3}\rho_{end}^{\frac{1}{6}}\right]^{-\frac{3}{4}} < \left[\frac{M_P}{\pi}\sqrt{\frac{10}{g_*(T_{rh})}}m_a T_{QCD}^4\right]^{\frac{1}{6}}, \tag{5.70}$$

and hence

$$\sigma_{\text{eff}}^2 < \frac{4\pi}{\sqrt{3}}2^{\frac{3}{2}}\frac{\lambda^{\frac{3}{2}}}{\rho_{end}^{\frac{1}{6}}}M_P^2\left(\frac{g_*(T_{rh})\pi^2}{30}\right)^{-\frac{1}{3}}\left[\frac{M_P}{\pi}\sqrt{\frac{10}{g_*(T_{rh})}}T_{QCD}^4 m_a\right]^{-\frac{2}{9}}. \tag{5.71}$$

If, instead, we look at the $T_{QCD} > T_{osc}$ regime, we can employ relation (5.62) and get the following inequality

$$\left(\frac{1}{\pi}\sqrt{\frac{10}{g_*(T_{rh})}}\frac{m_a M_P}{T_{rh}^2}\right)^{\frac{1+2l}{4}} > 1, \tag{5.72}$$

which results in

$$T_{rh} < \left(\frac{1}{\pi}\sqrt{\frac{10}{g_*(T_{rh})}}m_a M_P\right)^{\frac{1}{2}}. \tag{5.73}$$

Now, substituting the expression for T_{RH} found in (5.49), we get

$$\left(\frac{30}{g_*(T_{rh})\pi^2}\right)^{\frac{1}{4}}\left[\frac{2k}{k+8-6kl}\frac{\sqrt{3}\gamma_\phi}{M_P^{4l-1}}\right]^{\frac{1}{2-4l}} < \left(\frac{1}{\pi^2}\frac{10}{g_*(T_{RH})}\right)^{\frac{1}{4}}\sqrt{m_a M_P}, \tag{5.74}$$

yielding the wanted inequality

$$\gamma_\phi < \frac{k+8-6kl}{2k}\cdot\frac{M_P^{2l}}{\sqrt{3}}\left(\frac{1}{3}\right)^{\frac{1}{2}-l}\cdot m_a^{1-2l}. \tag{5.75}$$

The results for the couplings in this regime are:

$$y_{\text{eff}}^2 < \frac{8\pi}{\sqrt{k(k-1)}}\frac{7-k}{k}\frac{1}{\sqrt{3}}\left(\frac{1}{3}\frac{m_a^2}{M_P^2}\frac{1}{\lambda}\right)^{\frac{1}{k}} \tag{5.76}$$

for the fermionic decay;

$$\mu_{\text{eff}}^2 < \frac{4\pi}{3\sqrt{3}}\sqrt{\frac{k-1}{k}}(4k+2)(3\lambda M_P^2)^{\frac{1}{k}}m_a^{2-\frac{2}{k}} \tag{5.77}$$

for the bosonic decay;

$$\sigma_{\text{eff}}^2 < \frac{4\pi}{\sqrt{3}}\sqrt{k}(k-1)^{\frac{3}{2}}\frac{(4k-10)}{3M_P^2}(3\lambda M_P^2)^{\frac{3}{k}}m_a^{2-\frac{6}{k}} \tag{5.78}$$

for the bosonic annihilation in the case $k = 4, 6$. Similarly, for $k = 2$ in the $T_{QCD} > T_{osc}$ regime, the oscillation temperature becomes

$$T_{osc} = \left[\frac{M_P}{\pi}\sqrt{\frac{10}{g_*(T_{rh})}}m_a\right]^{\frac{1}{2}}. \tag{5.79}$$

The condition $T_{osc} > T_{RH}$ gives then the constraint

$$\left(\frac{30}{g_*(T_{RH})\pi^2}\right)^{\frac{1}{4}}\left[2\sqrt{3}\frac{\gamma_\phi}{M_P^3}\rho_{end}^{\frac{1}{6}}\right]^{-\frac{3}{4}} < \left[\frac{M_P}{\pi}\sqrt{\frac{10}{g_*(T_{RH})}}m_a\right]^{\frac{1}{2}}, \tag{5.80}$$

and hence

$$\sigma_{eff}^2 < \frac{4\pi}{\sqrt{3}} 2^{\frac{3}{2}} \frac{\lambda^{\frac{3}{2}}}{\rho_{end}^{\frac{1}{6}}} M_P^2 \left(\frac{g_*(T_{RH})\pi^2}{30} \right)^{-\frac{1}{3}} \left[\frac{M_P}{\pi} \sqrt{\frac{10}{g_*(T_{RH})}} m_a \right]^{-\frac{2}{3}}. \tag{5.81}$$

Taking the square root we can plot a curve corresponding to the upper bound of each coupling. Moreover we can make use of experimental constraints to find a specific range on the x-axis. Specifically, we will consider the following validity range regarding m_a in the case of QCD axions:

$$10^{-6}\text{eV} < m_a < 10^{-5}\text{eV}. \tag{5.82}$$

This choice is valid whenever the initial misalignment angle is considered to be of order $\theta_i \sim \mathcal{O}(1)$, as can be seen from [44]. We will therefore restrict to this regime of validity, considering $\theta_i \in [0.1; 1]$. Moreover, we can use the following expression for λ (see App. D):

$$\lambda \simeq \frac{18\pi^2 A_{S*}}{6^{\frac{k}{2}} N_*^2}. \tag{5.83}$$

From [31] we can see the values of λ used depending on the different values of k; for the case of $k = 2$ we can compute it from the formula, keeping in mind that the values used are $A_{S*} = 2.1 \cdot 10^{-9}$ [50] and $N_* = 55$. A note has to be made for the latter: the number of e-folds belongs to $N_* \in (50, 60)$; here, a fiducial value of $N_* = 55$ is adopted. Although a dependence on the specific channel probed exists, this difference is sufficiently small that the average value of 55 is considered to be a good approximation.

k	λ
2	$2.06 \cdot 10^{-11}$
4	$3.43 \cdot 10^{-12}$
6	$25.71 \cdot 10^{-13}$

Table 5.2: Values of λ used for each value of k.

Lastly, as far as the relativistic degrees of freedom are concerned, seing that their value is temperature dependent, we refer to [19] in order to derive them in the different regimes we are interested in.

$T_{QCD} < T_{osc}$		$T_{QCD} > T_{osc}$
$T_{QCD} < T_{RH} < T_{osc}$	$T_{RH} < T_{QCD} < T_{osc}$	
$g_* \in [61.75; 106.75]$	$g_* \in [10.75; 17.25]$	

Table 5.3: Summary of [19] results for $g_*(T)$. As we can see, we can take an average value for each of the two regimes, respectively 84.25 and 14.01, considering that the approximation will cause a variation of the order of at most 2, hence negligible.

If we check the dimensionalities of the couplings, we will see that y_{eff} and σ_{eff} are both dimensionless, whereas μ_{eff} has the dimension of a mass. To ensure consistent dimensionality in the plot, it has hence been divided by a quantity with mass-dimension 1. What could be used is either M_P or $m_{\phi(a_{end})}$, which can be evaluated from (5.14) inserting the condition that

$$\phi_{end} = \sqrt{\frac{3}{8}} M_P \ln\left[\frac{1}{2} + \frac{k}{3}(k + \sqrt{k^2+3})\right], \tag{5.84}$$

which comes from the approximated solution to $\dot{\phi}^2_{end} = V(\phi)$. In the end what we divide by will become

$$m_\phi = M_P \left[k(k-1)\lambda\left[\sqrt{\frac{3}{8}} \ln\left(\frac{1}{2} + \frac{k}{3}(k + \sqrt{k^2+3})\right)^{k-2}\right]\right]^{\frac{1}{2}}. \tag{5.85}$$

We are finally able to plot the bounds found for the couplings, in the different temperature regimes analysed.

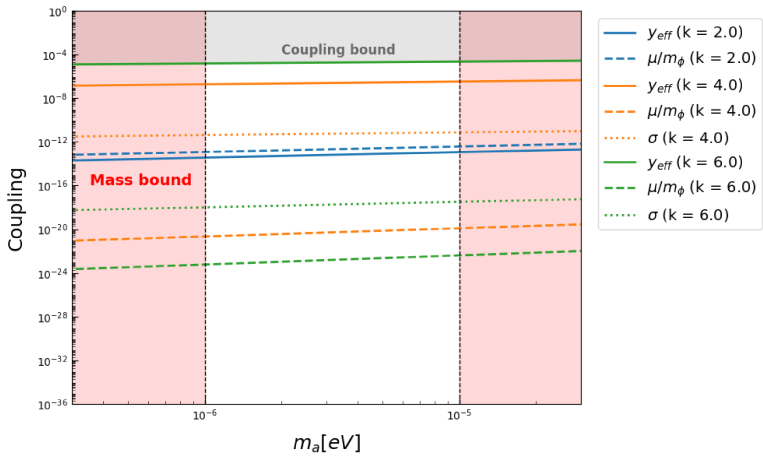

Figure 5.4: Plot of the bounds on the coupling for $T_{QCD} > T_{osc}$. As can be seen in table 5.3 the value of $g_*(T_{rh})$ has been taken to be ~ 14.1. The shaded grey region indicates the range of validity of this coupling due to the constraints found (in this case it refers to y_{eff} for $k = 6$, in general the excluded region is the one above the lines), whereas the red shading is due to the regime of m_a considered.

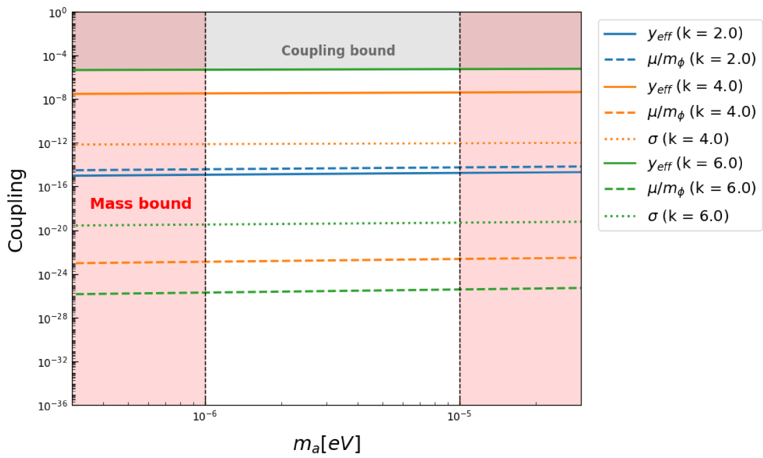

Figure 5.5: Plot of the bounds on the coupling for $T_{QCD} < T_{osc}$. Here the value of $g_*(T_{rh})$ has been taken to be ~ 14.1.

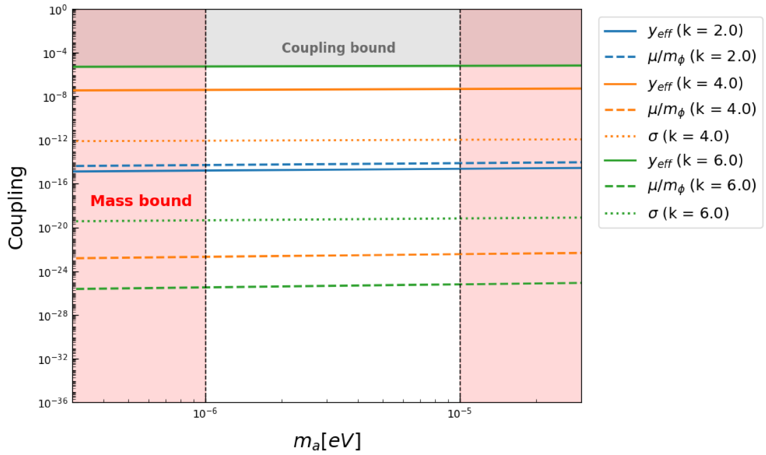

Figure 5.6: Plot of the bounds on the coupling for $T_{QCD} < T_{osc}$. In this case $g_*(T_{rh})$ has been taken to be ~ 84.25.

To conclude, one could also get the correspondence between the couplings and the reheating temperature, expliciting (5.49). For instance, for the fermionic coupling one would find

$$T_{rh} = \left(\frac{30}{g_*(T_{rh})\pi^2}\right)^{\frac{1}{4}} \cdot \left[\frac{k}{7-k}\sqrt{3}\sqrt{k(k-1)}\frac{(M_P^4\lambda)^{\frac{1}{k}}}{8\pi}\right]^{\frac{k}{4}} \cdot y_{\text{eff}}^{\frac{k}{2}}. \tag{5.86}$$

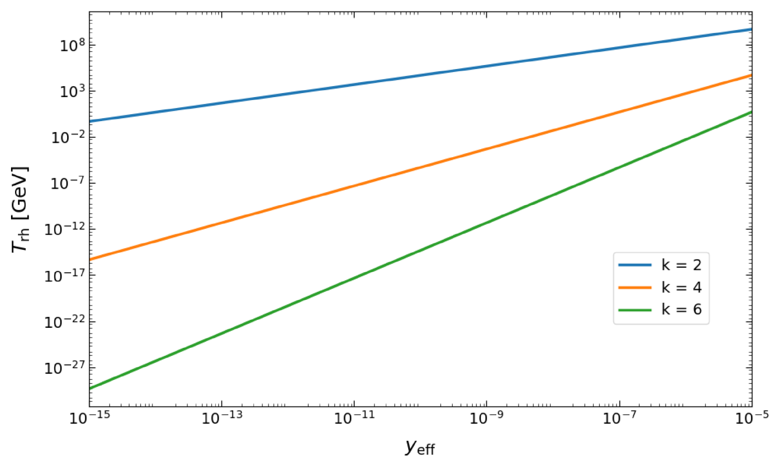

Figure 5.7: Plot of the behaviour of the reheating temperature as a function of the fermionic coupling as seen in Eq. (5.86).

5.2.3 ALPs

In the case of axion-like particles the mass m_a does not depend on time, therefore the oscillation temperature can be obtained in the same way as (5.62):

$$T_{osc} = T_{rh}\left(\frac{1}{\pi}\sqrt{\frac{10}{g_*(T_{rh})}}\frac{m_a \cdot M_P}{T_{rh}^2}\right)^{\frac{1+2l}{4}} \tag{5.87}$$

The calculations that follow and the bounds found will then coincide with the scenario in which $T_{QCD} > T_{osc}$.

5.3 Gravitational axions

In Section 5.2 we talked about axion production via the standard misalignment mechanism, where the axion behaved as a scalar field and its initial position led it to oscillate along the potential, leading to the observed DM production.

We now look at another production mechanism, specifically 2-to-2 processes mediated by a graviton, that can emerge from the thermal bath and from the scattering of the inflaton condensate.

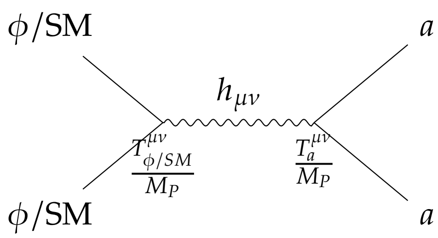

Figure 5.8: s-channel gravitational production of axions.

We want to understand how non-minimal couplings [55]

$$\xi_S S^2 R, \tag{5.88}$$

affect the production of gravitational dark matter during reheating. We can assume the scalar in the final state to be the DM particle produced from the graviton-mediated process [3]. We therefore consider couplings between matter particles, that are mediated by massless gravitons. Firstly, expanding the metric around the flat spacetime, $g_{\mu\nu} \simeq \eta_{\mu\nu} + \frac{2h_{\mu\nu}}{M_P}$, we can see the interaction term emerging from the action as

$$\sqrt{-g}\mathcal{L}_{int} = -\frac{1}{M_P} h_{\mu\nu}(T^{\mu\nu}_{SM} + T^{\mu\nu}_{\phi} + T^{\mu\nu}_{a}), \tag{5.89}$$

where the stress-energy tensors have indices representing SM fields, the inflaton and BSM fields (in our case, the axion), respectively. The form of the stress energy tensor $T^{\mu\nu}_i$ depends on the spin of the field [56]. In the case of scalar DM or the inflaton it looks like

$$T^{\mu\nu}_S = \partial^\mu S \partial^\nu S - g^{\mu\nu}\left[\frac{1}{2}\partial^\alpha S \partial_\alpha S - V(S)\right], \tag{5.90}$$

where $S = a, \phi$ is the scalar.

The objective is the analysis of these interactions, to determine if they can account for the correct amount of dark matter observed today.

The interaction considered will then be [60] [42]

$$\phi/SM^a(p_1) + \phi/SM^a(p_2) \to X^b(p_3) + X^b(p_4), \tag{5.91}$$

and it will be mediated by the graviton, which has momentum $k = p_1 + p_2$. We evaluate the tree level amplitude by contracting with the indices of the graviton's propagator:

$$\mathcal{M}^{ab} = M^a_{\mu\nu}\Pi^{\mu\nu\rho\sigma}M^b_{\rho\sigma}, \tag{5.92}$$

where the propagator for a massless graviton of momentum k has, in the De Donder gauge, the form

$$\Pi^{\mu\nu\rho\sigma}(k) = \frac{\eta^{\rho\nu}\eta^{\sigma\mu} + \eta^{\rho\mu}\eta^{\sigma\nu} - \eta^{\rho\sigma}\eta^{\mu\nu}}{2k^2}, \tag{5.93}$$

and the indices a, b denote respectively the spins of the SM and DM particles, the initial and final states of the process.

Considering that we are looking for axionic DM, we will restrict ourselves to the case of scalar dark matter. In this case, the partial amplitude for the final state can be expressed as

$$M^0_{\mu\nu} = \frac{1}{2}[p_{1\mu}p_{2\nu} + p_{1\nu}p_{2\mu} - \eta_{\mu\nu}(p_1 \cdot p_2 + m^2)]. \tag{5.94}$$

The rate will be evaluated assuming massless initial states, which is justified by the large energy associated to their momenta p_1 and p_2 at the end of inflation, so large that it dominates over electroweak scale massess.

There are two gravitational production mechanisms, both represented in Fig. 5.8:

- Production from the thermal plasma. The interactions considered will be $SM + SM \rightarrow a + a$ and the SM particles in the initial states will either be scalars, fermions or bosons.
- Production from the inflaton condensate. The interaction will be $\phi + \phi \rightarrow a + a$ and the evaluation of the matrix element will be done considering the inflaton not as made of particles with different energies, but as a coherent collection of non-relativistic quanta at rest, hence as an oscillating classical field.

In the following subsections the derivation of the matrix elements necessary to evaluate the rate of the two processes will be presented.

5.3.1 Thermal scattering

We first calculate the rate of production in the case of scattering of SM particles mediated by a graviton.

Scalar initial state

Let us start with the case in which the SM particles in the initial state are scalars. Assuming that we are in the high energy limit, neglecting then the mass term in (5.94), the evaluation required becomes

$$
\begin{aligned}
\mathcal{M}^{00} &= \frac{1}{8k^2}[p_{1\mu}p_{2\nu} + p_{1\nu}p_{2\mu} - \eta_{\mu\nu}p_1 \cdot p_2][\eta^{\rho\nu}\eta^{\sigma\mu} + \eta^{\rho\mu}\eta^{\sigma\nu} - \eta^{\rho\sigma}\eta^{\mu\nu}]\times \\
&\qquad \times [p_{3\rho}p_{4\sigma} + p_{3\sigma}p_{4\rho} - \eta_{\rho\sigma}p_3 \cdot p_4] \\
&= \frac{1}{8k^2}[p_{1\mu}p_{2\nu} + p_{1\nu}p_{2\mu} - \eta_{\mu\nu}p_1 \cdot p_2][2p_3^{\mu}p_4^{\nu} + 2p_3^{\nu}p_4^{\mu}] \\
&= \frac{1}{8k^2}[4(p_1 \cdot p_3)(p_2 \cdot p_4) + 4(p_1 \cdot p_4)(p_2 \cdot p_3) - 4(p_1 \cdot p_2)(p_3 \cdot p_4)].
\end{aligned}
\tag{5.95}
$$

It is easier to now introduce the Mandelstam variables. Using the fact that $s = (p_1 + p_2)^2 \simeq 2(p_1 \cdot p_2)$, $t = (p_1 - p_3)^2 \simeq -2(p_1 \cdot p_3)$, $u = (p_1 - p_4)^2 \simeq -2(p_1 \cdot p_4)$, moreover that by momentum conservation $p_1 + p_2 = k = p_3 + p_4$ and that in the massless limit $s + t + u \approx 0$, so that we can write $u = -(s + t)$, this equation becomes

$$\begin{aligned}\mathcal{M}^{00} &= \frac{1}{2s}\left[\left(\frac{t}{2}\right)^2 + \left(\frac{u}{2}\right)^2 - \left(\frac{s}{2}\right)^2\right] \\ &= \frac{1}{8s}[t^2 + (s+t)^2 - s^2] = \frac{1}{4s}(t^2 + st).\end{aligned} \tag{5.96}$$

Now, adding the coupling at the vertex and squaring, we get:

$$|\mathcal{M}^{00}|^2 = \frac{1}{16M_P^4}\frac{t^2(s+t)^2}{s^2}. \tag{5.97}$$

Fermionic initial state

The second matrix element that needs to be evaluated is the one in which the SM particles in the interaction are taken to be fermions; Eq. (5.92) gets then modified and one needs to consider the matrix element of the initial particles as the fermionic one, and the one of the final particles still as the scalar, being in our assumption the product again made of axions:

$$\mathcal{M}^{\frac{1}{2}0} = M^{\frac{1}{2}}_{\mu\nu}\Pi^{\mu\nu\rho\sigma}M^{0}_{\rho\sigma}. \tag{5.98}$$

In this case the fermionic partial amplitude is

$$M^{\frac{1}{2}}_{\mu\nu} = \frac{1}{4}\bar{v}(p_2)[\gamma_\mu(p_1-p_2)_\nu + \gamma_\nu(p_1-p_2)_\mu]u(p_1). \tag{5.99}$$

This leads to

$$\begin{aligned}\mathcal{M}^{\frac{1}{2}0} &= \frac{1}{16k^2}\bar{v}(p_2)[\gamma_\mu(p_1-p_2)_\nu + \gamma_\nu(p_1-p_2)_\mu]u(p_1)[\eta^{\rho\mu}\eta^{\sigma\nu} + \eta^{\rho\nu}\eta^{\sigma\mu} - \eta^{\rho\sigma}\eta^{\mu\nu}]\times \\ &\qquad \times [p_{3\rho}p_{4\sigma} + p_{3\sigma}p_{4\rho} - \eta_{\rho\sigma}p_3\cdot p_4] \\ &= \frac{1}{16k^2}\bar{v}(p_2)[\gamma_\mu(p_1-p_2)_\nu + \gamma_\nu(p_1-p_2)_\mu]u(p_1)\times \\ &\qquad \times (2p_3^\mu p_4^\nu + 2p_3^\nu p_4^\mu - 4\eta^{\mu\nu}p_3\cdot p_4 + 4\eta^{\mu\nu}p_3\cdot p_4) \\ &= \frac{1}{16k^2}\bar{v}(p_2)[4\not{p}_3(p_1-p_2)\cdot p_4 + 4\not{p}_4(p_1-p_2)\cdot p_3]u(p_1) \\ &= \frac{1}{4k^2}\bar{v}(p_2)[\not{p}_3(q\cdot p_4) + \not{p}_4(q\cdot p_3)]u(p_1),\end{aligned} \tag{5.100}$$

where, to make things easier, we defined $q = p_1 - p_2$. Moreover we have the momentum conservation relations $p_1 + p_2 = p_3 + p_4 = k$. We will use the Mandelstam variables that we had introduced for the scalar case, which allow us the rewriting of the amplitude in the form

$$\mathcal{M}^{\frac{1}{2}0} = \frac{1}{4k^2}\bar{v}(p_2)[\frac{s+2t}{2}\not{p}_3 - \frac{s+2t}{2}\not{p}_4]u(p_1) = \frac{s+2t}{4s}\bar{v}(p_2)[\not{p}_3]u(p_1), \quad (5.101)$$

where we used the Dirac equations $\not{p}_1 u(p_1) = 0$ and $\bar{v}(p_2)\not{p}_2 = 0$, together with the fact that from momentum conservation $p_3 - p_4 = 2p_3 - (p_1 + p_2)$. Squaring this we get

$$|\mathcal{M}^{\frac{1}{2}0}|^2 = \frac{(s+2t)^2}{16s^2} tr[\not{p}_2\not{p}_3\not{p}_1\not{p}_3]. \quad (5.102)$$

We now use the properties of the trace, specifically the ones concerning the trace over 4 γ-matrices:

$$tr[\not{a}\not{b}\not{c}\not{d}] = 4[(a\cdot b)(c\cdot d) - (a\cdot c)(b\cdot d) + (a\cdot d)(b\cdot c)]. \quad (5.103)$$

In our case this gives us

$$\begin{aligned}|\mathcal{M}^{\frac{1}{2}0}|^2 &= \frac{(s+2t)^2}{16s^2}4[(p_2\cdot p_3)(p_1\cdot p_3) + (p_2\cdot p_3)(p_3\cdot p_1)]\\ &= \frac{(s+2t)^2}{16s^2}[2ut]\\ &= \frac{(-t(s+t))(s+2t)^2}{8s^2}.\end{aligned} \quad (5.104)$$

Adding the coupling at the vertex, and averaging over all possible initial spin states ($|\bar{\mathcal{M}}|^2 = \frac{1}{1+2s_1}\frac{1}{1+2s_2}\sum_{allspins}|\mathcal{M}|^2$, where in our fermionic case $s_1 = s_2 = 1/2$) this is finally:

$$|\mathcal{M}^{\frac{1}{2}0}|^2 = \frac{(-t(s+t))(s+2t)^2}{32M_p^4 s^2}. \quad (5.105)$$

Bosonic initial state

Lastly, we consider a bosonic initial state, whose partial amplitude is

$$\begin{aligned}M^1_{\mu\nu} =& \frac{1}{2}[\epsilon_2^*\epsilon_1(p_{1\mu}p_{2\nu} + p_{1\nu}p_{2\mu}) - \epsilon_2^* p_1(p_{2\mu}\epsilon_{1\nu} + \epsilon_{1\mu}p_{2\nu}) - \epsilon_1 p_2(p_{1\nu}\epsilon_{2\mu}^*\\ &+ \epsilon_{2\nu}^* p_{1\mu}) + p_1 p_2(\epsilon_{1\mu}\epsilon_{2\nu}^* + \epsilon_{1\nu}\epsilon_{2\mu}^*) + \eta_{\mu\nu}(\epsilon_2^*\cdot p_1\epsilon_1\cdot p_2 - p_1\cdot_2 \epsilon_2^*\epsilon_1)].\end{aligned} \quad (5.106)$$

The contraction between the propagator and the scalar final state gives

$$\Pi^{\mu\nu\rho\sigma}\mathcal{M}^{0}_{\rho\sigma} = \frac{1}{s}(p_{3\mu}p_{4\nu} + p_{3\nu}p_{4\mu}), \tag{5.107}$$

which in the contraction with eq. (5.106) is symmetric in the μ and ν indices and therefore gives

$$\begin{aligned}\mathcal{M}^{10} = \frac{1}{s}\{&(\epsilon_2^* \cdot \epsilon_1)[(p_1 \cdot p_3)(p_2 \cdot p_4) + (p_1 \cdot p_4)(p_2 \cdot p_3)] - (\epsilon_2^* \cdot p_1)[(p_2 \cdot p_3)(\epsilon_1 \cdot p_4)\\ &+ (p_3 \cdot \epsilon_1)(p_2 \cdot p_4)] - (\epsilon_1 \cdot p_2)[(p_1 \cdot p_4)(p_3 \cdot \epsilon_2^*) + (p_1 \cdot p_3)(\epsilon_2^* \cdot p_4)] + (p_1 \cdot p_2)\\ &[(\epsilon_1 \cdot p_3)(\epsilon_2^* \cdot p_4) + (\epsilon_1 \cdot p_4)(\epsilon_2^* \cdot p_3)] + (p_3 \cdot p_4)[(\epsilon_2^* \cdot p_1)(\epsilon_1 \cdot p_2) - (p_1 \cdot p_2)(\epsilon_2^* \cdot \epsilon_1)]\}.\end{aligned} \tag{5.108}$$

Due to the length of this derivation, the intermediate steps are omitted. Substituting the Mandelstam variables and squaring the matrix element, together with the fact that

$$\sum_\lambda \epsilon_\mu(p,\lambda)\epsilon_\nu^*(p,\lambda) \simeq -\eta_{\mu\nu}, \tag{5.109}$$

we get the final result of

$$|\mathcal{M}^{10}|^2 = \frac{1}{8M_P^4}\frac{t^2(s+t)^2}{s^2}. \tag{5.110}$$

We evaluate the total matrix element factoring in the number of degrees of freedom of each kind of particle in the SM. The scalar sector has 4 dof coming from the fact that the Higgs is a complex doublet. The fermionic sector includes quarks, 2 flavours (up and down) x 3 colours x 2 chiralities (left and right), and leptons, 2 chiralities for the charged one and 1 for the neutrino; the total is 15 dof that need to be multiplied by 3 generations, for a total of 45. Lastly, the bosonic sector contains the mediators, 8 gluons for $SU(3)$, 3 weak bosons for $SU(2)$ and 1 $U(1)$ boson for the hypercharge, for a total of 12. The final matrix element squared is

$$\begin{aligned}|\mathcal{M}|^2 &= 4|\mathcal{M}^{00}|^2 + 45|\mathcal{M}^{\frac{1}{2}0}|^2 + 12|\mathcal{M}^{10}|^2\\ &= \frac{1}{4M_P^4}\frac{t^2(s+t)^2}{s^2} + \frac{45}{32M_P^4}\frac{[-t(s+t)(s+2t)^2]}{s^2} + \frac{3}{2M_P^4}\frac{t^2(s+t)^2}{s^2},\end{aligned} \tag{5.111}$$

which we will use in the evaluation of the rate

$$R(T) = \frac{1}{1024\pi^6} \int f_1 f_2 E_1 E_2 dE_1 dE_2 d\cos\theta_{12} \int |\mathcal{M}|^2 d\Omega_{13}, \tag{5.112}$$

where E_i are the energies of the particles $i = 1, 2$, θ_{12} is the angle formed between their momenta and the thermal distribution functions are

$$f_i = \frac{1}{e^{\frac{E_i}{T}} \pm 1}, \tag{5.113}$$

depending on the bosonic or fermionic nature of the particles. For the evaluation of the rate we can therefore follow the computations performed in App. A and consider the thermal scattering rate as the following:

$$R_a^T = \beta_0 \frac{T^8}{M_P^4}, \tag{5.114}$$

where $\beta_0 = \frac{3997}{41472000}\pi^3$ [3]. To evaluate the axionic number density through this channel, the equation to be solved is

$$\frac{dN_a^T}{da} = \frac{a^2}{H} R_a^T, \tag{5.115}$$

where $N_a = a^3 n_a$ and in which we can insert the following expressions:

$$T^4 = \left(\frac{30}{g_* \pi^2}\right) \rho_R, \tag{5.116}$$

that sees [2]

$$\rho_R = \rho_{RH} \left(\frac{a_{RH}}{a}\right)^4 \left[\frac{1 - (\frac{a}{a_{end}})^{\frac{k+8-6kl}{k+2}}}{1 - (\frac{a_{RH}}{a_{end}})^{\frac{k+8-6kl}{k+2}}}\right]. \tag{5.117}$$

Moreover we will use

$$H \simeq \frac{\sqrt{\rho_\phi}}{\sqrt{3} M_P}, \tag{5.118}$$

where

$$\rho_\phi = \rho_{RH} \left(\frac{a_{RH}}{a}\right)^{\frac{6k}{k+2}}. \tag{5.119}$$

Our equation becomes

$$\frac{dN_a^T}{da} = \frac{a^2}{H} R_a^T = a^2 \frac{\sqrt{3} M_P}{\sqrt{\rho_{RH}}} \left(\frac{a}{a_{RH}}\right)^{\frac{3k}{k+2}} \frac{\beta_0}{M_P^4} \left(\frac{30}{g_* \pi^2}\right)^2 \rho_{RH}^2 \left(\frac{a_{RH}}{a}\right)^8 \left[\frac{1 - (\frac{a}{a_{end}})^{\frac{k+8-6kl}{k+2}}}{1 - (\frac{a_{RH}}{a_{end}})^{\frac{k+8-6kl}{k+2}}}\right]^2. \tag{5.120}$$

To make it easier we define the constant factor

$$C = \frac{\beta_0 \sqrt{3}}{M_P^3} \left(\frac{30}{g_* \pi^2}\right)^2 \rho_{RH}^{\frac{3}{2}} \cdot a_{RH}^8 a_{RH}^{-\frac{3k}{k+2}} \cdot \left[\frac{1}{1 - (\frac{a_{RH}}{a_{end}})^{\frac{k+8-6kl}{k+2}}}\right]^2. \tag{5.121}$$

Then we can integrate it in the range $a_{end} < a < a_{RH}$, so:

$$N_a^T(a_{RH}) - N_a^T(a_{end}) = C \int_{a_{end}}^{a_{RH}} \left[a^{\frac{3k}{k+2}-6} \left(1 - 2\left(\frac{a}{a_{end}}\right)^{\frac{k+8-6kl}{k+2}} + \left(\frac{a}{a_{end}}\right)^{\frac{2(k+8-6kl)}{k+2}}\right)\right] da. \tag{5.122}$$

The second term in the difference can be neglected, as axions have not yet been produced at the end of inflation, when the interactions have yet to take place.
In the end, considering that

$$N_a^T(a_{RH}) = n_a^T(a_{RH}) \cdot a_{RH}^3, \tag{5.123}$$

we can simplify and get the final expression for the axion number density

$$\begin{aligned} n_a^T(a_{RH}) = \frac{\sqrt{3}}{M_P^3} \beta_0 (k+2) \rho_{RH}^{\frac{3}{2}} \left(\frac{30}{g_* \pi^2}\right)^2 \left[\frac{1}{1 - r^{\frac{k+8-6kl}{k+2}}}\right]^2 \Bigg[&- \frac{(k+8-6kl)^2}{6(k+5)(k+2+6kl)(1-2kl)} r^{\frac{2k+10}{k+2}} \\ &- \frac{1}{2k+10} + \frac{2}{k+2+6kl} r^{\frac{k+8-6kl}{k+2}} + \frac{1}{6-12kl} r^{\frac{2k+16-12kl}{k+2}} \Bigg]. \end{aligned} \tag{5.124}$$

The full result, substituting the expression for r is:

$$\begin{aligned} n_a^T(a_{RH}) = \frac{\sqrt{3}\beta_0}{M_P^3} \left(\frac{30}{g_*(T_{rh}) \pi^2}\right)^2 \frac{\rho_{RH}^{\frac{3}{2}}}{[1 - (\frac{a_{end}}{a_{rh}})^{\frac{k+8-6kl}{k+2}}]^2} (k+2) \Bigg[\frac{1}{6-12kl} + \frac{2}{6kl+k+2} \left(\frac{a_{rh}}{a_{end}}\right)^{\frac{6kl-k-8}{k+2}} + \\ \left(\frac{1}{12kl-6} - \frac{2}{6kl+k+2} + \frac{1}{10+2k}\right) \left(\frac{a_{rh}}{a_{end}}\right)^{\frac{12kl-6}{k+2}} - \frac{1}{10+2k} \left(\frac{a_{rh}}{a_{end}}\right)^{\frac{12kl-2k-16}{k+2}} \Bigg]. \end{aligned} \tag{5.125}$$

Exploiting the fact that

$$\frac{a_{rh}}{a_{end}} = \left(\frac{\rho_{rh}}{\rho_{end}}\right)^{-\frac{k+2}{6k}}, \tag{5.126}$$

we can rewrite it as:

$$n_a^T(a_{RH}) = \frac{\sqrt{3}\beta_0}{M_P^3}\left(\frac{30}{g_*(T_{rh})\pi^2}\right)^2 \frac{\rho_{RH}^{\frac{3}{2}}}{[1-(\frac{\rho_{rh}}{\rho_{end}})^{\frac{k+8-6kl}{6k}}]^2}(k+2)\left[\frac{1}{6-12kl}+\frac{2}{6kl+k+2}\left(\frac{\rho_{rh}}{\rho_{end}}\right)^{\frac{k+8-6kl}{6k}}+\right.$$
$$\left.\left(\frac{1}{12kl-6}-\frac{2}{6kl+k+2}+\frac{1}{10+2k}\right)\left(\frac{\rho_{rh}}{\rho_{end}}\right)^{\frac{6-12kl}{6k}}-\frac{1}{10+2k}\left(\frac{\rho_{rh}}{\rho_{end}}\right)^{\frac{2k+16-12kl}{6k}}\right]. \tag{5.127}$$

5.3.2 Inflaton scattering

The second process considered is through the inflaton condensate. We can express its rate as [55] [37]:

$$R_i^{\phi^k} = g_X \int d\Psi_{1,2,3,4}(2\pi)^4\delta^{(4)}(p_1+p_2-p_3-p_4)[|\mathcal{M}_{1+2\leftrightarrow 3+4}|^2 f_1 f_2(1\pm f_3)(1\pm f_4)-(3+4\leftrightarrow 1+2)]. \tag{5.128}$$

Ignoring the Bose enhancement and Pauli blocking effects this can be simply rewritten as

$$R_i^{\phi^k} = g_X \int \frac{d^3\vec{p}_3}{(2\pi)^3 2p_3^0}\frac{d^3\vec{p}_4}{(2\pi)^3 2p_4^0}(2\pi)^4\delta^{(4)}(p_1+p_2-p_3-p_4)|\mathcal{M}|^2. \tag{5.129}$$

We can use the computation in appendix C to understand that the phase space integral can be written as

$$\frac{\beta_n}{8\pi} = \frac{1}{8\pi}\sqrt{1-4\frac{m_X^2}{s}}, \tag{5.130}$$

if the DM particles have the same mass and, including the symmetry factor l that accounts for identical particles in the final state, the rate becomes

$$R_i^{\phi^k} = g_X \cdot \frac{1}{l!}\sum_{n=1}^{\infty}|\mathcal{M}_n|^2\frac{\beta_n}{8\pi}. \tag{5.131}$$

Now the matrix element can be obtained by considering again

$$\mathcal{M} \sim \frac{1}{M_P^2} T_\phi^{\mu\nu} \Pi_{\mu\nu\rho\sigma} T_X^{\rho\sigma}. \tag{5.132}$$

Having considered the inflaton as a classical oscillating field with only time-dependance, the energy momentum tensor,

$$T_\phi^{\mu\nu} = \partial^\mu \phi \partial^\nu \phi - \eta^{\mu\nu} \mathcal{L}, \tag{5.133}$$

will have non-vanishing derivatives only for the $0-$ th components. Moreover, since the condensate satisfies $T_\phi^{00} \sim \rho_\phi$, specifically expanding the potential energy in terms of the Fourier modes

$$V(\phi) = V(\phi_0) \sum_{n=-\infty}^{\infty} \mathcal{P}_n e^{-in\omega t} = \rho_\phi \sum_{n=-\infty}^{\infty} \mathcal{P}_n e^{-in\omega t}. \tag{5.134}$$

Hence:

$$\begin{aligned} \mathcal{M} &\sim \frac{1}{M_P^2} T_\phi^{00} \Pi_{00\rho\sigma} T_X^{\rho\sigma} \\ &= \frac{1}{M_P^2} \cdot \rho_\phi (\mathcal{P}^k)_n \frac{1}{2k^2} [\eta^{\rho 0}\eta^{\sigma 0} + \eta^{\rho 0}\eta^{\sigma 0} - \eta^{\rho\sigma}\eta^{00}] \frac{1}{2} [p_{3\rho} p_{4\sigma} + p_{3\sigma} p_{4\rho} - \eta_{\rho\sigma}(p_3 \cdot p_4 + m_X^2)] \\ &= \frac{1}{M_P^2} \cdot \rho_\phi (\mathcal{P}^k)_n \frac{1}{4s} [4 p_3^0 p_4^0 + 2 m_X^2]. \end{aligned} \tag{5.135}$$

In the centre of mass frame, where $E_3 = E_4 = \frac{E_n}{2}$ we can write $2p_3^0 p_4^0 = \frac{E_n^2}{2} = \frac{s}{2}$, so:

$$\mathcal{M} = \frac{1}{M_P^2} \cdot \rho_\phi (\mathcal{P}^k)_n \frac{1}{4} \left(1 + \frac{2m_X^2}{s}\right). \tag{5.136}$$

Squaring it and taking into account symmetry factors, this becomes:

$$|\mathcal{M}|^2 = \frac{\rho_\phi^2}{M_P^4} \cdot |(\mathcal{P}^k)_n|^2 \left(1 + \frac{2m_X^2}{s}\right)^2. \tag{5.137}$$

We can now insert the result found in (5.131), with $g_X = l = 2$, to get the rate

$$R_i^{\phi^k} = \frac{2}{16\pi} \cdot \frac{\rho_\phi^2}{M_P^4} \sum_{n=1}^{\infty} \left(1 + \frac{2m_X^2}{s}\right)^2 |(\mathcal{P}^k)_n|^2 \langle \beta_n(m_X, m_X) \rangle. \tag{5.138}$$

To lighten the notation, we define

$$\Sigma_0^k = \sum_{n=1}^{\infty} \left(1 + \frac{2m_X^2}{s}\right)^2 |(\mathcal{P}^k)_n|^2 \sqrt{1 - \frac{4m_X^2}{E_n^2}}. \tag{5.139}$$

In the end, the rate considered is

$$R_a^\phi = \frac{2\rho_\phi^2}{16\pi M_P^4} \Sigma_0^k. \tag{5.140}$$

Again using

$$\rho_\phi = \rho_{RH} \left(\frac{a}{a_{RH}}\right)^{-\frac{6k}{k+2}}, \tag{5.141}$$

$$H \simeq \frac{\sqrt{\rho_\phi}}{\sqrt{3} M_P}, \tag{5.142}$$

one gets

$$\frac{dN_a}{da} = \frac{a^2 R_a^\phi}{H} = \frac{\sqrt{3}}{8\pi M_P^3} \Sigma_0^k \rho_{RH}^{\frac{3}{2}} a^2 \left(\frac{a}{a_{RH}}\right)^{-\frac{9k}{k+2}}. \tag{5.143}$$

From now on we will define the constant term

$$C' = \frac{\sqrt{3}}{8\pi M_P^3} \Sigma_0^k \rho_{RH}^{\frac{3}{2}}. \tag{5.144}$$

Integrating in the same limit as last section, and again considering $N_a(a_{end}) = 0$, we find

$$\begin{aligned} N_a(a_{RH}) = n_a(a_{RH}) \cdot a_{RH}^3 &= C' \cdot a_{RH}^{\frac{9k}{k+2}} \int_{a_{end}}^{a_{RH}} a^{-\frac{9k}{k+2}+2} da \\ &= C' \cdot a_{RH}^{\frac{9k}{k+2}} \cdot \frac{k+2}{-9k+3k+6} a^{-\frac{9k}{k+2}+3} \Big|_{a_{end}}^{a_{RH}} \\ &= C' \frac{(k+2)}{6-6k} \cdot a_{RH}^{\frac{9k}{k+2}} \cdot a_{RH}^{\frac{6-6k}{k+2}} \left[1 - \left(\frac{a_{end}}{a_{RH}}\right)^{\frac{6-6k}{k+2}}\right], \end{aligned} \tag{5.145}$$

so that in the end:

$$
\begin{aligned}
n_a^{\phi}(a_{RH}) &= C' \frac{(k+2)}{6-6k}[1 - r^{\frac{6k-6}{k+2}}] \\
&= \frac{\sqrt{3}}{8\pi M_P^3}\Sigma_0^k \rho_{RH}^{\frac{3}{2}} \frac{(k+2)}{6-6k}\left[1 - \left(\frac{a_{RH}}{a_{end}}\right)^{\frac{6k-6}{k+2}}\right] \\
&= \frac{\sqrt{3}}{8\pi M_P^3}\Sigma_0^k \rho_{RH}^{\frac{3}{2}} \frac{(k+2)}{6-6k}\left[1 - \left(\frac{\rho_{end}}{\rho_{RH}}\right)^{1-\frac{1}{k}}\right],
\end{aligned}
\tag{5.146}
$$

where again the notation is $r = a_{RH}/a_{end}$. In the limit $r \gg 1$ we simply have

$$
n_a^{\phi}(a_{RH}) = \frac{\sqrt{3}}{8\pi M_P^3}\Sigma_0^k \rho_{RH}^{\frac{3}{2}} \frac{k+2}{6k-k} r^{\frac{6k-6}{k+2}}. \tag{5.147}
$$

5.4 Relic abundance

Let us now evaluate the relic abundance contributions that we would get from the number densities obtained in Sections 5.2 and 5.3. Specifically, considering axions as dark matter, we can evaluate which production mechanism dominates over the other.

As far as the calculation of the relic abundance, it can be obtained from the number density using the following expression [36]

$$
\Omega_a h^2 = 1.6 \cdot 10^8 \frac{g_*(T_0)}{g_*(T_{rh})} \frac{n_a(T_{rh})}{T_{rh}^3} \frac{\tilde{m}_a(T_{rh})}{1GeV}. \tag{5.148}
$$

5.4.1 Standard misalignment production

Again, we will have to make a distinction based on whether oscillations start during or after the reheating period. We will therefore use (5.55), (5.60) and (5.62) to express T_{osc} in these two regimes.

$T_{rh} \geq T_{osc}$

Let us firstly evaluate the $T_{rh} \geq T_{osc}$. In this case, the axionic number density can be expressed through

$$
n_a(T_{rh}) = \frac{\rho_a(T_{rh})}{\tilde{m}_a(T_{rh})}, \tag{5.149}
$$

where the energy density can be found manipulating the following expression, which comes from the conservation of the axions' number densities and the assumption of entropy conservation:

$$\rho_a(T_{rh}) = \rho_a(T_{osc})\frac{\tilde{m}_a(T_{rh})}{\tilde{m}_a(T_{osc})}\frac{s(T_{rh})}{s(T_{osc})}. \tag{5.150}$$

Now, the energy density associated to oscillations is related to the potential, and considering the time (and therefore temperature) dependance of the mass it can be written as:

$$\rho_a(T_{osc}) = \frac{1}{2}\tilde{m}_a^2(T_{osc})f_a^2\theta_i^2. \tag{5.151}$$

We immediately see the appeareance of the initial misalignment angle, which makes sense considering that our DM candidate are axions, which are assumed here to be produced trough the misalignment mechanism. The entropy ratio, on the other hand, gets simplified if we consider that

$$s(T) = \frac{2\pi^2}{45}g_{*s}(T)T^3. \tag{5.152}$$

Inserting all these expressions in (5.148) we find the relic axionic abundance to be

$$\Omega_a h^2 = \frac{1.6\cdot 10^8}{2}\frac{g_*(T_0)}{g_*(T_{rh})}\frac{g_{*s}(T_{rh})}{g_{*s}(T_{osc})}\frac{f_a^2\theta_i^2}{T_{osc}^3\cdot 1GeV}\tilde{m}_a(T_{osc})\tilde{m}_a(T_{rh}). \tag{5.153}$$

Now, we can again make a distinction between the case in which $T_{osc} \geq T_{QCD}$ and the one in which $T_{osc} \leq T_{QCD}$, as $\tilde{m}_a$ and T_{osc} will be different (see Eqs. (5.53) (5.55)). As we will be working with many different temperature regimes, to simplify the understanding, each of them will be labelled by a circled number ①-⑥.

The relic abundance for regime ④, $T_{osc} \geq T_{QCD}$, will be

$$\begin{aligned}\Omega_a h^2 &= \frac{1.6\cdot 10^8}{2}\frac{g_*(T_0)}{g_*(T_{rh})}\frac{g_{*s}(T_{rh})}{g_{*s}(T_{osc})}(5.7\cdot 10^{-3}GeV^2)^2\frac{\theta_i^2}{1GeV}\frac{T_{QCD}^8}{T_{osc}^7T_{rh}^4}\\ &= \frac{1.6\cdot 10^8}{2}\frac{g_*(T_0)}{g_*(T_{rh})}\frac{g_{*s}(T_{rh})}{g_{*s}(T_{osc})}(5.7\cdot 10^{-3}GeV^2)^2\frac{\theta_i^2}{1GeV}\left(\frac{\pi}{M_P}\sqrt{\frac{g_*(T_{osc})}{10}}\right)^{\frac{7}{6}}\frac{T_{QCD}^{\frac{10}{3}}}{T_{rh}^4}m_a^{-\frac{7}{6}},\end{aligned} \tag{5.154}$$

whereas for regime ⑤, $T_{osc} \leq T_{QCD}$ but $T_{rh} \geq T_{QCD}$, it will be

$$\begin{aligned}\Omega_a h^2 &= \frac{1.6 \cdot 10^8}{2} \frac{g_*(T_0)}{g_*(T_{rh})} \frac{g_{*s}(T_{rh})}{g_{*s}(T_{osc})} (5.7 \cdot 10^{-3} GeV^2)^2 \frac{\theta_i^2}{1GeV} \frac{T_{QCD}^4}{T_{osc}^3 T_{rh}^4} \\ &= \frac{1.6 \cdot 10^8}{2} \frac{g_*(T_0)}{g_*(T_{rh})} \frac{g_{*s}(T_{rh})}{g_{*s}(T_{osc})} (5.7 \cdot 10^{-3} GeV^2)^2 \frac{\theta_i^2}{1GeV} \left(\frac{\pi}{M_P} \sqrt{\frac{g_*(T_{osc})}{10}} \right)^{\frac{3}{2}} \frac{T_{QCD}^4}{T_{rh}^4} m_a^{-\frac{3}{2}}.\end{aligned} \tag{5.155}$$

Finally, for regime ⑥, $T_{QCD} \geq T_{rh} \geq T_{osc}$, as $\tilde{m}_a(T_{rh}) = \tilde{m}_a(T_{osc}) = m_a$:

$$\begin{aligned}\Omega_a h^2 &= \frac{1.6 \cdot 10^8}{2} \frac{g_*(T_0)}{g_*(T_{rh})} \frac{g_{*s}(T_{rh})}{g_{*s}(T_{osc})} (5.7 \cdot 10^{-3} GeV^2)^2 \frac{\theta_i^2}{1GeV} \frac{1}{T_{osc}^3} \\ &= \frac{1.6 \cdot 10^8}{2} \frac{g_*(T_0)}{g_*(T_{rh})} \frac{g_{*s}(T_{rh})}{g_{*s}(T_{osc})} (5.7 \cdot 10^{-3} GeV^2)^2 \frac{\theta_i^2}{1GeV} \left(\frac{\pi}{M_P} \sqrt{\frac{g_*(T_{osc})}{10}} \right)^{\frac{3}{2}} m_a^{-\frac{3}{2}}.\end{aligned} \tag{5.156}$$

$T_{osc} \geq T_{rh}$

Let us now turn to the case in which $T_{osc} > T_{rh}$. First of all, we have seen that T_{osc} becomes dependent on the reheating temperature (Eqs. (5.60), (5.62)). Additionally, the energy density expression gets modified by another ratio

$$\rho_a(T_{rh}) = \rho_a(T_{osc}) \frac{m_a}{\tilde{m}_a(T_{osc})} \frac{s(T_0)}{s(T_{osc})} \cdot \frac{S(T_{osc})}{S(T_{rh})}, \tag{5.157}$$

which accounts for the entropy injection in the thermal bath due to the fact that the inflaton is decaying during reheating. This ratio can be equivalently expressed as

$$\frac{S(T_{osc})}{S(T_{rh})} = \frac{g_{*s}(T)}{g_{*s}(T_{rh})}. \tag{5.158}$$

This implies that the relic abundance is expressed, in this regime, as

$$\Omega_a h^2 = \frac{1.6 \cdot 10^8}{2} \frac{g_*(T_0)}{g_*(T_{rh})} \frac{f_a^2 \theta_i^2}{T_{osc}^3 \cdot 1GeV} \tilde{m}_a(T_{osc}) \tilde{m}_a(T_{rh}). \tag{5.159}$$

Doing the same calculations as before, just taking into account the different expressions for T_{osc}, we get:

$$\begin{aligned}
\Omega_a h^2 &= \frac{1.6\cdot 10^8}{2}\frac{g_*(T_0)}{g_*(T_{rh})}(5.7\cdot 10^{-3}GeV^2)^2\frac{\theta_i^2}{1GeV}\frac{T_{QCD}^8}{T_{osc}^7 T_{rh}^4} \\
&= \frac{1.6\cdot 10^8}{2}\frac{g_*(T_0)}{g_*(T_{rh})}(5.7\cdot 10^{-3}GeV^2)^2\frac{\theta_i^2}{1GeV}\frac{T_{QCD}^8}{T_{rh}^{11}}\left(\frac{\pi}{M_P}\sqrt{\frac{g_*(T_{rh})}{10}}\frac{T_{rh}^6}{T_{QCD}^4}\right)^{\frac{7}{8}\frac{1+2l}{1+l}} m_a^{-\frac{7}{8}\frac{1+2l}{1+l}},
\end{aligned} \tag{5.160}$$

whenever $T_{QCD} < T_{osc}$ and $T_{QCD} < T_{rh}$, which we define to be regime ①. If, instead, $T_{QCD} < T_{osc}$ but $T_{QCD} > T_{rh}$, regime ②, we get

$$\begin{aligned}
\Omega_a h^2 &= \frac{1.6\cdot 10^8}{2}\frac{g_*(T_0)}{g_*(T_{rh})}(5.7\cdot 10^{-3}GeV^2)^2\frac{\theta_i^2}{1GeV}\frac{T_{QCD}^4}{T_{osc}^7} \\
&= \frac{1.6\cdot 10^8}{2}\frac{g_*(T_0)}{g_*(T_{rh})}(5.7\cdot 10^{-3}GeV^2)^2\frac{\theta_i^2}{1GeV}\frac{T_{QCD}^4}{T_{rh}^{7}}\left(\frac{\pi}{M_P}\sqrt{\frac{g_*(T_{rh})}{10}}\frac{T_{rh}^6}{T_{QCD}^4}\right)^{\frac{7}{8}\frac{1+2l}{1+l}} m_a^{-\frac{7}{8}\frac{1+2l}{1+l}}.
\end{aligned} \tag{5.161}$$

Lastly, for $T_{QCD} > T_{osc} > T_{rh}$, regime ③:

$$\begin{aligned}
\Omega_a h^2 &= \frac{1.6\cdot 10^8}{2}\frac{g_*(T_0)}{g_*(T_{rh})}(5.7\cdot 10^{-3}GeV^2)^2\frac{\theta_i^2}{1GeV}\frac{1}{T_{osc}^3} \\
&= \frac{1.6\cdot 10^8}{2}\frac{g_*(T_0)}{g_*(T_{rh})}(5.7\cdot 10^{-3}GeV^2)^2\frac{\theta_i^2}{1GeV}\frac{1}{T_{rh}^{3}}\left(\frac{\pi}{M_P}\sqrt{\frac{g_*(T_{rh})}{10}}T_{rh}^2\right)^{\frac{3}{4}(1+2l)} m_a^{-\frac{3}{4}(1+2l)}.
\end{aligned} \tag{5.162}$$

	T Regime	$\Omega_a^{MIS}h^2$
①	$T_{osc} > T_{rh} > T_{QCD}$	$2.6 \cdot 10^{-5} \cdot \theta_i^2 \frac{(GeV)^{11}}{T_{rh}^{11}} \left[\frac{M_P}{\pi}\sqrt{\frac{10}{g_*(T_{rh})}}\frac{T_{QCD}^4}{T_{rh}^6} m_a\right]^{-\frac{7(2l+1)}{8(1+l)}}$
②	$T_{osc} > T_{QCD} > T_{rh}$	$0.3 \cdot \theta_i^2 \frac{(GeV)^7}{T_{rh}^7} \left[\frac{M_P}{\pi}\sqrt{\frac{10}{g_*(T_{rh})}}\frac{T_{QCD}^4}{T_{rh}^6} m_a\right]^{-\frac{7(2l+1)}{8(1+l)}}$
③	$T_{QCD} > T_{osc} > T_{rh}$	$6.2 \cdot 10^2 \cdot \theta_i^2 \frac{(GeV)^3}{T_{rh}^3} \left[\frac{M_P}{\pi}\sqrt{\frac{10}{g_*(T_{rh})}}\frac{m_a}{T_{rh}^2}\right]^{-\frac{3}{4}(1+2l)}$
④	$T_{rh} > T_{osc} > T_{QCD}$	$8.6 \cdot 10^{-22}\theta_i^2 \frac{(GeV)^{\frac{31}{6}}}{T_{rh}^4} m_a^{-\frac{7}{6}}$
⑤	$T_{rh} > T_{QCD} > T_{osc}$	$5.9 \cdot 10^{-28}\theta_i^2 \frac{(GeV)^{\frac{11}{2}}}{T_{rh}^4} m_a^{-\frac{3}{2}}$
⑥	$T_{QCD} > T_{rh} > T_{osc}$	$1.2 \cdot 10^{-24}\theta_i^2 (GeV)^{\frac{3}{2}} m_a^{-\frac{3}{2}}$

Table 5.4: Summary of the misalignment abundances in the 6 different temperature regimes. The numerical factors have been evaluated so that the dependance between the reheating temperature and the axion mass is evident. The number of relativistic degrees of freedom as of today has been taken to be $g_*(T_0) \approx 3.36$, whereas the others depend on T_{rh} or T_{osc} and, as they depend on the regime, they can be read off from Tab. 5.3.

5.4.2 Gravitational production

Let us first comment on the relative dominance between the two gravitational production processes; comparing equations (5.127) and (5.146) we find that

$$\frac{n_a^T}{n_a^\phi} \ll 1, \tag{5.163}$$

meaning that gravitational production is always dominated by the scattering of the inflaton zero modes.

	$k=2$	$k=4$	$k=6$
Σ_0^k	$1/16$	0.063	0.056
ρ_{end}	$(5.2 \cdot 10^{15} GeV)^4$	$(4.8 \cdot 10^{15} GeV)^4$	$(4.6 \cdot 10^{15} GeV)^4$

Table 5.5: Values of Σ_0^k and ρ_{end} used for each value of k [56].

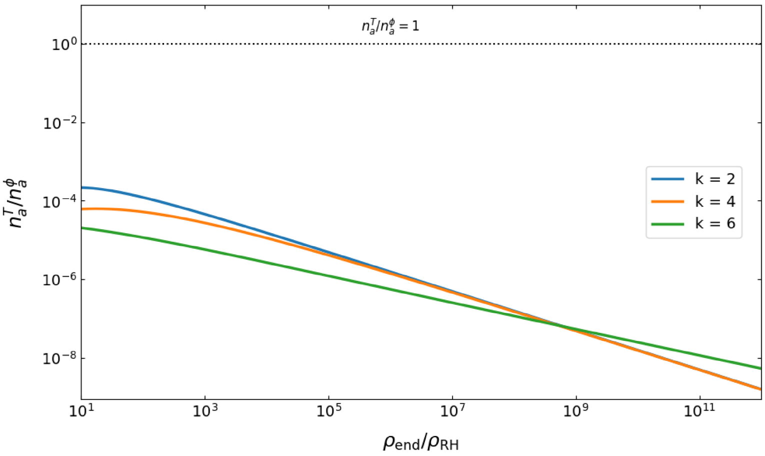

Figure 5.9: Plot showing how the ratio between the thermal and the inflaton contribution is always $\ll 1$, hence defining the inflaton scattering as the dominating gravitational production mechanism.

Nevertheless, let us now remain general. In the gravitational production case, one needs to consider the sum of the two processes contributing to the axionic production, namely $n_a^{TOT}(T_{rh}) = n_a^\phi(T_{rh}) + n_a^T(T_{rh})$. This implies

$$\Omega_a h^2 = 1.6 \cdot 10^8 \frac{g_*(T_0)}{g_*(T_{rh})} \frac{\tilde{m}_a(T_{rh})}{1GeV \cdot T_{rh}^3} (n_a^\phi + n_a^T). \tag{5.164}$$

Again, being the mass temperature dependent, we will have different regimes. In this case we simply divide the 6 regimes summed up in Tab. 5.4. On the one hand, $T_{rh} \geq T_{QCD}$, which corresponds to regimes ①, ④, ⑤ and whose relic abundance will be

$$\Omega_a h^2 = 1.6 \cdot 10^8 \frac{g_*(T_0)}{g_*(T_{RH})} \frac{m_a}{1GeV} \frac{T_{QCD}^4}{T_{rh}^7} (n_a^\phi + n_a^T), \tag{5.165}$$

where the number densities can be read from Eqs. (5.127) and (5.147). On the other hand, $T_{rh} \leq T_{QCD}$, which corresponds to regimes ②, ③, ⑥ and has

$$\Omega_a h^2 = 1.6 \cdot 10^8 \frac{g_*(T_0)}{g_*(T_{RH})} \frac{m_a}{1GeV} \frac{1}{T_{rh}^3} (n_a^\phi + n_a^T). \tag{5.166}$$

T Regime	$\Omega_a^{GRAV} h^2$
①, ④, ⑤ $\quad T_{rh} > T_{QCD}$	$\Omega_a h^2 = 3.2 \cdot 10^3 \cdot m_a \frac{(GeV)^3}{T_{rh}^7}(n_a^\phi + n_a^T)$
②, ③, ⑥ $\quad T_{rh} < T_{QCD}$	$\Omega_a h^2 = 3.8 \cdot 10^7 \frac{m_a}{1GeV} \frac{1}{T_{rh}^3}(n_a^\phi + n_a^T)$

Table 5.6: Summary of the gravitational abundances in the 6 different temperature regimes.

Having now evaluated all the wanted relic abundances, we can check which production mechanism is more relevant with respect to the other. To do so we take the ratio between the expressions of their abundances and evaluate its discrepancy with respect to 1. Since this function depends on some known parameters but also on T_{rh} and m_a, we can restrict ourselves to a certain regime of validity considering the range of validity of the latter to which we previously restricted ourselves. Focusing on the case in which $T_{osc} > T_{rh}$, as we did in section 5.2, we can determine which contribution is more relevant by considering the first three different regimes:

- ① $T_{QCD} < T_{rh} < T_{osc}$

$$\frac{(\Omega_a h^2)^{MIS}}{(\Omega_a h^2)^{GRAV}} = \frac{(5.7 \cdot 10^{-3} GeV^2)^2 \frac{\theta_i^2}{2} \frac{T_{QCD}^4}{T_{rh}^4}}{(n_a^\phi + n_a^T)} \left[\sqrt{\frac{g_*(T_{rh})}{10}} \frac{\pi}{M_P} \frac{T_{rh}^6}{T_{QCD}^4} \right]^{\frac{7}{8}\frac{(1+2l)}{1+l}} \cdot m_a^{-\frac{7}{8}\frac{(1+2l)}{1+l} - 1}. \tag{5.167}$$

We can manipulate this expression to determine when this ratio exceeds unity and hence when the standard misalignment production becomes the dominating production mechanism over the gravitational production, by expressing T_{rh} as a function of m_a. The plot 5.10 shows the ratio in this first case, dividing the plane in two regions depending on whether the misalignment mechanism comes to dominate over the gravitational production or viceversa.

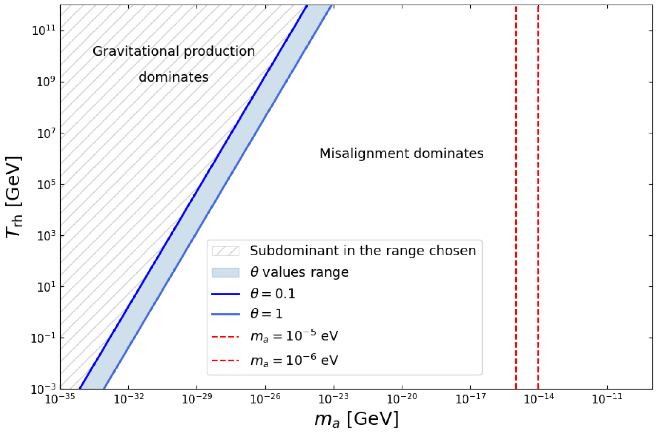

Figure 5.10: Ratio of the axionic abundances evaluated respectively through misalignment mechanism and gravitational production in the temperature regime ①. In this plot, the choice was to consider the fermionic decay, hence $k = 2$ and $l = 0$. As it can be seen, in the mass range of validity chosen for our analysis, mislignment dominates over gravitational production.

This can be done for the other regimes:

- ② $T_{rh} < T_{QCD} < T_{osc}$

$$\frac{(\Omega_a h^2)^{MIS}}{(\Omega_a h^2)^{GRAV}} = \frac{(5.7\cdot 10^{-3}GeV^2)^2 \frac{\theta_i^2}{2}\frac{T_{QCD}^4}{T_{rh}^4}}{(n_a^{\phi} + n_a^{T})} \left[\sqrt{\frac{g_*(T_{rh})}{10}}\frac{\pi}{M_P}\frac{T_{rh}^6}{T_{QCD}^4}\right]^{\frac{7}{8}\frac{(1+2l)}{1+l}} \cdot m_a^{-\frac{7}{8}\frac{(1+2l)}{1+l}-1}; \tag{5.168}$$

- ③ $T_{rh} < T_{osc} < T_{QCD}$

$$\frac{(\Omega_a h^2)^{MIS}}{(\Omega_a h^2)^{GRAV}} = \frac{(5.7\cdot 10^{-3}GeV^2)^2 \frac{\theta_i^2}{2}}{(n_a^{\phi} + n_a^{T})} \left[\sqrt{\frac{g_*(T_{rh})}{10}}\frac{\pi}{M_P}T_{rh}^2\right]^{\frac{3}{4}(1+2l)} \cdot m_a^{-\frac{3}{4}(1+2l)-1}. \tag{5.169}$$

Having now distinguished the regimes in which one production mechanism comes to dominate over the other, we can concentrate on just one of them. If, for instance, the misalignment mechanism dominates, the main relic contribution is given by Eq. (5.160). We impose the upper bound $\Omega_a h^2 < 0.12$ so that we can express T_{rh} as a function of m_a. For instance in regime ①

$$T_{rh}^{\frac{21}{4}\frac{(1+2l)}{(1+l)}-11} < \frac{0.12}{1.6\cdot 10^8}\frac{g_*(T_{rh})}{g_*(T_0)}\frac{2}{(5.7\cdot 10^{-3}GeV^2)^2}\frac{1GeV}{\theta_i^2}\cdot\frac{1}{T_{QCD}^8}\left[\sqrt{\frac{10}{g_*(T_{rh})}}\frac{M_P}{\pi}T_{QCD}^4\right]^{\frac{7}{8}\frac{(1+2l)}{(1+l)}} \cdot m_a^{\frac{7}{8}\frac{(1+2l)}{(1+l)}}. \tag{5.170}$$

We can again plot the relation between T_{rh} and m_a depending on the different values of k and considering that the initial misalignment angle spans the interval $\theta_i \in [0.1; 1]$.

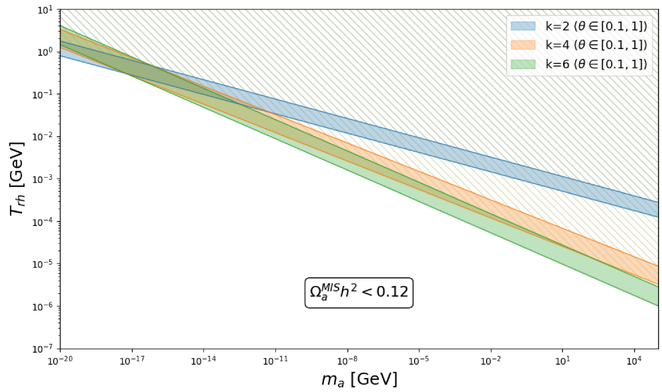

Figure 5.11: Misalignment contribution only, in the case of a fermionic decay, $l = \frac{1}{2} - \frac{1}{k}$, for different values of k. The shaded region highlights the area excluded by experimental constraints on the DM relic abundance.

Even though the plot shown in Fig. 5.10 shows a specific dominance, we can nevertheless proceed with the evaluation of the relic abundance of axions as a DM candidate by considering both contributions, misalignment and gravitational production, where the latter will simply be subdominant. Since the upper bound on the relic abundance is $\Omega_a h^2 = 0.12$, we set that as a limit and get T_{rh} as a function of m_a from the composite expression coming from the sum of the results presented in Tables 5.4 and 5.6 (obviously corresponding to the same regime). The following plots sum up the parameters space of $\{m_a; T_{rh}\}$ for the 6 different regimes.

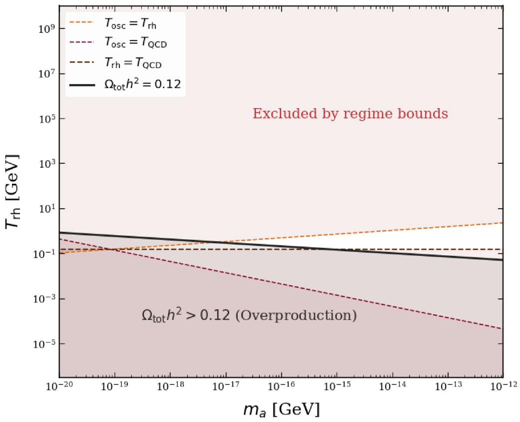

(a) ① $T_{osc} > T_{rh} > T_{QCD}$

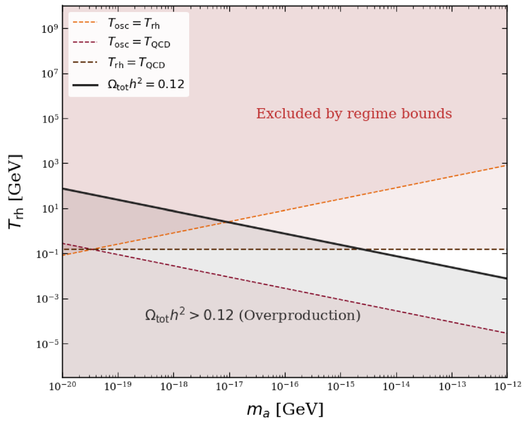

(b) ② $T_{osc} > T_{QCD} > T_{rh}$

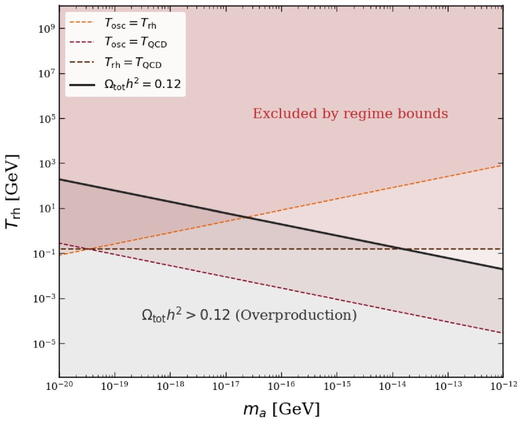

(c) ③ $T_{QCD} > T_{osc} > T_{rh}$

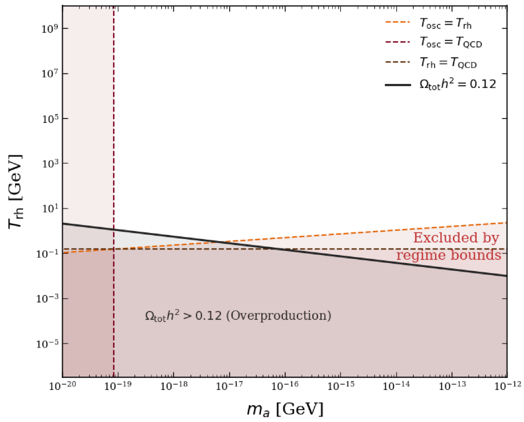

(d) ④ $T_{rh} > T_{osc} > T_{QCD}$

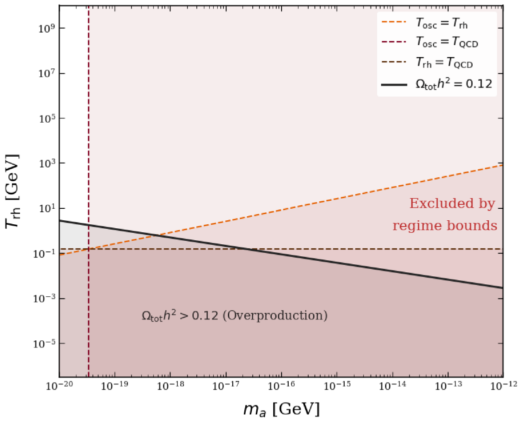

(e) ⑤ $T_{rh} > T_{QCD} > T_{osc}$

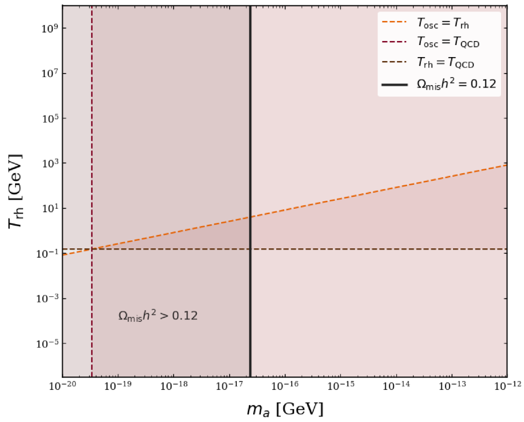

(f) ⑥ $T_{QCD} > T_{rh} > T_{osc}$

Figure 5.12: The plots show the range of validity of the reheating temperature as a function of the axion mass if we assume axions as a good DM candidate, imposing therefore an upperbound on their abundance of $\Omega_a h^2 < 0.12$, and considering their production during the reheating epoch, both via misalignement and gravitational production.

5.5 PBH reheating

We now introduce a new factor into our analysis, Primordial Black Holes, and compare the inflaton driven reheating that we have seen up until now with the PBH reheating.

5.5.1 Primordial Black Holes

Black Holes are predicted by General Relativity to be regions of a certain mass where the gravitational field is so strong that not even light can escape [7]. There are different types of Black Holes, depending on their mass scale, both those that derive from the collapse of astrophysical objects and those produced in the Early Universe, which gives them the name of ”Primordial Black Holes”. PBHs are therefore objects that could have been produced in the Early Universe, through various mechanisms, after the collapse of a region with large energy density fluctuations, usually considered $\frac{\delta\rho}{\rho} \gtrsim \delta_c \sim 1$.

We assume that the mass of the PBH is monochromatic [34], peaked around a specific mass that we define as M_{in}, so that the mass distribution is simply

$$f_{PBH}(M) = \delta(M - M_{in}). \tag{5.171}$$

This initial mass is assumed to be a fraction of the Hubble mass at the time of collapse, meaning that it can be rewritten as

$$M_{in} = \gamma M_H = \gamma \frac{4}{3}\pi \frac{\rho(t_{in})}{H^3(t_{in})} = 4\pi\gamma \frac{M_P^2}{H(t_{in})}, \tag{5.172}$$

where $\gamma = \omega^{\frac{2}{3}}$ is a parameter determining the efficiency of the collapse.

As PBHs decay [33], the evolution equation for their mass will have the form

$$\frac{dM_{BH}}{dt} = -\epsilon \frac{M_P^4}{M_{BH}^2}, \tag{5.173}$$

where $\epsilon = \frac{27}{4}\frac{\pi g_*(T_{BH})}{480}$. Solving this equation one finds the evaporation time, meaning the time at which the PBH mass has fully evaporated:

$$t_{ev} = \frac{M_P^3}{3\epsilon M_P^4} \simeq 1s \left(\frac{M_{in}}{10^8 g}\right)^3. \tag{5.174}$$

This imposes an upper bound on the value of the initial PBH mass, because evaporation must occur before BBN (which happened at around $t \sim 1s$) in order not to have perturbative effects given by the entropy injection in the thermal bath, that would follow the PBH evaporation. Moreover, for the mass to have been inside of the horizon at the end of inflation one sees that

$$M_{in} \gtrsim \rho_{end}/H^3_{end} \simeq 1g. \tag{5.175}$$

These two constraints give us the range of validity in which the initial mass can be restricted:

$$1g \lesssim M_{in} \lesssim 10^8 g. \tag{5.176}$$

One last parameter needs to be introduced for the sake of the following analysis. We therefore define

$$\beta = \frac{\rho_{BH}(t_{in})}{\rho_{TOT}(t_{in})}, \tag{5.177}$$

which tells us what fraction of the total energy density is associated to Black Holes.

Constraints on the β parameter arise from requiring that the abundance of gravitational waves generated from the density fluctuations due to the inhomogeneities of the PBH is not in conflict with BBN constraints. The upper bound on β was derived in [12]:

$$\beta < 1.1 \cdot 10^{-6} \left(\frac{\gamma}{0.2}\right)^{-\frac{1}{2}} \left(\frac{g_{BH}}{108}\right)^{\frac{17}{48}} \left(\frac{g_{ev}}{106.75}\right)^{\frac{1}{16}} \left(\frac{M_{in}}{10^4 g}\right)^{-\frac{17}{24}}. \tag{5.178}$$

Solving Eq. (5.173) gives

$$M^3_{BH}(a) = M^3_{in} + \frac{\epsilon M_P^2 M_{in}}{2\pi\gamma(1+\omega)} \left[1 - \left(\frac{a}{a_{in}}\right)^{\frac{3}{2}(1+\omega)}\right], \tag{5.179}$$

where we employed $\sqrt{\rho_{in}} = 4\pi\gamma\sqrt{3}\frac{M_P^3}{M_{in}}$. One can also use the fact that

$$\frac{a_{in}}{a_{end}} = \left(\frac{M_{in}\sqrt{\rho_{end}}}{4\pi\gamma\sqrt{3}M_P^3}\right)^{\frac{2}{3(1+\omega)}}, \tag{5.180}$$

which comes from the fact that $\rho_{in} = \rho_{end}(\frac{a_{end}}{a_{in}})^{\frac{3}{2}(1+\omega)}$ and from the relation of ρ_{in} with the initial mass already presented. The mass expression can therefore be rewritten, in the limit of $a \gg a_{in}$, as

$$M_{BH}^3(a) \simeq M_{in}^3 \left[1 - \frac{2\sqrt{3}\epsilon M_P^5}{\sqrt{\rho_{end}} M_{in}^3 (1+\omega)} \left(\frac{a}{a_{end}} \right)^{\frac{3}{2}(1+\omega)} \right]. \tag{5.181}$$

Another useful equation to write is the equation describing the evolution of the energy density of PBHs, namely:

$$\dot{\rho}_{BH} + 3H\rho_{BH} = \frac{\rho_{BH}}{M_{BH}} \frac{dM_{BH}}{dt} \theta(t - t_{in})\theta(t_{ev} - t). \tag{5.182}$$

This comes from the Boltzmann equation for matter components with a negative term on the RHS, highlighting the decreasing in time due to evaporation. The two Heaviside functions ensure the validity between the formation of PBHs and their complete evaporation. This can be rewritten changing the time variable into the scale factor:

$$aH\frac{d\rho_{BH}}{da} + 3H\rho_{BH} = \frac{\rho_{BH}}{M_{BH}} aH \frac{dM_{BH}}{da}. \tag{5.183}$$

Dividing by aH and separating the variables:

$$\frac{1}{\rho_{BH}} \frac{d\rho_{BH}}{da} = \frac{dM_{BH}}{M_{BH}} - 3\frac{da}{a}, \tag{5.184}$$

which integrated gives

$$\rho_{BH}(a) = \rho_{BH}(a_{in}) \left(\frac{a_{in}}{a} \right)^3 \left(\frac{M_{BH}(a)}{M_{in}} \right). \tag{5.185}$$

Implementing Eq. (5.181) in the latter, one finally gets the expression for the PBHs' energy density:

$$\rho_{BH}(a) = \beta\rho_{end} \left(\frac{4\pi\gamma\sqrt{3}M_P^3}{M_{in}\sqrt{\rho_{end}}} \right)^{\frac{2\omega}{(1+\omega)}} \left(\frac{a_{end}}{a} \right)^3 \left[1 - \frac{2\sqrt{3}\epsilon M_P^5}{\sqrt{\rho_{end}} M_{in}^3 (1+\omega)} \left(\frac{a}{a_{end}} \right)^{\frac{3}{2}(1+\omega)} \right]^{\frac{1}{3}}. \tag{5.186}$$

There is a threshold value for β, that we call β_{crit}^{BH}, above which PBHs dominate over the total energy density. Specifically, to evaluate its expression one needs to ensure that PBHs come to dominate before their evaporation, in other words whenever $a_{BH} < a_{ev}$. We obtain the expressions of the redshifts as follows: to get the evaporation time we impose that the mass of the BH vanishes at

a_{ev}, in other words we require from (5.181) that $M(a_{ev}) = 0$. This clearly gives:

$$\frac{a_{ev}}{a_{end}} = \left(\frac{\sqrt{\rho_{end}} M_{in}^3 (1+\omega)}{2\sqrt{3}\epsilon M_P^5}\right)^{\frac{2}{3(1+\omega)}}. \tag{5.187}$$

To get the redshift of the BH domination, instead, we identify the moment in which the PBH crosses the inflaton, which we know to have an energy density that goes as $\rho_\phi \propto a^{-3(1+\omega)}$. Neglecting the second subdominant term in Eq. (5.186), and imposing the resulting expression (evaluated for $a = a_{BH}$) to be equal to the inflaton's, this gives:

$$\frac{a_{BH}}{a_{end}} = \left(\frac{M_{in}\sqrt{\rho_{end}}}{4\pi\gamma\sqrt{3}M_P^3}\right)^{\frac{2}{3(1+\omega)}} \beta^{-\frac{1}{3\omega}}. \tag{5.188}$$

Imposing (5.187) and (5.195) to be equal, the critical value is then found at [35]

$$\beta_{crit}^{BH} = \left(\frac{\epsilon}{(1+\omega)2\pi\gamma}\right)^{\frac{2\omega}{1+\omega}} \left(\frac{M_P}{M_{in}}\right)^{\frac{4\omega}{1+\omega}}. \tag{5.189}$$

5.5.2 PBH reheating temperature

In order to evaluate the PBH temperature we need to distinguish between two separate cases.

PBH domination

Whenever the parameter β crosses the critical threshold (5.189), $\beta > \beta_{crit}^{BH}$, PBHs dominate the energy density of the Universe over the inflaton. In this case reheating ends with their decay, that generates entropy which is then transferred to the thermal bath. The condition for that to happen is identified by:

$$\Gamma_{BH} = H. \tag{5.190}$$

Using the fact that

$$\Gamma_{BH} = \epsilon \frac{M_P^4}{M_{in}^3}, \tag{5.191}$$

where $\epsilon = \frac{\pi g_{BH}}{480}$, and using $\rho_{RH} = \alpha_T T_{RH}^4$, one gets

$$T_{rh} = M_P \left(\frac{3\epsilon^2}{\alpha_T}\right)^{\frac{1}{4}} \left(\frac{M_P}{M_{in}}\right)^{\frac{3}{2}}. \tag{5.192}$$

Without PBH domination

On the other hand, if $\beta < \beta_{crit}^{BH}$, PBHs are not the dominant component of the energy density of the Universe, but they are still decaying, hence transferring entropy to the thermal bath. This allows us to identify the reheating temperature with the value corresponding to ρ_R^{BH} at the time in which they evaporate. In the end the reheating temperature is found to be:

$$T_{rh} \simeq M_P \left[\frac{\delta^{\frac{3(\omega_\phi+1)}{4(1-3\omega_\phi)}}}{\alpha_T^{\frac{1}{4}}}\right] \left(\frac{M_P}{M_{in}}\right)^{\frac{3(1-\omega_\phi)}{2(1-3\omega_\phi)}} \beta^{\frac{3(\omega_\phi+1)}{12\omega_\phi-4}}, \tag{5.193}$$

where

$$\delta = \frac{5+3\omega_\phi}{2\sqrt{3}\epsilon} (4\pi\sqrt{3}\gamma)^{\frac{-2\omega_\phi}{1+\omega_\phi}} \left[\frac{2\sqrt{3}\epsilon}{1+\omega_\phi}\right]^{\frac{5+3\omega_\phi}{3+3\omega_\phi}}. \tag{5.194}$$

We now focus on the first scenario, meaning when PBHs come to dominate the energy budget of the Universe after a certain point. We have different situations, let us first consider the situation in which the inflaton decays, allowing PBHs to dominate the energy density over radiation.

Having gotten the expressions of the PBH reheating temperatures in this regime, it is now interesting to evaluate how the analysis previously done in section 5.4, where only the inflaton was decaying and reheating the Universe, changes. In addition to the T_{rh} difference, in a Universe where PBHs dominate the energy density, also the oscillating conditions for the axions are different. For simplicity we consider at first only PBHs, ignoring the presence of the inflaton and assuming radiation domination before the PBH starts to dominate. We can identify with t_{eq} the time at which ρ_R and ρ_{BH} cross each other. Having assumed a PBH dominated Universe, the evaporation of the PBH, which happens at t_{ev}, will always be after t_{eq}. Constraining oscillations to happen before the evaporation of the PBH we identify two regimes: either $T_{rh,BH} < T_{osc} < T_{eq}$ or $T_{rh,BH} < T_{eq} < T_{osc}$. The Hubble rate will be different for the two cases, as it goes like radiation domination case for the second case and like matter for the first.

$$H(T_{osc}) = H_{eq} \begin{cases} \left(\frac{T_{osc}}{T_{eq}}\right)^2 & \text{for } T_{osc} > T_{eq} \\ \left(\frac{T_{osc}}{T_{eq}}\right)^{\frac{3}{2}} & \text{for } T_{osc} < T_{eq} \end{cases} . \tag{5.195}$$

Performing the same analysis as the previous section, we can then identify the oscillation temperature in different regimes. Specifically, we again require $T_{rh,BH} < T_{osc}$ and, imposing $3H(T_{osc}) = \tilde{m}_a(T_{osc})$ while using Eq. (5.195), we get the oscillation temperature.

We can now evaluate the relic abundance, which, seeing that misalignment is the dominating production mechanism, will be given by

$$\Omega_a h^2 = \frac{\rho_a(T_0)}{\rho_c/h^2}, \tag{5.196}$$

where the energy density will simply be

$$\rho_a(T_0) = \rho_a(T_{osc}) \frac{m_a}{\tilde{m}_a(T_{osc})} \left(\frac{a_0}{a_{osc}}\right)^{-3}, \tag{5.197}$$

and $\rho_a(T_{osc}) = \frac{1}{2}\tilde{m}_a^2(T_{osc}) f_a^2 \theta_i^2$.

In order to proceed we then need to determine the redshift between when axions start oscillating and the present time. To begin, assume that axions start oscillating before PBHs start dominating the energy density budget; in this case the expressions for the oscillation temperature will be:

- $T_{osc} > T_{eq}, T_{QCD}$:

$$T_{osc} = \left[\frac{M_P}{\pi}\sqrt{\frac{10}{g_*(T_{osc})}} T_{QCD}^4 m_a\right]^{\frac{1}{6}}; \tag{5.198}$$

- $T_{eq} < T_{osc} < T_{QCD}$:

$$T_{osc} = \left[\frac{M_P}{\pi}\sqrt{\frac{10}{g_*(T_{osc})}} m_a\right]^{\frac{1}{2}}. \tag{5.199}$$

We can hence split the redshift in three phases:

$$\frac{a_{in}}{a_0} = \frac{a_{in}}{a_{eq}} \frac{a_{eq}}{a_{ev}} \frac{a_{ev}}{a_0}, \tag{5.200}$$

due to the different behaviours of the dominating components at different times.

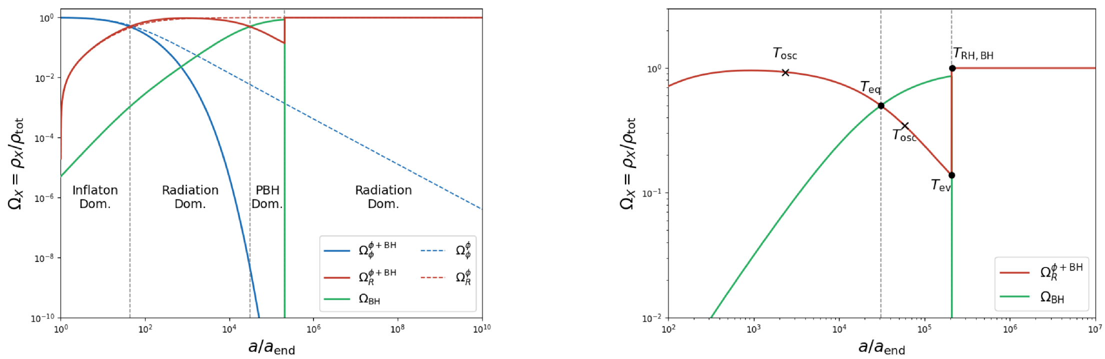

Figure 5.13: On the left the renormalized energy densities, presented in order to show the different regimes of domination. The used parameters are $k = 6$, the coupling is $y = 0.1$, $\beta = 10^{-6}$, $\lambda = 5 \cdot 10^{-11}$, $M_{in} = 10g$. In the example considered above, we mentioned PBHs coming to dominate after a radiation dominated phase. On the right a zoom in has been proposed to show the splitting between the redshifts. For the sake of brevity only one case will be here analyzed, specifically the one in which oscillations happen in radiation domination.

The first phase can be determined by imposing the crossing of ρ between radiation and PBHs at equality.

$$\rho_{BH}(a_{eq}) = \rho_R(a_{eq}). \tag{5.201}$$

Considering the redshift from the initial time, which we will identify with the time the axion starts oscillating, and equality we can rewrite it as

$$\rho_{BH,in}\left(\frac{a_{in}}{a_{eq}}\right)^3 = \rho_{R,in}\left(\frac{a_{in}}{a_{eq}}\right)^4, \tag{5.202}$$

and using the β relation

$$\beta = \frac{\rho_{BH,in}}{\rho_{R,in}}, \tag{5.203}$$

this gives us

$$\frac{a_{in}}{a_{eq}} = \beta. \tag{5.204}$$

Next we consider the time from equality until the PBH evaporates. We know that the latter is the moment in which $H = \Gamma_{BH}$ and we already got the reheating temperature result in Eq. (5.192). The relation will then be

$$\rho_{BH}(a_{ev}) = \rho_R(a_{ev}). \tag{5.205}$$

We will use the fact that evaporation and reheating happen almost simultaneously, so that $\rho_R(a_{ev}) = \alpha_T T^4_{rh,BH}$, with $\alpha_T = \frac{\pi^2}{30} g_*(T_{rh,BH})$. Moreover we can express

$$\rho_{BH}(a_{ev}) = \rho_{BH,eq}\left(\frac{a_{eq}}{a_{ev}}\right)^3 = \rho_{BH,in}\left(\frac{a_{in}}{a_{eq}}\right)^3\left(\frac{a_{eq}}{a_{ev}}\right)^3. \tag{5.206}$$

Additionally, we will express $\rho_{BH,in} = \beta\rho_{R,in}$ to express it in terms of the initial mass, seen that:

$$M_{in} = \gamma\frac{4\pi}{3}\frac{\rho_{R,in}}{H^3(t_{in})}, \tag{5.207}$$

which implies

$$\rho_{R,in} = 48\pi^2\gamma^2\frac{M_P^6}{M_{in}^2}. \tag{5.208}$$

Therefore the condition (5.205) will become:

$$\alpha_T\left[\left(\frac{12\epsilon^2}{\alpha_T}\right)^{\frac{1}{4}}\frac{M_P^{\frac{5}{2}}}{M_{in}^{\frac{3}{2}}}\right]^4 = \beta^4 48\pi^2\gamma^2\frac{M_P^6}{M_{in}^2}\left(\frac{a_{eq}}{a_{ev}}\right)^3, \tag{5.209}$$

and hence

$$\frac{a_{eq}}{a_{ev}} = \left(\frac{\epsilon}{2\pi\gamma}\frac{M_P^2}{M_{in}^2}\right)^{\frac{2}{3}}\beta^{-\frac{4}{3}}. \tag{5.210}$$

Lastly, the remaining piece is

$$\frac{a_{ev}}{a_0} = \frac{T_0}{T_{RH,BH}}\left(\frac{g_0}{g_{RH}}\right)^{\frac{1}{3}}. \tag{5.211}$$

Combining the three different pieces, one finds

$$\begin{aligned}\frac{a_{in}}{a_0} &= \frac{a_{in}}{a_{eq}}\frac{a_{eq}}{a_{ev}}\frac{a_{ev}}{a_0} \\ &= \left(\frac{\epsilon}{2\pi\gamma}\right)^{\frac{2}{3}} T_0\left(\frac{\alpha_T}{12\epsilon^2}\right)^{\frac{1}{4}}\left(\frac{M_{in}}{M_P^7}\right)^{\frac{1}{6}}\left(\frac{g_0}{g_{RH}}\right)^{\frac{1}{3}}\beta^{-\frac{1}{3}}.\end{aligned} \tag{5.212}$$

Having now gotten the total redshift we can compute the relic abundance, assuming $a_{osc} = a_{in}$ and, again, that axions get produced mainly through misalignement mechanism:

$$\Omega_a h^2 = \frac{\rho_a(T_0)}{\rho_c/h^2} = \frac{1}{2}\frac{\tilde{m}_a(T_{osc})}{m_a}\frac{(5.7\cdot 10^{-3}GeV^2)^2\theta_i^2}{\rho_c/h^2}\left[\left(\frac{\epsilon}{2\pi\gamma}\right)^2\frac{g_0}{g_{RH}}T_0^3\left(\frac{\alpha_T}{12\epsilon^2}\right)^{\frac{3}{4}}\left(\frac{M_{in}}{M_P^7}\right)^{\frac{1}{2}}\right]\beta^{-1}. \tag{5.213}$$

As always, we impose the usual $\Omega_a h^2 < 0.12$ upper bound, so that we can identify a parameter space relating the axionic m_a to the pbh's β.

Before showing this, we might also mention the fact that axions are not exclusively produced through misalignment in this context, but they can also come from PBH evaporation. If we add this density contribution to the relic abundance evaluation, we find a β independent term:

$$\begin{aligned}\Omega_a^{ev}h^2 = \frac{\rho_a^0}{\rho_c/h^2} &= \frac{1}{\rho_c/h^2}\left(\frac{a_{ev}}{a_0}\right)^3\rho^{ev} \\ &= \frac{1}{\rho_c/h^2}\frac{g_0}{g_{ev}}\frac{T_0^3}{T_{ev}^3}\tilde{m}_a(T_{ev})n_{PBH}^{ev}.\end{aligned} \tag{5.214}$$

We can substitute

$$\begin{aligned}n_{PBH}^{ev} &= n_{PBH}^{i}\left(\frac{a_i}{a_{ev}}\right)^3 \\ &= \frac{\beta\rho_{rad}^i}{M_{in}}\cdot\left(\frac{\epsilon}{2\pi\gamma}\frac{M_P^2}{M_{in}^2}\right)^2\beta^{-1},\end{aligned} \tag{5.215}$$

where $\rho_{rad}^i = \alpha_T T_{osc}^4$. To be precise there's a coefficient that should be added in this expression, to indicate how much of the decay actually contributes to this density, but, as it is at most of order 1 (or 10^{-2} which is even smaller), we neglect it. In any case, as will be shown by the total result, in the low axion mass regime that we consider, the evaporation contribution is negligible with respect to the misalignment production.

So in the end:

$$\begin{aligned}\Omega_a h^2 = \frac{1}{2}\frac{\tilde{m}_a(T_{osc})}{m_a}\frac{(5.7\cdot 10^{-3}GeV^2)^2\theta_i^2}{\rho_c/h^2}\left[\left(\frac{\epsilon}{2\pi\gamma}\right)^2\frac{g_0}{g_{RH}}T_0^3\left(\frac{\alpha_T}{12\epsilon^2}\right)^{\frac{3}{4}}\left(\frac{M_{in}}{M_P^7}\right)^{\frac{1}{2}}\right]\beta^{-1} + \\ \frac{1}{\rho_c/h^2}\frac{g_0}{g_{ev}}\frac{T_0^3}{T_{ev}^3}\tilde{m}_a(T_{ev})\left(\frac{\epsilon}{2\pi\gamma}\frac{M_P^2}{M_{in}^2}\right)^2\frac{\alpha_T T_{osc}^4}{M_{in}}.\end{aligned} \tag{5.216}$$

A note has to be made here: the considered range of M_{in} values is more stringent than the $1g < M_{in} < 10^8 g$ mentioned before. The reasoning behind this is that, being the axion mass temperature dependant, as temperature rises in the evaporation process, the mass decreases. In this situation we could go back to the regime in which $3H > m_a$, where the axion is frozen, as an intermediate phase between two oscillating regimes. This would forbid us from evaluating the energy densities, and consequently the relic abundances, through the redshifts, as we would not have $\rho \propto a^{-3}$ but $\rho \sim$ const in that period. The lower bound that we can consider in this analysis will then be obtained as

$$M_{in} > 10^8 g \cdot \left(\frac{T_{BBN}}{T_{osc}}\right)^{2/3}, \tag{5.217}$$

due to the fact that $T_{rh,BH} \propto M_{in}^{-\frac{3}{2}}$. Using $T_{BBN} \sim 1MeV$ and $T_{osc} \sim 1GeV$, we find a lower bound of the order of $M_{in} > 10^6 g$.

We can now impose the usual upper bound on the relic abundance in order to plot (5.216). We will restrict to the case in which $T_{osc} > T_{QCD}$ so that the appearence of the oscillation temperature (5.198) entails the axion mass.

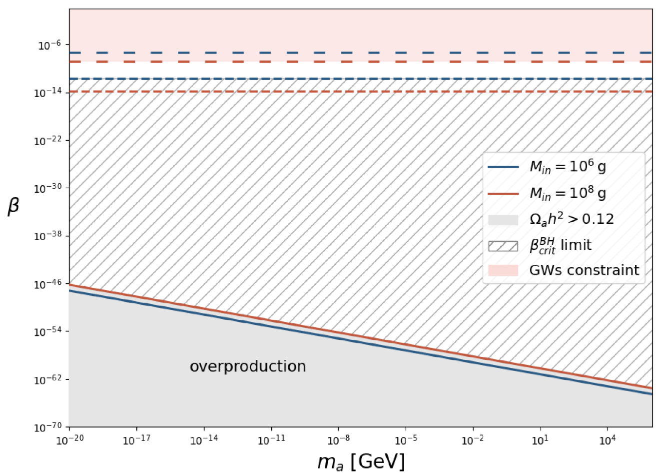

Figure 5.14: Plot of the β parameter as a function of the axion mass. As we can see, the lines corresponding to the relic abundance upper bound lie well below the horizontal constraints identified by the β^{BH}_{crit} classifying the pbh domination. This implies that in this regime we are always underproducing. The fact that PBH domination requires higher values of β, however, implies that we have just a small range of possible β values to produce the right amount.

6

Conclusions

6.1 Summing up

This thesis focused on axions as possible Dark Matter candidates. After a brief contextualization of the Physics models currently used, namely the Standard Model and the ΛCDM model, and their issues in Chapter 1, axions were introduced and later presented in Chapters 2 and 3, respectively. Chapter 4 focuses on the Inflationary phase and Reheating, which will constitute the framework of the analysis. The main work was then developed in Chapter 5.

Axions emerge theoretically as a solution to the strong CP problem that appears in the context of the Standard Model, but can also be useful in a cosmological framework, as they can serve as Dark Matter candidates. The context in which axions were studied in this thesis is the Reheating epoch, a post-inflationary phase needed in order to thermalize the Universe. Axions were considered to have been produced through two different mechanisms: the misalignment mechanism, in which the axion oscillates around the minimum of the potential, and gravitational production, in which they are produced after SM particles interactions or from the inflaton condensate, both cases being graviton-mediated. The goal was to restrict the parameter space, which in this analysis consisted of the reheating temperature T_{rh} and the axion mass m_a at T_0, which we chose in the range $10^{-6}\text{eV} < m_a < 10^{-5}\text{eV}$. To do so, one can consider the experimental upper bound on the abundance of axions in the case they constitute DM, namely $\Omega_{DM} h^2 < 0.12$.

In the following sections the main results of the thesis will be summarized.

6.1.1 Axions produced during Misalignment Mechanism

A T-attractor potential was considered, $V(\phi) \simeq \lambda \frac{\phi^k}{M_P^{k-4}}$, with three possible interactions for the inflaton field, namely fermionic and bosonic decay and bosonic annihilation, each characterized by a different k-dependant l parameter. After evaluating the explicit expressions for the radiation and inflaton energy densities, the two were equated, allowing the evaluation of the reheating temperature.

After this preliminary analysis, axions were considered to have been produced through misalignment mechanism, meaning initially displaced from a position θ_i along their potential and being later able to roll down and start oscillating. Imposing the oscillating condition $3H(T_{osc}) = \tilde{m}_a(T_{osc})$, it was possible to derive the oscillation temperature in different temperature regimes.

Wanting to study axions in the case they were produced during Reheating, one can compare these oscillation temperatures to the reheating temperature previously derived, imposing oscillations to have started during reheating ($T_{osc} > T_{rh}$). In the end we could find some upper bounds on the couplings of each of the three inflaton interactions.

$T_{osc} > T_{RH}$	
$T_{QCD} < T_{osc}$	$y_{\text{eff}}^2 < \frac{4\pi}{\sqrt{3}} \frac{14-2k}{k^{\frac{3}{2}}\sqrt{k-1}} \left(\frac{\pi^4 g_*(T_{RH})^2}{3 \cdot 900} \frac{1}{\lambda^3 M_P^{10}} T_{QCD}^8 \right)^{\frac{1}{3k}} \cdot m_a^{\frac{2}{3k}}$
	$\mu_{\text{eff}}^2 < \frac{4\pi}{\sqrt{3}} \sqrt{\frac{k-1}{k}} (4k+2) M_P^{\frac{4}{k}-2} \lambda^{\frac{1}{k}} \left(\frac{\sqrt{10} \cdot g_*(T_{RH})}{30^{\frac{3}{2}}} \cdot \pi^2 M_P T_{QCD}^4 \right)^{\frac{2}{3}(1-\frac{1}{k})} \cdot m_a^{\frac{2}{3}(1-\frac{1}{k})}$
	$\sigma_{\text{eff}}^2 < \frac{4\pi}{\sqrt{3}} \sqrt{k} (k-1)^{\frac{3}{2}} (4k-10) \lambda^{\frac{3}{k}} \left(\frac{\sqrt{10}}{M_P^5} \frac{g_*(T_{RH})}{30^{\frac{3}{2}}} \pi^2 T_{QCD}^4 \right)^{\frac{2}{3}(1-\frac{3}{k})} \cdot m_a^{\frac{2}{3}(1-\frac{3}{k})}$
$T_{QCD} > T_{osc}$	$y_{\text{eff}}^2 < \frac{8\pi}{\sqrt{k(k-1)}} \frac{7-k}{k} \frac{1}{\sqrt{3}} \left(\frac{1}{3} \frac{m_a^2}{M_P^2} \frac{1}{\lambda} \right)^{\frac{1}{k}}$
	$\mu_{\text{eff}}^2 < \frac{4\pi}{3\sqrt{3}} \sqrt{\frac{k-1}{k}} (4k+2) (3\lambda M_P)^{\frac{1}{k}} m_a^{2-\frac{2}{k}}$
	$\sigma_{\text{eff}}^2 < \frac{4\pi}{\sqrt{3}} \sqrt{k} (k-1)^{\frac{3}{2}} \frac{(4k-10)}{3M_P^2} (3\lambda M_P^2)^{\frac{3}{k}} m_a^{2-\frac{6}{k}}$

Table 6.1: Summary of the coupling constraints. (Note: the bosonic annihilation coupling σ_{eff} is here derived only for $k = 4, 6$).

The Table above shows the final bounds on the couplings found. Seen the axion mass dependence, and knowing it can be restrained to a certain range in our analysis, we could plot the resulting parameter space in Plots 5.4, 5.5 and 5.6.

6.1.2 Gravitational axions

The second production mechanism considered comes from 2-to-2 processes, either from SM particles interacting (thermal scattering) or from the inflaton condensate (inflaton scattering), mediated by a massless graviton. The evaluation of the rates of these gives respectively the following number densities:

$$n_a^T(a_{RH}) = \frac{\sqrt{3}\beta_0}{M_P^3}\left(\frac{30}{g_*(T_{rh})\pi^2}\right)^2 \frac{\rho_{RH}^{\frac{3}{2}}}{[1-(\frac{a_{end}}{a_{rh}})^{\frac{k+8-6kl}{k+2}}]^2}(k+2)\left[\frac{1}{6-12kl} + \frac{2}{6kl+k+2}\left(\frac{a_{rh}}{a_{end}}\right)^{\frac{6kl-k-8}{k+2}} + \left(\frac{1}{12kl-6} - \frac{2}{6kl+k+2} + \frac{1}{10+2k}\right)\left(\frac{a_{rh}}{a_{end}}\right)^{\frac{12kl-6}{k+2}} - \frac{1}{10+2k}\left(\frac{a_{rh}}{a_{end}}\right)^{\frac{12kl-2k-16}{k+2}}\right]; \tag{6.1}$$

$$n_a^\phi(a_{RH}) = \frac{\sqrt{3}}{8\pi M_P^3}\Sigma_0^k \rho_{RH}^{\frac{3}{2}} \frac{(k+2)}{6-6k}\left[1-\left(\frac{a_{RH}}{a_{end}}\right)^{\frac{6k-6}{k+2}}\right]. \tag{6.2}$$

6.1.3 Relic abundances

The number densities previously derived can be employed in the evaluation of the relic abundance through:

$$\Omega_a h^2 = 1.6\cdot 10^8 \frac{g_*(T_0)}{g_*(T_{RH})}\frac{n_a(T_{RH})}{T_{RH}^3}\frac{\tilde{m}_a(T_{RH})}{1GeV}. \tag{6.3}$$

T Regime		$\Omega_a^{GRAV}h^2$
①, ④, ⑤	$T_{rh} > T_{QCD}$	$\Omega_a h^2 = 3.2\cdot 10^3 \cdot m_a \frac{(GeV)^3}{T_{rh}^7}(n_a^\phi + n_a^T)$
②, ③, ⑥	$T_{rh} < T_{QCD}$	$\Omega_a h^2 = 3.8\cdot 10^7 \frac{m_a}{1GeV}\frac{1}{T_{rh}^3}(n_a^\phi + n_a^T)$

Table 6.2: Gravitational abundances.

In the same way, for the misalignment mechanism production:

	T Regime	$\Omega_a^{MIS} h^2$
①	$T_{osc} > T_{rh} > T_{QCD}$	$2.6 \cdot 10^{-5} \cdot \theta_i^2 \frac{(GeV)^{11}}{T_{rh}^{11}} \left[\frac{M_P}{\pi} \sqrt{\frac{10}{g_*(T_{rh})}} \frac{T_{QCD}^4}{T_{rh}^6} m_a \right]^{-\frac{7(2l+1)}{8(1+l)}}$
②	$T_{osc} > T_{QCD} > T_{rh}$	$0.3 \cdot \theta_i^2 \frac{(GeV)^7}{T_{rh}^7} \left[\frac{M_P}{\pi} \sqrt{\frac{10}{g_*(T_{rh})}} \frac{T_{QCD}^4}{T_{rh}^6} m_a \right]^{-\frac{7(2l+1)}{8(1+l)}}$
③	$T_{QCD} > T_{osc} > T_{rh}$	$6.2 \cdot 10^2 \cdot \theta_i^2 \frac{(GeV)^3}{T_{rh}^3} \left[\frac{M_P}{\pi} \sqrt{\frac{10}{g_*(T_{rh})}} \frac{m_a}{T_{rh}^2} \right]^{-\frac{3}{4}(1+2l)}$
④	$T_{rh} > T_{osc} > T_{QCD}$	$8.6 \cdot 10^{-22} \theta_i^2 \frac{(GeV)^{\frac{31}{6}}}{T_{rh}^4} m_a^{-\frac{7}{6}}$
⑤	$T_{rh} > T_{QCD} > T_{osc}$	$5.9 \cdot 10^{-28} \theta_i^2 \frac{(GeV)^{\frac{11}{2}}}{T_{rh}^4} m_a^{-\frac{3}{2}}$
⑥	$T_{QCD} > T_{rh} > T_{osc}$	$1.2 \cdot 10^{-24} \theta_i^2 (GeV)^{\frac{3}{2}} m_a^{-\frac{3}{2}}$

Table 6.3: Misalignment abundances.

These two tables sum up the main results of the thesis. Summing both mechanisms contributions and imposing the DM experimental upper bound, the plots 5.12 were realized. Additionally to the excluded region due to overproduction, each regime imposes further constraints on the parameter space, leaving in white colour the only acceptable co-existing region between m_a and T_{rh}. One can clearly see how the different regimes leave more or less space to the right amount of axion DM produced; for example in regime ④: $T_{rh} > T_{osc} > T_{QCD}$ the allowed white region is much more extended than the other cases, some of which are all cancelled by overproduction or regime constraints.

6.1.4 PBH reheating

In the last section, the total energy density was hypothesized to be dominated by matter after a certain point, specifically by objects formed in the Early Universe and known as Primordial Black Holes. This domination phase depends on the parameter β seen in Eq. (5.177). If they do dominate at a certain point, they are said to drive reheating, modifying T_{rh}.

A previously radiation dominated phase is assumed, which implies a certain expression for the reheating and the oscillation temperature.

In the end, the axion abundance in this scenario was evaluated, considering that they were produced both via misalignment and through the PBH evaporation:

$$\Omega_a h^2 = \frac{1}{2}\frac{\tilde{m}_a(T_{osc})}{m_a}\frac{(5.7\cdot 10^{-3}GeV^2)^2\theta_i^2}{\rho_c/h^2}\left[\left(\frac{\epsilon}{2\pi\gamma}\right)^2\frac{g_0}{g_{RH}}T_0^3\left(\frac{\alpha_T}{12\epsilon^2}\right)^{\frac{3}{4}}\left(\frac{M_{in}}{M_P^7}\right)^{\frac{1}{2}}\right]\beta^{-1}+ \\ \frac{1}{\rho_c/h^2}\frac{g_0}{g_{ev}}\frac{T_0^3}{T_{ev}^3}\tilde{m}_a(T_{ev})\left(\frac{\epsilon}{2\pi\gamma}\frac{M_P^2}{M_{in}^2}\right)^2\frac{\alpha_T T_{osc}^4}{M_{in}}. \tag{6.4}$$

This expression was used to plot 5.14, which shows the restricted range of β allowed in order not to have overproduction of axions, in the case they are DM. As the relic abundance line lies well below the β_{crit}^{BH} limits considered in this analysis, the m_a range chosen does not really affect the range of validity of the β parameter.

6.2 Discussion and future prospects

In this work we have discussed the production of axions as DM candidates, in the epoch of reheating, through different mechanisms: misalignment, gravitational production and from PBH evaporation. The goal was to restrict the parameter space $\{m_a\,;T_{rh}\}$ in different temperature regimes. Depending on the production mechanism, other parameters come into play, such as the initial misalignment angle θ_i, or β and M_{in} in the case of PBHs. Many of the plots have been shown for a single situation, the case in which the potential had a $k = 2$ and the inflaton was decaying into fermions during reheating, hence $l = 0$. The analysis can therefore be extended to see how this behaviour changes for different k-powers or different decay channels. Regarding the PBH analysis, we focused on the case in which the inflaton decays, we get to radiation domination and afterwards the PBH dominates over the total energy budget of the Universe. Of course, there are many other scenarios that could be explored. One could study the situation in which PBHs never come to dominate, hence having a reheating temperature as the one presented in Eq. (5.193), which brings an additional β dependence and therefore enriches the parameter space analysis. Otherwise the inflaton can be thought not to decay beforehand, bypassing the radiation era, and therefore implying a different temperature dependence in Eq. (5.195).

A

Equilibrium thermodynamics

In this appendix, we review some thermodynamic relations used throughout this thesis, focusing on the evolution of number densities in an expanding Universe, governed by the Boltzmann equation.

A common form for the equations encountered will be

$$\frac{dn}{dt} + kHn = C, \tag{A.1}$$

where n is the number density of the species, C stands for the collision term representing interactions, and $H = \frac{1}{a}\frac{da}{dt}$, with a being the scale factor. The constant k is typically taken to be $k = 3$ in the case of matter and $k = 4$ in the case of radiation.

It is easy to see that they can be recast into a compact form defining

$$Y = a^k n. \tag{A.2}$$

We can see that

$$\frac{dY}{dt} = \frac{d(a^k n)}{dt} = \frac{dn}{dt} \cdot a^k + n \cdot k a^{k-1} \frac{da}{dt}. \tag{A.3}$$

In analogy to (A.1) we can write

$$\frac{1}{a^k}\frac{dY}{dt} = \frac{dn}{dt} + nkH, \tag{A.4}$$

or simply

$$\frac{dY}{dt} = a^k C. \tag{A.5}$$

A.1 Number density equation

In Section 5.3 we use Eqs. (5.115) and (5.143). This comes from the Boltzmann equation

$$\frac{dn_X}{dt} + 3Hn_X = R_X^i, \tag{A.6}$$

where X is the produced species considered, in our case $X = a$ are the axions, R_X^i is the rate at which the process happens, so either thermal R_a^T or inflaton scatterings R_a^ϕ. We use the Hubble rate $H = \frac{\dot{a}}{a} = \frac{da}{dt}\frac{1}{a}$ to change variable, from t to a

$$\frac{d}{dt} = aH\frac{d}{da}, \tag{A.7}$$

so that our equation becomes

$$aH\frac{dn_X}{da} + 3Hn_X = R_X^i \Rightarrow \frac{dn_X}{da} + 3\frac{n_X}{a} = \frac{R_X^i}{aH}. \tag{A.8}$$

Then, using the fact that $Y_X = n_X a^3$:

$$\frac{dY_X}{dt} = \frac{dn_X}{dt} \cdot a^3 + 3a^2\dot{a}n_X \Rightarrow \frac{dY_X}{da} = \frac{dn_X}{da} \cdot a^3 + 3a^2 n_X. \tag{A.9}$$

Comparing the two equations (A.8) and (A.9) we are left with

$$\frac{dY_X}{da} = \frac{a^2 R_X^i}{H}. \tag{A.10}$$

A.2 The rate

Consider the scattering

$$SM(p_1) + SM(p_2) \longrightarrow a(p_3) + a(p_4), \tag{A.11}$$

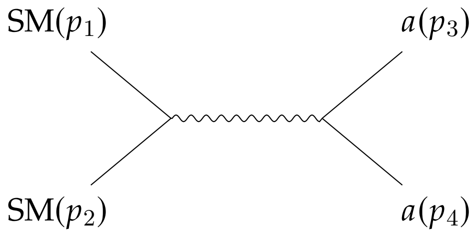

Figure A.1: s-channel gravitational production of axions.

and let us evaluate the rate of this process. We know that

$$R(T) = \int \frac{d^3\vec{p}_1}{(2\pi)^3}\frac{d^3\vec{p}_2}{(2\pi)^3}\frac{f_1}{2E_1}\frac{f_2}{2E_2}\int \frac{d^3\vec{p}_3}{(2\pi)^3 2E_3}\frac{d^3\vec{p}_4}{(2\pi)^3 2E_4}|\mathcal{M}|^2(2\pi)^4\delta^{(4)}(p_1+p_2-p_3-p_4). \tag{A.12}$$

We will consider the centre-of-mass frame for particles with momenta p_3, p_4, meaning that $\vec{p}_3+\vec{p}_4 = 0$ and hence $E_3 = E_4$; moreover, assuming to be in a regime in which masses are negligible compared to the temperature $m_1, m_2, m_3, m_4 \ll T$.

First of all, let us show that this expression is equivalent to equation (5.112). In order to do that we exploit the masslessness of the particles considered, which implies $p_i = E_i$. This means that the phase space elements can be written as:

$$d\Pi_i = \frac{d^3p_i}{(2\pi)^3 2E_i} = \frac{E_i^2 dE_i d\Omega_i}{(2\pi)^3 2E_i}. \tag{A.13}$$

For the case of $i = 1, 2$ we additionally consider that $\int d\Omega_1 = 4\pi$ and $\int d\Omega_2 = \int d\phi_{12} d\cos\theta_{12} = 2\pi \int d\cos\theta_{12}$. As far as the final state:

$$\int d\Pi_3 d\Pi_4 (2\pi)^4\delta^{(4)}(p_1+p_2-p_3-p_4) = \frac{1}{16\pi^2}\int d\Omega_{13}. \tag{A.14}$$

Plugging everything back, and considering the additional internal symmetry factor of $1/2$ due to the identical particles, we get:

$$R(T) = \frac{1}{1024\pi^6}\int f_1 f_2 E_1 E_2 dE_1 dE_2 d\cos\theta_{12}\int |\mathcal{M}|^2 d\Omega_{13}, \tag{A.15}$$

where E_i are the energies of the particles $i = 1, 2$, θ_{12} is the angle formed between their momenta and the thermal distribution functions are

$$f_i = \frac{1}{e^{\frac{E_i}{T}} \pm 1}, \tag{A.16}$$

depending on the bosonic or fermionic nature of the particles. For the evaluation of the rate it is useful to perform some variable change. In particular we see that $d\Omega_{13} = 2\pi d\cos\theta_{13}$, where we will call $\cos\theta_{13} = x$, with $x \in [-1;1]$. Moreover $t = \frac{s}{2}(\cos\theta_{13} - 1)$ and $s = 2E_1E_2(1 - \cos\theta_{12})$, where we will call $\cos\theta_{12} = z$ with $z \in [-1;1]$.

We will now present the general resolution, not considering numerical factors, that will be used in Chapter 5. Let us first consider the scalar and bosonic cases, which have a matrix element $|\mathcal{M}|^2 \propto \frac{t^2(s+t)^2}{s^2}$ and a positive sign in Eq. (A.16). Performing the variable change above described, the rate reduces to

$$R(T) = \frac{1}{2048\pi^5}\left(\int_0^{+\infty} \frac{E^3}{e^{\frac{E}{T}} - 1}\right)\int_{-1}^{+1} (x-1)^2(x+1)^2 dx \int_{-1}^{+1} (1-z)^2 dz, \quad \text{(A.17)}$$

where the two integrals for E_1 and E_2 have been grouped under a generic E integral squared, seen as they are the same and each equal to $\frac{\pi^4}{15}T^4$.

For the fermionic case, instead, $|\mathcal{M}|^2 \propto \frac{[-t(s+t)(s+2t)^2]}{s^2}$ and a negative sign in Eq. (A.16). The rate reduces to

$$R(T) = \frac{1}{512\pi^5}\left(\int_0^{+\infty} \frac{E^3}{e^{\frac{E}{T}} + 1}\right)\int_{-1}^{+1} -x^2(x^2-1) dx \int_{-1}^{+1} (1-z)^2 dz. \quad \text{(A.18)}$$

In this case the energy integral equates to $\frac{7}{120}\pi^4 T^4$.

Evaluating the numerical parts of the integrals and summing them respecting the coefficients of each matrix element, leads to Eq. (5.114).

B

Equations of motion for a scalar field

From the minimal action principle one can get the equations of motion for the inflaton field ϕ:

$$\frac{\partial S}{\partial \phi} = 0. \tag{B.1}$$

Having considered the following action,

$$S_\phi = \frac{1}{16\pi G}\int d^4x\sqrt{-g}\mathcal{L}_\phi, \tag{B.2}$$

with

$$\mathcal{L}_\phi = -\frac{1}{2}g^{\mu\nu}\partial_\mu\phi\partial_\nu\phi - V(\phi), \tag{B.3}$$

varying the action gives

$$\begin{aligned} 0 &= -\int d^4x\left\{\delta[\sqrt{-g}V(\phi)] + \frac{1}{2}\delta[\sqrt{-g}g^{\mu\nu}\phi_{,\mu}\phi_{,\nu}]\right\} \\ &= -\int d^4x\left\{\sqrt{-g}\frac{\partial V(\phi)}{\partial\phi}\delta\phi + \sqrt{-g}g^{\mu\nu}\delta(\phi_{,\mu})\phi_{,\nu}\right\}. \end{aligned} \tag{B.4}$$

The second half of this equation can be rewritten using integration by parts

$$\sqrt{-g}g^{\mu\nu}\delta(\phi_{,\mu})\phi_{,\nu} = -\partial_\mu[\sqrt{-g}g^{\mu\nu}\phi_{,\nu}]\delta\phi + \partial_\mu[\sqrt{-g}g^{\mu\nu}\delta\phi\phi_{,\nu}]. \tag{B.5}$$

Putting to zero the second term, which is a boundary term, and inserting this relation in (B.4) we get:

$$\frac{1}{\sqrt{-g}}[\sqrt{-g}g^{\mu\nu}\phi_{,\nu}]_{,\mu} = \frac{\partial V}{\partial\phi} \Rightarrow \Box\phi = \frac{\partial V}{\partial\phi}. \tag{B.6}$$

The D'Alambertian operator can be written as

$$\begin{aligned}
\Box\phi &= \frac{1}{\sqrt{-g}}(g^{\mu\nu}\sqrt{-g}\phi_{,\mu})_{,\nu} \\
&= \frac{1}{a^3}(g^{00}a^3\phi_{,0})_{,0} + \frac{1}{a^3}(g^{ii}a^3\phi_{,i})_{,i} \\
&= \frac{1}{a^3}(-a^3\phi_{,0})_{,0} + \frac{1}{a^3}(a\phi_{,i})_{,i} \\
&= -\ddot{\phi} - \frac{3a^2\dot{a}\dot{\phi}}{a^3} + \frac{\nabla^2\phi}{a^2} \\
&= -\ddot{\phi} - 3H\dot{\phi} + \frac{\nabla^2\phi}{a^2}.
\end{aligned} \tag{B.7}$$

Unifying (B.6) and (B.7) one gets the Klein-Gordon equation for the scalar field ϕ:

$$\ddot{\phi} + 3H\dot{\phi} - \frac{\nabla^2\phi}{a^2} = -\frac{\partial V}{\partial\phi}. \tag{B.8}$$

C

Decay rates

C.1 Decay rate of the inflaton field oscillating about a quadratic potential

Let us evaluate the decay rate of the inflaton field into two fermions, given the interaction coupling y.

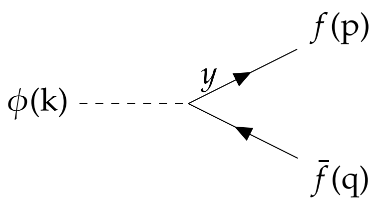

Figure C.1: Decay of scalar ϕ into a fermion-antifermion pair.

The matrix element reads

$$i\mathcal{M}(\phi \to \bar{f} f) = iy\bar{u}(p)v(q), \tag{C.1}$$

so that

$$\begin{aligned} |\mathcal{M}|^2 &= y^2 tr[\bar{v}(q)u(p)\bar{u}(p)v(q)] \\ &= y^2 tr[(\not{p} + m_f)(\not{q} - m_f)] \\ &= y^2[p_\alpha q_\beta 4\eta^{\alpha\beta} - 4m_f^2] \\ &= 4y^2(p \cdot q - m_f^2). \end{aligned} \tag{C.2}$$

In the inflaton rest frame we have $k^\mu = (m_\phi, 0, 0, 0)$, $p^\mu = (\sqrt{m_f^2 + p_*^2}, p_*, 0, 0)$ and $q^\mu = (\sqrt{m_f^2 + p_*^2}, -p_*, 0, 0)$. The momentum conservation $k^\mu = p^\mu + q^\mu$ allows us to rewrite $p \cdot q = \frac{m_\phi^2}{2} - m_f^2$, hence:

$$|\mathcal{M}|^2 = 4y^2\left(\frac{m_\phi^2}{2} - 2m_f^2\right) = 8y^2\frac{m_\phi^2}{4}\left(1 - 4\frac{m_f^2}{m_\phi^2}\right). \tag{C.3}$$

Energy conservation on the other hand translates into

$$m_\phi = 2\sqrt{m_f^2 + p_*^2}, \tag{C.4}$$

which inverted is

$$p_* = \frac{m_\phi}{2}\sqrt{1 - 4\frac{m_f^2}{m_\phi^2}}. \tag{C.5}$$

The decay rate can be evaluated from

$$\Gamma_{\phi\to\bar{f}f} = \frac{1}{2E_\phi}\int |\mathcal{M}|^2 d\Phi_2 = \frac{1}{2m_\phi}\frac{p_*}{4\pi m_\phi}|\mathcal{M}|^2. \tag{C.6}$$

Substituting the result just found one gets

$$\begin{aligned} \Gamma_{\phi\to\bar{f}f} &= \frac{1}{2m_\phi}\frac{m_\phi}{2}\sqrt{1 - 4\frac{m_f^2}{m_\phi^2}}\frac{1}{4\pi m_\phi}8y^2\frac{m_\phi^2}{4}\left(1 - 4\frac{m_f^2}{m_\phi^2}\right) \\ &= \frac{m_\phi}{8\pi}y^2\left(1 - 4\frac{m_f^2}{m_\phi^2}\right)^{\frac{3}{2}}. \end{aligned} \tag{C.7}$$

In the limit $m_f \ll m_\phi$ the decay rate reads simply

$$\Gamma = \frac{y^2 m_\phi}{8\pi}, \tag{C.8}$$

where y is the effective Yukawa coupling that determines the strength of the decay.

C.2 Decay rate of the inflaton field oscillating about a T-model potential

The evaluation of the phase space reads

$$\int d\Phi_2 = \int \frac{d^3\vec{p}_A}{(2\pi)^3 2E_A} \frac{d^3\vec{p}_B}{(2\pi)^3 2E_B} (2\pi)^4 \delta^{(4)}(p_n - p_A - p_B). \tag{C.9}$$

In the rest frame of the decaying mode we have $p_n = (E_n, 0, 0, 0)$, meaning that $\vec{p}_n = 0$ and consequently, from the 3-dimensional delta function, $\vec{p}_B = -\vec{p}_A$. This allows us to integrate only over one of the two, say for instance $d^3\vec{p}_B$, using the shorthand $p \equiv |\vec{p}_A| \equiv |\vec{p}_B|$, that in spherical coordinates can be rewritten as $p^2 dp d\Omega$. Moreover the energy conservation gives the relation

$$E_n = \sqrt{p^2 + m_A^2} + \sqrt{p^2 + m_B^2}. \tag{C.10}$$

We are left with

$$\begin{aligned} \int d\Phi_2 &= \frac{1}{(2\pi)^2} \frac{1}{4} \int \frac{p^2 dp d\Omega}{E_A E_B} \delta(E_n - E_A - E_B) \\ &= \frac{4\pi}{16\pi^2} \int \frac{p^2}{E_A E_B} \delta(E_n - E_A - E_B) dp, \end{aligned} \tag{C.11}$$

where we used the fact that $\int d\Omega = 4\pi$. We define $f(p) = \sqrt{p^2 + m_A^2} + \sqrt{p^2 + m_B^2} - E_n$ and thanks to the delta property

$$\delta(f(p)) = \frac{\delta(p - p^*)}{|f'(p^*)|}, \tag{C.12}$$

where p^* is the momentum that satisfies $E_n = E_A + E_B$, and to the fact that we can evaluate the derivative as

$$\frac{df}{dp}(p^*) = \frac{dE_A}{dp}(p^*) + \frac{dE_B}{dp}(p^*) = \frac{p^*}{E_A} + \frac{p^*}{E_B} = p^*\left(\frac{E_A + E_B}{E_A E_B}\right), \tag{C.13}$$

so that $|f'(p^*)| = \frac{p^* E_n}{E_A E_B}$. Now putting everything together it's easy to see that

$$\int d\Phi_2 = \frac{1}{4\pi}\left[\frac{(p^*)^2}{E_A E_B} \cdot \frac{1}{|f'(p^*)|}\right] = \frac{p^*}{4\pi E_n}. \tag{C.14}$$

Let us now manipulate Eq. (C.10) to find an expression for p^* that we can substitute in the result just found. Specifically, squaring it once and then a second time gives:

$$E_n^2 = p^{*2} + m_A^2 + p^{*2} + m_B^2 + 2\sqrt{(p^{*2} + m_A^2)(p^{*2} + m_B^2)}; \tag{C.15}$$

$$4(p^{*2} + m_A^2)(p^{*2} + m_B^2) = (E_n^2 - 2p^{*2} - m_A^2 - m_B^2)^2. \tag{C.16}$$

Simplifying we are left with

$$4p^{*2}E_n^2 = (E_n^2 - m_A^2 - m_B^2)^2 - 4m_A^2 m_B^2, \tag{C.17}$$

so that finally

$$p^{*2} = \frac{(E_n^2 - m_A^2 - m_B^2)^2 - 4m_A^2 m_B^2}{4E_n^2}. \tag{C.18}$$

Using the difference of squares property:

$$\begin{aligned} p^{*2} &= \frac{(E_n^2 - m_A^2 - m_B^2 - 2m_A m_B)(E_n^2 - m_A^2 - m_B^2 + 2m_A m_B)}{4E_n^2} \\ &= \frac{(E_n^2 - (m_A + m_B)^2)(E_n^2 - (m_A - m_B)^2)}{4E_n^2} \\ &= \frac{1}{4}\left(1 - \frac{(m_A + m_B)^2}{E_n^2}\right)\left(1 - \frac{(m_A - m_B)^2}{E_n^2}\right). \end{aligned} \tag{C.19}$$

Finally

$$
\begin{aligned}
\int d\Phi_2 &= \frac{1}{4\pi E_n}\cdot\frac{1}{2}\sqrt{\left(1-\frac{(m_A+m_B)^2}{E_n^2}\right)\left(1-\frac{(m_A-m_B)^2}{E_n^2}\right)} \\
&= \frac{1}{8\pi E_n}\beta_n(m_A,m_B),
\end{aligned} \tag{C.20}
$$

where we defined

$$
\beta_n(m_A,m_B) = \sqrt{\left(1-\frac{(m_A+m_B)^2}{E_n^2}\right)\left(1-\frac{(m_A-m_B)^2}{E_n^2}\right)}. \tag{C.21}
$$

This will appear in the evaluation of the decay rate which is written as

$$
\Gamma_n = \frac{1}{2E_n}\int |\mathcal{M}_n|^2 d\Phi_2 = \frac{\beta_n}{16\pi^2 E_n^2}|\mathcal{M}_n|^2. \tag{C.22}
$$

In our case we can write the decay rate as

$$
\Gamma_\phi = \frac{1}{8\pi(1+\omega_\phi)\rho_\phi}\sum_{n=1}^{\infty}|\mathcal{M}_n|^2 E_n\beta_n(m_A,m_B). \tag{C.23}
$$

Exploiting the fact that ϕ is oscillating with a certain frequency ω, the energy can be written as $E_n = n\omega$. We recall that the field could be factorized as $\phi(t) = \phi_0(t)\cdot\mathcal{P}(t)$, where $\mathcal{P}(t)$ varies rapidly with respect to ϕ_0, that we approximate as constant over a short time range. Therefore we get:

$$
\begin{aligned}
\rho_\phi &= \frac{1}{2}\dot{\phi}^2 + V(\phi) \\
&= \frac{1}{2}\phi_0^2\dot{\mathcal{P}}^2 + V(\phi_0\mathcal{P}),
\end{aligned} \tag{C.24}
$$

and since we have been considering $V(\phi)\propto\phi^k$, then we can say that $V(\phi_0\mathcal{P}) = \mathcal{P}^k V(\phi_0)$. Moreover, at the maximum of the oscillation $\mathcal{P} = 1$, $E_K = 0$ and consequently $\rho_\phi = V(\phi_0)$. Using these relations, we can then rewrite our time derivative as:

$$
\dot{\mathcal{P}}^2 = \frac{2}{\phi_0^2}[\rho_\phi - V(\phi_0\mathcal{P})] = \frac{2V(\phi_0)}{\phi_0^2}[1-\mathcal{P}^k]. \tag{C.25}
$$

Furthermore, the mass can be expressed as a function of the envelope via the second derivative of the potential:

$$m_\phi^2 = V''(\phi_0) = \lambda k(k-1)\phi_0^{k-2}. \tag{C.26}$$

Substituting this in the previous equation, we finally find

$$\dot{\mathcal{P}}^2 = \frac{2m_\phi^2}{k(k-1)}(1-\mathcal{P}^k), \tag{C.27}$$

We integrate this, assuming that the oscillating function $\mathcal{P}(t)$ starts at its maximum $\mathcal{P} = 1$ at $t = 0$ and drops to its minimum $\mathcal{P} = 0$ at a quarter of a period $t = T/4$.

$$\int_0^1 \frac{d\mathcal{P}}{\sqrt{1-\mathcal{P}^k}} = \int_0^{T/4} m_\phi \sqrt{\frac{2}{k(k-1)}}dt. \tag{C.28}$$

We relate the period to the frequency $T = \frac{2\pi}{\omega}$ and perform the computation, knowing that the left hand side integral equates to $\frac{1}{k}\frac{\Gamma(1/k)\Gamma(1/2)}{\Gamma(1/k+1/2)}$. This leads to:

$$\omega = m_\phi \sqrt{\frac{\pi k}{(k-1)}} \frac{\Gamma(\frac{1}{k}+\frac{1}{2})}{\Gamma(1/k)}. \tag{C.29}$$

$\mathcal{P}(t)$ can be expanded as a Fourier series in terms of this frequency ω:

$$\mathcal{P}(t) = \sum_{n=-\infty}^{\infty} \mathcal{P}_n e^{-in\omega t}. \tag{C.30}$$

C.2.1 Inflaton decay into two fermions

In the case on the inflaton decay into two fermions we have a matrix element structure similar to (C.1), with the difference that in this model the field can be rewritten in an oscillating and an envelope part. Thus

$$\mathcal{M}_n = y\phi_0\mathcal{P}_n\bar{u}(p_A)v(p_B). \tag{C.31}$$

The matrix element squared will be, looking at the calculation done for (C.3), fixing the coupling and writing E_n instead of m_ϕ,

$$|\mathcal{M}_n|^2 = y^2\phi_0^2\mathcal{P}_n^2 2E_n^2\left(1-4\frac{m_f^2}{m_\phi^2}\right) = y^2\phi_0^2\mathcal{P}_n^2 2E_n^2\beta_n^2(m_f, m_f), \tag{C.32}$$

which we can plug in the expression for the decay rate:

$$\begin{aligned}\Gamma_\phi &= \frac{1}{8\pi(1+\omega_\phi)\rho_\phi}\sum_{n=1}^{\infty}|\mathcal{M}_n|^2 E_n\beta_n(m_A, m_B) \\ &= \frac{y^2\phi_0^2}{4\pi(1+\omega_\phi)\rho_\phi}\sum_{n=1}^{\infty}|\mathcal{P}_n|^2 E_n^2\beta_n^2(m_f, m_f)\cdot E_n\beta_n(m_f, m_f),\end{aligned} \tag{C.33}$$

because in our case the two particles A and B have the same mass m_f. Averaging over one oscillation we can exploit the fact that $\rho_\phi = \frac{1}{2}\dot{\phi}^2 + V(\phi)$ so that

$$\langle\rho_\phi\rangle = V(\phi_0) = \frac{\phi_0^2 V''(\phi_0)}{k(k-1)}. \tag{C.34}$$

Together with $1+\omega_\phi = \frac{2k}{k+2}$ and $E_n = n\omega$ we can rewrite the rate as

$$\begin{aligned}\Gamma_{\phi\to\bar{f}f} &= \frac{y^2\phi_0^2\omega^3}{4\pi(1+\omega_\phi)\langle\rho_\phi\rangle}\sum_{n=1}^{\infty}|\mathcal{P}_n|^2 n^3\langle\beta_n^3(m_f, m_f)_+\rangle \\ &= \frac{y^2(k+2)(k-1)}{2\cdot 4\pi}\cdot\frac{\omega^3}{m_\phi^2}\sum_{n=1}^{\infty}|\mathcal{P}_n|^2 n^3\left\langle\left(1-\left(\frac{2m_f}{n\omega}\right)^2\right)_+^{\frac{3}{2}}\right\rangle \\ &= \frac{y^2}{8\pi}\omega\left[(k+2)(k-1)\left(\frac{\omega}{m_\phi}\right)^2\sum_{n=1}^{\infty}|\mathcal{P}_n|^2 n^3\left\langle\left(1-\frac{\mathcal{R}}{n^2}\mathcal{P}^2\right)_+^{\frac{3}{2}}\right\rangle\right] \\ &= \frac{y^2}{8\pi}\omega\alpha_y(k,\mathcal{R}),\end{aligned} \tag{C.35}$$

where $\mathcal{R} = (2m_f/\omega)^2|_{\phi\to\phi_0}$. Moreover we used the notation

$$(1-x)_+ \equiv (1-x)\theta(1-x), \tag{C.36}$$

in order to only include kinematically allowed decays, so that in the case in which $n\omega < 2m_f$ there is not enough energy to create the two fermions.

We can conclude that the fermionic decay has the final form

$$\Gamma_{\phi\to\bar{f}f}(t) \equiv \frac{y_{eff}^2(k)}{8\pi}m_\phi(t), \tag{C.37}$$

where we identify

$$y_{eff}^2(k) = \alpha_y(k,\mathcal{R})\frac{\omega}{m_\phi}y^2. \tag{C.38}$$

C.2.2 Inflaton decay into two bosons

In this case, the interaction considered is different and we parametrize it with $\mathcal{L}_I = \zeta^{2-\gamma}\phi^\gamma b_1 b_2$, so that we can express the two bosonic interactions just by modifying the value of γ. The matrix element is just $\mathcal{M}_n = \zeta^{2-\gamma}\phi_0^\gamma(\mathcal{P}^\gamma)_n$ that squared in the decay rate gives

$$\begin{aligned}\Gamma_{\phi^\gamma\to b_1 b_2} &= \frac{\zeta^{4-2\gamma}\phi_0^{2\gamma}}{8\pi(1+\omega_\phi)\rho_\phi}\sum_{n=1}^{\infty}|(\mathcal{P}^\gamma)_n|^2 E_n\langle\beta_n(m_A, m_B)_+\rangle \\ &= \frac{\zeta^{4-2\gamma}\phi_0^{2\gamma}}{8\pi(1+\omega_\phi)\rho_\phi}\omega\sum_{n=1}^{\infty}|(\mathcal{P}^\gamma)_n|^2 n\langle\beta_n(m_b, m_b)_+\rangle.\end{aligned} \tag{C.39}$$

From here we can set $\gamma = 1$ and $\zeta = \mu$ to get the inflaton decay into two bosons:

$$\Gamma_{\phi\to bb} = \frac{\mu^2\phi_0^2}{8\pi\cdot 2k}\frac{(k+2)}{\phi_0^2 m_\phi^2}k(k-1)\omega\sum_{n=1}^{\infty}n|\mathcal{P}_n|^2\langle\beta_n(m_b, m_b)_+\rangle, \tag{C.40}$$

which can be written in the form

$$\Gamma_{\phi\to bb}(t) = \frac{\mu_{eff}^2(k)}{8\pi m_\phi(t)}, \tag{C.41}$$

if one, including symmetry factors, defines

$$\mu_{eff}^2(k) = \frac{\mu^2}{4m_\phi}(k+2)(k-1)\omega\alpha_\mu(k,\mathcal{R}), \tag{C.42}$$

where

$$\alpha_\mu(k,\mathcal{R}) = 4\sum_{n=1}^{\infty}n|\mathcal{P}_n|^2\left\langle\left(1-\frac{\mathcal{R}}{n^2}\mathcal{P}^2\right)_+^{\frac{1}{2}}\right\rangle. \tag{C.43}$$

Similarly, the annihilation into 2 bosons is represented by a σ coupling, through a matrix element which looks like is $\mathcal{M}_n = 2\sigma\phi_0^2(\mathcal{P}^2)_n$. We can therefore write, including symmetry factors,

$$\Gamma_{\phi\to bb} = \frac{\sigma^2\rho_\phi}{8\pi}\frac{k(k+2)(k-1)^2}{m_\phi^4}\omega\sum_{n=1}^{\infty}n|(\mathcal{P}^2)_n|^2\langle\beta_n(m_b, m_b)_+\rangle. \tag{C.44}$$

The decay rate can be compared to

$$\Gamma_{\phi\phi\to bb} = \frac{\sigma^2_{eff}}{8\pi}\frac{\rho_\phi(t)}{m^3_\phi(t)}, \tag{C.45}$$

provided that

$$\sigma^2_{eff}(k) = \frac{\sigma^2}{8m_\phi}k(k+2)(k-1)^2\omega\alpha_\sigma(k,\mathcal{R}), \tag{C.46}$$

where, similarly to before, $\mathcal{R} = (2m_b/\omega)^2|_{\phi\to\phi_0}$.

D

Evaluation of λ

Starting from our T-model potential, we want to get an expression for the values of λ that are presented in Tab. 5.2. To derive it we will use the following relations between hyperbolic functions:

$$\frac{d}{dx}(\tanh x) = \mathrm{sech}^2 x; \tag{D.1}$$

$$\frac{\mathrm{sech}^2 x}{\tanh x} = 2\mathrm{csch}(2x); \tag{D.2}$$

$$\frac{1}{\mathrm{csch} x} = \sinh x; \tag{D.3}$$

$$\int \sinh(ax)dx = \frac{1}{a}\cosh(ax). \tag{D.4}$$

We start from the ϵ slow-roll parameter:

$$\begin{aligned} \epsilon \equiv \frac{1}{2}M_P^2\left(\frac{V'}{V}\right)^2 &= \frac{1}{2}M_P^2\left[k\frac{\mathrm{sech}^2\left(\frac{\phi}{\sqrt{6}M_P}\right)}{\tanh\left(\frac{\phi}{\sqrt{6}M_P}\right)}\cdot\frac{1}{\sqrt{6}M_P}\right]^2 \\ &= \frac{k^2}{3}\mathrm{csch}^2\left(\frac{\phi}{\sqrt{6}M_P}\right). \end{aligned} \tag{D.5}$$

This comes in useful when evaluating the number of e-folds at the end of inflation:

$$\begin{aligned} N_* &\simeq \frac{1}{M_P^2}\int_{\phi_{end}]}^{\phi_*}\frac{V(\phi)}{V'(\phi)}d\phi \simeq \frac{1}{M_P^2}\int_{\phi_{end}]}^{\phi_*}\frac{d\phi}{\sqrt{2\epsilon}} \\ &\simeq \sqrt{\frac{3}{2}}\frac{1}{M_P k}\int_{\phi_{end}]}^{\phi_*}\frac{d\phi}{\sqrt{\mathrm{csch}(\sqrt{\frac{2}{3}}\frac{\phi}{M_P})}} \simeq \frac{3}{2k}\cosh\left(\sqrt{\frac{2}{3}}\frac{\phi}{M_P}\right). \end{aligned} \tag{D.6}$$

Inverting this we can express ϕ_* in terms of N_*:

$$\phi_* = \sqrt{\frac{3}{2}}M_P\cosh^{-1}\left(\frac{2kN_*}{3}\right). \tag{D.7}$$

Then we evaluate the amplitude of the curvature power spectrum

$$\begin{aligned} A_{S*} &\simeq \frac{V_*}{24\pi^2\epsilon_* M_P^4} \\ &\simeq \lambda M_P^4 6^{\frac{k}{2}}\tanh^k\left(\frac{\phi_*}{\sqrt{6}M_P}\right)\cdot\frac{1}{24\pi^2 M_P^4}\cdot\frac{3}{k^2}\cdot\frac{1}{\mathrm{csch}^2(\sqrt{\frac{2}{3}}\frac{\phi}{M_P})} \\ &\simeq \lambda\frac{6^{\frac{k}{2}}}{8\pi^2k^2}\tanh^k\left(\frac{\phi_*}{\sqrt{6}M_P}\right)\cdot\sinh^2\left(\sqrt{\frac{2}{3}}\frac{\phi}{M_P}\right) \end{aligned} \tag{D.8}$$

.

Inverting it, we get an expression for λ which is

$$\lambda \simeq \frac{8\pi^2k^2}{6^{\frac{k}{2}}}\cdot A_{S*}\cdot\frac{1}{\tanh^k\left(\frac{\phi_*}{\sqrt{6}M_P}\right)\cdot\sinh^2\left(\sqrt{\frac{2}{3}}\frac{\phi}{M_P}\right)}. \tag{D.9}$$

From (D.6) we can write

$$\cosh\left(\sqrt{\frac{2}{3}}\frac{\phi}{M_P}\right) \simeq \frac{2kN_*}{3}, \tag{D.10}$$

and

$$\sinh^2\left(\sqrt{\frac{2}{3}}\frac{\phi}{M_P}\right) \simeq \cosh^2\left(\sqrt{\frac{2}{3}}\frac{\phi}{M_P}\right) = \frac{4k^2N_*^2}{9}, \tag{D.11}$$

which comes from $\sinh^2 x = \cosh^2 x - 1$, where we can neglect the -1 for large values of x. Moreover for large ϕ_*, $\tanh^k\left(\frac{\phi_*}{\sqrt{6}M_P}\right) \to 1$. The simplified expression is then

$$\lambda \simeq \frac{18\pi^2 A_{S*}}{6^{\frac{k}{2}} N_*^2}. \tag{D.12}$$

References

[1] A. Batra, P. Bharadwaj, S. Mandal, R. Srivastava and J. W. F. Valle. *Phenomenology of the simplest linear seesaw mechanism*. 2023. arXiv: `2305.00994v2 [hep-ph]`.

[2] B. Barman, S. Cléry, R. T. Co, Y. Mambrini and K. A. Olive. *Gravity as a Portal to Reheating, Leptogenesis and Dark Matter*. 2022. arXiv: `2210.05716v2 [hep-ph]`.

[3] B. Barman and A. Datta. *Testing Axionic Dark Matter during Gravitational Reheating*. 2024. arXiv: `2312.13821v2 [hep-ph]`.

[4] S. M. Barr and D. Seckel. "Planck-Scale Corrections to Axion Models". In: *Physical Review D* 46.2 (1992), pp. 539–549. DOI: `10.1103/PhysRevD.46.539`.

[5] D. Baumann. *TASI Lectures on Inflation*. 2012. arXiv: `0907.5424v2 [hep-th]`.

[6] Quentin Bonnefoy. "Heavy fields and the axion quality problem". In: *Physical Review D* 108.3 (2023), p. 035023. DOI: `10.1103/PhysRevD.108.035023`.

[7] B. J. Carr and A. M. Green. *The History of Primordial Black Holes*. 2025. arXiv: `2406.05736v4 [astro-ph]`.

[8] M. Dine and A. Kusenko. *The Origin of the Matter-Antimatter Asymmetry*. 2003. arXiv: `0303065v3 [hep-ph]`.

[9] S. Dodelson. *Modern Cosmology*. Academic Press, 2003.

[10] G. Efstathiou. *Challenges to the ΛCDM Cosmology*. 2024. arXiv: `2406.12106v2 [astro-ph]`.

[11] F. Capozzi, E. Lisi, A. Marrone, D. Montanino and A. Palazzo. *Neutrino masses and mixings: Status of known and unknown 3ν parameters*. 2016. arXiv: `1601.07777v1 [hep-ph]`.

[12] G. Domènech, C. Lin and M. Sasaki. *Gravitational wave constraints on the primordial black hole dominated early universe*. 2025. arXiv: 2012.08151v3 [gr-qc].

[13] G. B. Gelmini. *TASI 2014 Lectures: the Hunt for Dark Matter*. 2015. arXiv: 1502.01320v2 [hep-ph].

[14] D. Griffiths. *Introduction to Elementary Particles*. John Wiley and Sons, 2008.

[15] B. Gripaios. *Physics Beyond the Standard Model*. 2015. arXiv: 1503.02636v1 [hep-ph].

[16] H. Shao, J. J. Givans, J. Dunkley, M. Madhavacheril, F. Qu, G. Farren and B. Sherwin. *Cosmological limits on the neutrino mass sum for beyond-ΛCDM models*. 2024. arXiv: 2409.02295 [astro-ph].

[17] M. Herrera. *The Standard Model*. 1998. arXiv: 9812242 [hep-ph].

[18] A. Hook. *TASI Lectures on the Strong CP Problem and Axions*. 2023. arXiv: 1812.02669v3 [hep-ph].

[19] L. Husdal. *On Effective Degrees of Freedom in the Early Universe*. 2016. arXiv: 1609.04979v3 [astro-ph].

[20] J. Asorey, J. de Cruz Pérez. *Revisiting ΛCDM extensions in light of re-analyzed CMB data*. 2025. arXiv: 2506.13537v1 [astro-ph].

[21] K. Arun, S. B. Gudennavar and C. Sivaram. *Dark matter, dark energy, and alternate models: A review*. 2017. arXiv: 1704.06155 [hep-ph].

[22] R. Kallosh and A. Linde. *Universality Class in Conformal Inflation*. 2013. arXiv: 1306.5220v3 [hep-th].

[23] E. W. Kolb and M. S. Turner. *The Early Universe*. Addison-Wesley, 1993.

[24] E. Nardi L. Di Luzio M. Giannotti and L. Visinelli. *The landscape of QCD axion models*. 2022. arXiv: 2003.01100v4 [hep-ph].

[25] K. Lozanov. *Lectures on Reheating after Inflation*. 2019. arXiv: 1907.04402v1 [astro-ph].

[26] O. Luongo and M. Muccino. *Dark energy reconstructions combining BAO data with galaxy clusters and intermediate redshift catalogs*. 2024. arXiv: 2411.04901v1 [astro-ph].

[27] D. H. Lyth and A. R. Liddle. *The Primordial Density Perturbation*. Cambridge University Press, 2009.

[28] M. A. G. Garcia, K. Kaneta, W. Ke, Y. Mambrini, K. A. Olive and S. Verner. *The Role of Vectors in Reheating*. 2023. arXiv: 2311.14794v1 [hep-ph].

[29] M. A. G. Garcia, K. Kaneta, Y. Mambrini and K. A. Olive. *Inflaton Oscillations and Post-Inflationary Reheating*. 2021. arXiv: 2012.10756v2 [hep-ph].

[30] M. A. G. Garcia, K. Kaneta, Y. Mambrini and K. A. Olive. *Reheating and Post-inflationary Production of Dark Matter*. 2020. arXiv: 2004.08404v2 [hep-ph].

[31] M. A. G. Garcia, M. Gross, Y. Mambrini, K. A. Olive, M. Pierre and J. H. Yoon. *Effects of Fragmentation on Post-Inflationary Reheating*. 2023. arXiv: 2308.16231v2 [hep-ph].

[32] M. Bauera, M. Neubertb, S. Rennere, M. Schnubelb and A. Thammf. *The Low-Energy Effective Theory of Axions and ALPs*. 2021. arXiv: 2012.12272v2 [hep-ph].

[33] M. Gross, E. Kpatcha, Y. Mambrini, M. O. Olea-Romacho and R. Roshan. *Gravitational Wave Production During Reheating: From the Inflaton to Primordial Black Holes*. 2024. arXiv: 2411.04189v1 [hep-ph].

[34] M. R. Haque, E. Kpatcha, D. Maity and Y. Mambrini. *Primordial Black Hole Reheating*. 2023. arXiv: 2305.10518v1 [hep-ph].

[35] M. R. Haque,E.Kpatcha, D. Maity and Y Mambrini. *Primordial black hole versus inflaton*. 2024. arXiv: 2309.06505v2 [hep-ph].

[36] Y. Mambrini. *Particles in the Dark Universe*. Springer, 2021.

[37] Y. Mambrini and K. A. Olive. *Gravitational production of dark matter during reheating*. 2021. arXiv: 2102.06214v2 [hep-ph].

[38] D. J. E. Marsh. *Axion Cosmology*. 2016. arXiv: 1510.07633v2 [astro-ph].

[39] D. J. E. Marsh. *Axions and ALPs: a very short introduction*. 2017. arXiv: 1712.03018v1 [hep-ph].

[40] V. F. Mukhanov. *Physical Foundations of Cosmology*. Cambridge University Press, 2012.

[41] H. Murayama. *Physics Beyond the Standard Model and Dark Matter*. 2007. arXiv: 0704.2276 [hep-ph].

[42] N. Bernal, M. Dutra, Y. Mambrini, K. Olive, M. Peloso and M. Pierre. *Spin-2 Portal Dark Matter*. 2018. arXiv: 1803.01866v1 [hep-ph].

[43] N. Bhusal, E. Chavez M., M. A. Garcia, A. G. Menkara and M. Pierre. *Fermion reheating with a quartic inflaton potential*. 2025. arXiv: 2512.16203v1 [hep-ph].

[44] Ciaran O'Hare. *AxionLimits*. https://github.com/cajohare/AxionLimits. 2020. DOI: 10.5281/zenodo.3932430.

[45] C. A. J. O'Hare. *Cosmology of axion dark matter*. 2024. arXiv: 2403.17697v2 [hep-ph].

[46] R. D. Peccei. *Discrete and Global Symmetries in Particle Physics*. 1998. arXiv: 9807516 [hep-ph].

[47] R. D. Peccei. *Why PQ?* 2010. arXiv: 1005.0643v1 [hep-ph].

[48] R.D. Peccei. *The Strong CP Problem and Axions*. 2006. arXiv: 0607268v1 [hep-ph].

[49] A. Pich. *The Standard Model of Electroweak Interactions*. 2021. arXiv: 1201.0537 [hep-ph].

[50] Planck Collaboration. *Planck 2018 results. X. Constraints on inflation*. 2020. arXiv: 1807.06211 [astro-ph.CO].

[51] F. Quevedo and A. Schachner. *Cambridge Lectures on The Standard Model*. 2024. arXiv: 2409.09211 [hep-th].

[52] A. Riotto. *Inflation and the Theory of Cosmological Perturbations*. 2017. arXiv: 0210162v2 [hep-ph].

[53] A. Riotto. *Theories of Baryogenesis*. 1998. arXiv: 9807454v2 [hep-ph].

[54] S. Borsanyi, Z. Fodor, K.-H. Kampert, S. D. Katz, T. Kawanai, T. G. Kovacs, S. W. Mages, A. Pasztor, F. Pittler, J. Redondo, A. Ringwald and K. K. Szabo. *Lattice QCD for Cosmology*. 2016. arXiv: 1606.07494v2 [hep-lat].

[55] S. Cléry, Y. Mambrini, K. A. Olive, A. Shkerin and Sarunas Verner. *Gravitational Portals with Non-Minimal Couplings*. 2022. arXiv: 2203.02004v1 [hep-ph].

[56] S. Cléry, Y. Mambrini, K. A. Olive and Sarunas Verner. *Gravitational portals in the early Universe*. 2022. arXiv: 2112.15214v2 [hep-ph].

[57] V. Gorini S. L. Cacciatori and F. Re. *Dark Energy*. 2024. arXiv: 2410.10435v1 [gr-qc].

[58] P. Sikivie. *Axion Cosmology*. 2006. arXiv: 0610440v2 [astro-ph].

[59] D. Tong. *Lectures on Gauge Theory*. 2018.

[60] S. Verner. *Gravitational Production of Massive Spin-2 Particles During Reheating*. 2025. arXiv: 2512.19041v1 [hep-ph].

[61] O. Wantz and E.P.S. Shellard. *Axion Cosmology Revisited*. 2011. arXiv: 0910.1066v3 [astro-ph].

[62] S. Weinberg. *Principles and Applications of the General Theory of Relativity*. John Wiley and Sons, 1972.

[63] Steven Weinberg. "The Cosmological Constant Problem". In: *Reviews of Modern Physics* 61.1 (1989), pp. 1–23. DOI: 10.1103/RevModPhys.61.1.

[64] Steven Weinberg. "The U(1) Problem". In: *Physical Review D* 11.12 (1975), pp. 3583–3593. DOI: 10.1103/PhysRevD.11.3583.

[65] Yong Xu. "Constraining Axion and ALP Dark Matter from Misalignment during Reheating". In: *Physical Review D* 108.8 (2023), p. 083536. DOI: 10.1103/PhysRevD.108.083536.

Acknowledgments

First and foremost I would like to thank my supervisor, Professor Francesco D'Eramo, for giving me the opportunity to work on this thesis under his guidance. I am deeply grateful for the trust he placed in me, for the flexibility he provided me with, which allowed me to complete a part of this work during my Erasmus exchange, and for introducing me to the team in Paris. Furthermore, I am thankful for all the advice regarding my future career in research.

I would also like to thank my cosupervisor, Professor Yann Mambrini, for giving me the opportunity to work on part of my thesis in Paris, allowing me to live an amazing experience and to work in an inspiring environment. His enthusiasm and passion for physics have been a source of inspiration for my future in the academic field.

Lastly, I would like to thank PhD candidate Mathieu Gross, who put a huge effort into making sure that I was able to come to the IJCLab. I am incredibly thankful for his daily guidance, his patient explanations and for all the insightful suggestions he shared with me.